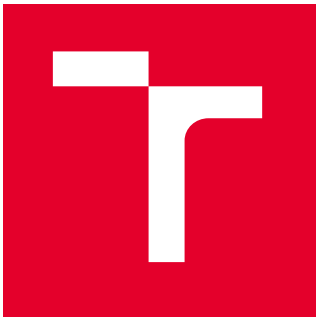

BRNO UNIVERSITY OF TECHNOLOGY

VYSOKÉ UČENÍ TECHNICKÉ V BRNĚ

FACULTY OF MECHANICAL ENGINEERING

FAKULTA STROJNÍHO INŽENÝRSTVÍ

INSTITUTE OF MACHINE AND INDUSTRIAL DESIGN

ÚSTAV KONSTRUOVÁNÍ

AN INVESTIGATION OF BIOTRIBOLOGICAL PERFORMANCE OF HYDROGELS FOR CARTILAGE REPLACEMENT

STUDIUM BIOTRIBOLOGICKÝCH VLASTNOSTÍ HYDROGELŮ PRO NÁHRADU KLOUBNÍ CHRUPAVKY

MASTER'S THESIS

DIPLOMOVÁ PRÁCE

AUTHOR — **Bc. Daniel Němeček**

AUTOR PRÁCE

SUPERVISOR — **doc. Ing. David Nečas, Ph.D.**

VEDOUCÍ PRÁCE

BRNO 2025

BRNO UNIVERSITY OF TECHNOLOGY
FACULTY OF MECHANICAL ENGINEERING

Assignment Master's Thesis

Institut:	Institute of Machine and Industrial Design
Student:	**Bc. Daniel Němeček**
Degree programm:	Mechanical Engineering Design
Branch:	no specialisation
Supervisor:	**doc. Ing. David Nečas, Ph.D.**
Academic year:	2024/25

As provided for by the Act No. 111/98 Coll. on higher education institutions and the BUT Study and Examination Regulations, the director of the Institute hereby assigns the following topic of Master's Thesis:

An investigation of biotribological performance of hydrogels for cartilage replacement

Brief Description:

A crucial issue in orthopaedics, which has significant socio–economic implications, is the substantial increase in the number of hip and knee replacements. In terms of the total number of surgeries, joint replacement due to osteoarthritis in its various forms represents a significant proportion. In this case, the irreversible degradation of joint cartilage plays a key role. If it were possible to develop a sufficiently high–quality technical material based on hydrogel that could replace damaged cartilage, it would not only significantly improve patients' quality of life but also lead to enormous financial savings for the healthcare system.

Thesis type: research
Thesis output: publication result (J, D)
Project: OP JAK

Master's Thesis goals:

The main objective is to describe the biotribological properties of hydrogel–based materials using standard tribological tests in various model configurations. Different types of materials, ranging from simple models to composite (lamellar) hydrogels, will be compared.
The partial objectives of the thesis are as follows:
– provide a critical review of current scientific papers dealing with joint cartilage replacement,
– prepare hydrogel samples using various manufacturing technologies (cast–drying, freezing/thawing),
– conduct tests focused on evaluating the coefficient of friction and wear of the hydrogels,
– discuss the obtained findings in the context of current scientific studies.

Required outputs: report.
Work extent: approximately 72,000 characters (40–50 pages of text without images).
The timeline, structure of the work, and report template must follow:
http://www.ustavkonstruovani.cz/texty/bakalarske–studium–ukonceni/

Recommended bibliography:

NEČAS, David, Seido YARIMITSU, David REBENDA, Hironori SHINMORI, Martin VRBKA, Yoshinori SAWAE, Teruo MURAKAMI and Ivan KŘUPKA. 2023. On the replacement of articular cartilage: The friction of PVA hydrogel layer in hip simulator test. Tribology International. 178.

MURAKAMI, Teruo, Seido YARIMITSU, Kazuhiro NAKASHIMA, Tetsuo YAMAGUCHI, Yoshinori SAWAE, Nobuo SAKAI and Atsushi SUZUKI. 2014. Superior lubricity in articular cartilage and artificial hydrogel cartilage. Proceedings of the Institution of Mechanical Engineers, Part J: Journal of Engineering Tribology. 228(10), 1099-1111.

GONG, Jian Ping. 2006. Friction and lubrication of hydrogels—its richness and complexity. Soft Matter. 2(7), 544-552.

Deadline for submission Master's Thesis is given by the Schedule of the Academic year 2024/25

In Brno,

L. S.

prof. Ing. Martin Hartl, Ph.D.
Director of the Institute

doc. Ing. Jiří Hlinka, Ph.D.
FME dean

ABSTRACT

Articular cartilage, a superior nature's bearing, is a hidden treasure supporting us throughout our very lives, without us even noticing. The downside of such maintainless function is that once the cartilage is damaged, it cannot repair itself. Approaches to cartilage' treatment are many. An engineering one is to make a cartilage-like replica as its replacement. For that water-based materials (hydrogel) have been studied – dealing with a prevailing issue of combining a high strength material with wear-resistant low frictional surface.

The aim of the present work was to find out how hydrogel stiffness affects its resistance to wear and reveal the corresponding frictional mechanisms. It was found that hydrogel that was preloaded for a long time (e.g. sitting), exhibits a different frictional mechanism – corresponded to its solid friction properties, than rehydrated hydrogel in motion – corresponded to fluid load properties (e.g. walking, running). The lubricating properties of the hydrogel's solid phase were associated with cross-linking polymer structure inducing either abrasive friction or non-destructive adhesion friction. For dominant fluid lubrication, properties such as hydrogel' water content and water permeability are crucial for low friction.

In conclusion, compliant hydrogels were found to create wear-resistant polymer brush layer – contributing both to better lubrication at solid (boundary) and fluid (biphasic) phase dominant lubrication. Stiffer hydrogels usually perform worse due to deficiency of protruding polymers to the surface, resulting in excessive wear.

KEYWORDS

biotribology, artificial cartilage, PVA, hydrogel, boundary lubrication, friction, wear, pHEMA, biphasic lubrication

ABSTRAKT

Kloubní chrupavka, jedinečné přírodní ložisko, které podporuje naši pohybovou činnost po celý život – aniž bychom si toho byli vědomi. Nevýhodou této bezúdržbové funkce je, že jakmile dojde k poškození chrupavky, nedokáže se sama opravit. Existuje mnoho přístupů k léčbě chrupavky. Mezi hlavní inženýrské přístupy je vytvoření její umělé náhrady – napodobeniny chrupavky. K tomuto účelu se zkoumají materiály na bázi vody (hydrogely). Ty však čelí zásadnímu problému: jak spojit vysokou pevnost materiálu s nízkým třením a odolností proti opotřebení.

Cílem této práce bylo pokusit se objasnit, jak tuhost hydrogelu ovlivňuje jeho odolnost proti opotřebení a odhalit související třecí mechanismy. Bylo zjištěno, že hydrogel, který byl dlouho zatížen (podobně jako při sezení na židli), vykazuje třecí mechanismus jiné chování (dochází totiž k přímému kontaktu spolu zabírajících povrchů), než plně hydratovaný hydrogel při pohybu, kde jsou povrchy převážně oddělené tenkou mazací vrstvou (podobně jako při chůzi nebo běhu). Mazací vlastnosti pevné fáze hydrogelu souvisely s jeho polymerní strukturou. Polymerní struktura způsobovala buď abrazivní tření, nebo ochranné adhezivní tření. Při dominantě kapalinovém mazání jsou pro nízké tření zásadní vlastnosti jako obsah vody v hydrogelu a jeho propustnost.

Závěrem bylo zjištěno, že poddajné hydrogely vytvářejí na povrchu odolnou polymerní vrstvu („polymerový kartáč“), která přispívá k menšímu opotřebení. A to jak v případě přímého kontaktu povrchů, tak v kapalinné fázi. Naopak tužší hydrogely zpravidla vykazují horší vlastnosti kvůli nedostatku vyčnívajících polymerních řetězců na povrchu, což vede k nadměrnému opotřebení.

KLIČOVÁ SLOVA

biotribologie, umělá chrupavka, PVA, hydrogel, mezné mazání, tření, opotřebení, pHEMA, dvojfázové mazání

BIBLIOGRAPHICAL REFERENCE

NĚMEČEK, Daniel. *An investigation of biotribological performance of hydrogels for cartilage replacement*. Brno, 2025, 103 p. Brno University of Technology, Faculty of Mechanical Engineering, Institute of Machine and Industrial Design. Thesis supervisor: doc. Ing. David Nečas, Ph.D.

ACKNOWLEDGMENT

I would like to express my gratitude to those who made my master's studies an amazing and memorable experience and gave me an opportunities I could have never dreamt of. Most importantly, I would like to thank doc. Ing. David Nečas, Ph.D., not only for being overwhelmingly helpful throughout the years but also for arranging internships in Japan and Chile for me – something I will remember for the rest of my life. The deepest gratitude belongs to my parents, without whose boundless support none of what you are about to read would have been possible.

AUTHOR'S DECLARATION ON THE ORIGIN OF THE WORK

I herby declare that I have written the master's thesis *An investigation of biotribological performance of hydrogels for cartilage replacement* on my own according to the advice of my supervison Ing. David Nečas, Ph.D., and using the sources listed in references.

…….

Author's signature

CONTENT

1 INTRODUCTION

The first attempts to replace natural cartilage with manmade material have begun in the early 20th century, focusing primarily on hip and knee joints, by using stainless steel, ceramics, or polyethylene components. This was shown as an efficient replacement enabling patients to restore their active lives. However, due to insufficient lubrication causing excessive wear and inflammation, the possible lifespan was fairly limited. Up until today, this method of replacing the articular cartilage is understood as the most effective, with an estimated lifespan of 15 years. It is believed that with some improvements enhancing the lubrication regime via surface modification (topography, coatings) the lifespan could be higher.

The main issue related to the total replacement components is the cost, which together with the gradually increasing need for the replacements, is unsustainable.

One of the possible answers to this particular issue besides others, is to create a material based on our knowledge of natural cartilage and make a material that would work on the same superior lubricating mechanisms as cartilage. Achieving this would get us access to a mechanism of superlubricity, whose applications might go far beyond biological applications and have the potential to change the whole bearing industry – nevertheless, this problem is extremely complex and has been investigated for many years without a clear solution, despite the knowledge progress that has been made.

A sort of material, believed to be able to replace cartilage in the future is hydrogel, consisting of a solid and liquid phase, specifically Poly(vinyl alcohol) (PVA) hydrogel. PVA hydrogel possess a crucial property that other materials lack, high fluid load support, enabling the maintenance of minimal contact between opposing surfaces – similar to cartilage.

Material property, structure, and expected resultant behavior are derived from the articular cartilage. The long-term aim is to develop a material that could equally represent natural cartilage in terms of its superior behavior. For a better understanding of what obstacles stand in the way of achieving this goal, let me first introduce the current understanding of natural cartilage behavior and why it is so difficult for us to replace this particular human body part equally.

2 OVERVIEW OF THE CURRENT STATE OF KNOWLEDGE

2.1 Research methods

The aim of the research section is to identify the limitations and current challenges in the existing state of knowledge. It explores and summarizes the fundamental concepts necessary to understand articular cartilage and hydrogel material. Based on the identified gaps in the current understanding of hydrogel materials, the main themes were selected for the diploma thesis. The scientific publications were searched based on the following questions:

1. What is the current state of knowledge of articular cartilage? Which parts are crucial to understand regarding its superior lubricating mechanism?
   Keywords: friction, lubrication, articular cartilage, boundary lubrication, biphasic lubrication, hydration lubrication, tribology, review

2. Which types of hydrogels and their properties are suited for the simulation of articular cartilage?
   Keywords: artificial cartilage, cartilage replacement, hydrogel, Poly (vinyl alcohol)

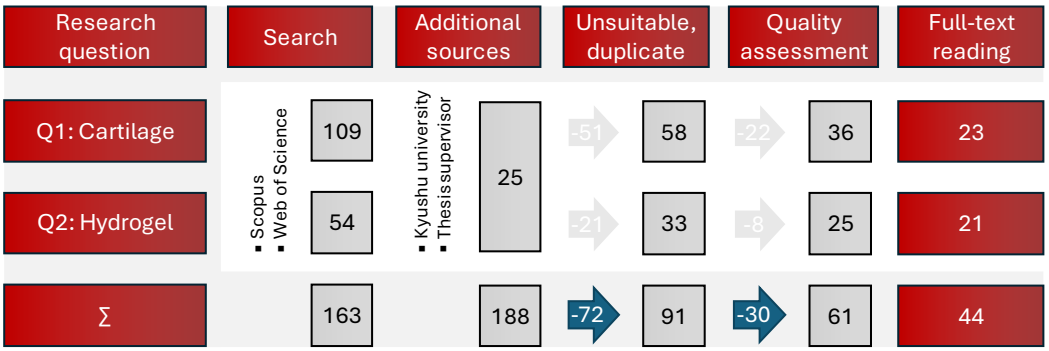

Figure 2-1: Prisma diagram of scientific research articles.

2.2 Articular cartilage

A synovial joint is an essential component of most living animals. A component we would not be able to do very basic activities involving any kind of movement. Imagine how many cartilage tissues and joints we incorporate when we just sit at our computer: spine, neck, or even fingertips. All those parts work amazingly well, even when we barely move. Even at extreme loads (e.g. weightlifting, rock climbing, or athletics), cartilage always provides smooth movement. Only when it is injured, causing extreme pain, does it begin to attract all our attention.

Healthy articular cartilage is often assigned to friction as low as 0.001 under pressure exceeding our body weight by many folds and represents the most effective lubricated surface in nature. [1] Such low friction, often compared to that in ice skating, has not yet been replicated on the same scale, despite the many years of intensive work effort of many researchers. Understanding is a crucial factor for us to be able to intervene correctly when some degeneration of this tissue occurs. Joint degeneration is recently on a steep rise as the population is getting older, due to available heath care. This raises the demand for effective cartilage tissue replacements with equivalent performance. Current joint replacements standing primarily on metal or polyethylene materials. These are costly and do not guarantee long-term solutions. Bringing a detailed inside look into the function of natural cartilage and developing a material with similar properties would be revolutionary.

2.2.1 Friction of articular cartilage

Maintaining such minimal friction is an essential condition for decades-long good functioning in human cartilage, keeping wear at the minimum possible level. Deviations from this low friction might indicate tissue degradation related to osteoarthritis – the prevalent joint disease.

Friction is generally understood as energy dissipation caused by surfaces mutually sliding against each other. Lost energy might be emitted in the form of heat and noise. Lubrication, on the other hand, reduces this energy loss by separating the surfaces. By studying further friction mechanisms, we can sort the main mechanisms corresponding to those losses: viscous friction and boundary friction. Viscous friction is meant by contactless sliding, where dissipation is carried out by sheared fluid film layers. Boundary friction is rather complicated and is considered as molecular contact between sliding surfaces. Dissipation is made via intermolecular bonding, their elastic stretching and breakage or passage of the same charge molecules over local repulsive maxima. In order to simplify those effects, friction is traditionally described as coefficient of friction (COF) = (force to slide the surfaces) / (load compressing the surfaces) known as Amontons' law, simplifying the dissipation energies into one force acting against performed movement [1, 2].

2.2.2 Structure and composition

We can think of articular cartilage as a well-structured water-based tissue (~80 % water) at the end of an articulating bone, with a typical thickness ranging from 1 to 4 mm. Besides maintaining smooth movement, cartilage also damps sudden impacts and supports high stresses otherwise transmitted on subchondral bone. Apart from cartilage and bone, joint consists of joint cavity filled with synovial fluid (SF) and the synovial membrane covering the cavity, Figure 2-2 a) [1].

Articular cartilage structure is composed of collagen fibrils, proteoglycans, other non-collagenous proteins, and chondrocytes with a high content of water [1].

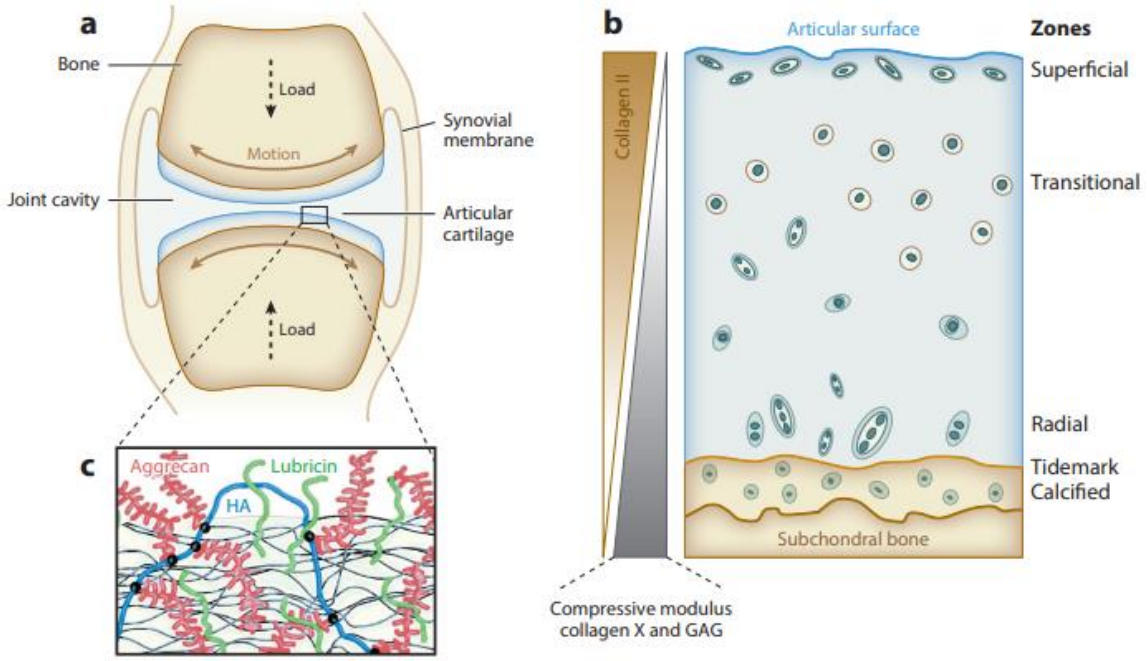

Figure 2-2: a) Schema of a synovial joint. a) A synovial joint is composed of opposing bones covered with thin layer of cartilage and embedded in SF filing up the joint cavity surrounded by synovial membrane. b) Cartilage structure is categorized into four zones. Cartilage cells (chondrocytes) occupy less than 5 % of the tissue. Cartilage structure, composition and mechanical properties vary with depth. c) Superficial cartilage layer showing molecules incorporated in cartilage lubrication: hyaluronic acid (HA), aggrecan and lubricin. Phospholipids are not depicted here, although they are important constituents as well [2].

Collagen fibrils, primarily type II, provide structure with strength and stiffness. Collagen arrangement in the cartilage varies in depth and can be classified into three zones, Figure 2-3 a) – the superficial zone, the middle/transitional zone, and the deep/radial zone. In the superficial zone, the collagen fibrils are oriented parallelly with the articular surface to withstand mechanical loading. The density of collagen here is the highest and its content gradually decreases with depth. Passing through the middle and deep zone, the fibers change their orientation towards the articular surface until they are perpendicular to the subchondral bone. The diameter of the deep fibrils is larger than in the upper zones. Proteoglycan's concentration is inverse to collagen fibrils, with the highest content at the deep zone and the lowest at the superficial zone [1, 3].

The compressive modulus of the tissue is higher with depth and is proportionally connected with proteoglycan concentration. However, the transverse modulus (parallel with the articulating surface) is the highest at the superficial layer and rapidly decreases as the collagen changes its arrangement. [4] This nonhomogeneous and anisotropic behavior has implications for the permeability of fluid flow through the cartilage matrix. Permeability in the parallel direction is lower than in the compressive direction; this is very important for interstitial fluid load support [3, 5].

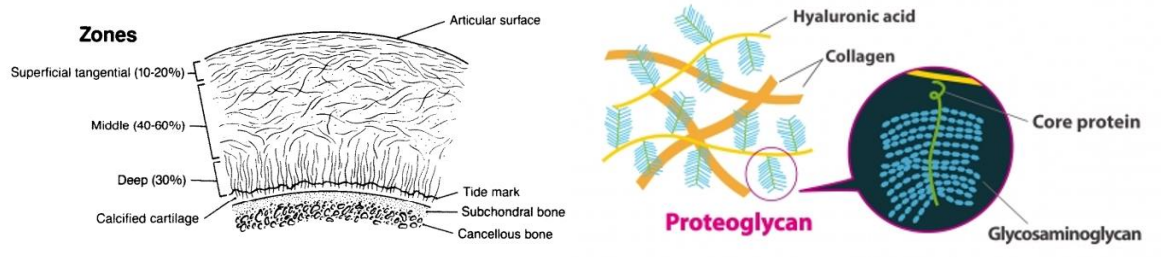

Figure 2-3: a) Collagen network organization in natural cartilage. b) Schema of proteoglycan macromolecule.

Proteoglycans are composed of core protein and attached glycosaminoglycan (GAG) chains forming bush-like structure, which are further linked to HA, Figure 2-3 b). They have a dense negative charge and are highly hydrated, contributing to water retention of cartilage. The dense negative charge induces osmotic pressure, leading to the swelling and expansion of cartilage. The collagen fibers inside the cartilage resist this, resulting in tension in fibers and contribution to the high stiffness of the cartilage [1–3].

Important representants of proteoglycans in cartilage surfaces are aggrecan and lubricin. Aggrecan is non-covalently linked to hyaluronic acid (HA) and forms a bottle-brush-like structure. Lubricin, also known as proteoglycan 4, plays an important role in the superficial zone along with HA and phospholipids and is also present in the synovial fluid [2], this will be described in detail later.

Phospholipids (PLs) form long chain monolayer or bilayers consisting of many headgroups and protruding hydrophobic acyl tails. It is present both in SF and at cartilage surface [2].

Water content increases from roughly 65 % near the subchondral bone to 80 % at the outer superficial zone. Natural cartilage does not have any blood vessels, therefore, any regeneration of major damage of cartilage tissue is unlikely. The only cell type in cartilage is chondrocytes. The cell have an ability to locally repair and maintain the tissue as well as synthesizing other cartilage' molecules. Chondrocytes occupy less than 5 % of cartilage volume, the absence of blood vessels emphasizes the role of water within the cartilage, which plays a key role in transporting nutrients. Chondrocytes' behavior is governed by shear and compressive stresses. Compressive forces are needed for the proper healthy circulation of nutrients and SF within the matrix. Increase in shear force may indicate degradation and non-standard cell behavior. It is believed that chondrocytes play a crucial role in recognizing pathological changes in cartilage [1, 2].

Cartilage dysfunction, such as osteoarthritis (OA) might be a result of several events, beginning with damage to articular cartilage, initiated by some trauma (or by old age). This leads to disruption of lubrication, resulting in an increase of friction and progressive structural changes which ultimately lead to joint failure. Damaged cartilage is not capable of healing itself due to its lack of blood vessels and low density of chondrocytes. Initiating damage is accompanied with friction increase and correspondingly higher shear strain influences chondrocyte cells and causes significant changes to the microstructural organization of the cartilage; degraded tissue is then abraded, and high friction then causes repeating of this so-called self-reinforcing cycle, which is destructive, see Figure 2-4 [1, 6].

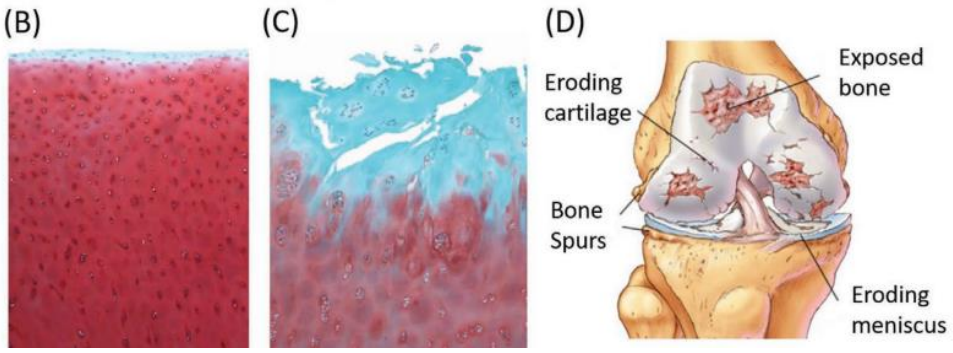

Figure 2-4: b) A histology image shows smooth and likely healthy articular cartilage, c) A histology image of degenerated cartilage affected by osteoarthritis. A rougher surface and extensive matrix loss result from cartilage stiffening caused by shear strain and subsequent chondrocytes irregular behavior. d) Schematic image of degenerated cartilage suffering of osteoarthritis. [1]

2.2.3 Models of Lubrication at Cartilage Surfaces

COF in synovial joints is commonly reported to be within the range of ≈ 0.001 – 0.01, performed on living cartilage, however, it is believed that friction between cartilage-cartilage contact might be even lower, as the dissipation energy includes losses connected with viscoelastic deformation of neighboring tissues (ligaments, muscles, synovial membrane) [1, 2].

The reason why synovial joints exhibit such a low friction and what is the precise lubrication mechanism behind represents a phenomenon that has been studied for decades, and still partially remains unknown. Researchers have been coming up with multiple suggestions, however, explaining the phenomenon only under specific conditions, not applicable to all. It was found that a crucial role in maintaining low friction plays interstitial fluid pressurization [7] in cartilage and substantial molecular interaction separating articulated surfaces at boundary interface even at low levels of movement, and their synergic cooperation of both together [8].

Early models primarily considered hydrodynamic fluid-film models, influenced by advances in hydrodynamic lubrication in machine theory. Over the years, various theories, such as electrohydrodynamic and micro-electrohydrodynamic lubrication were proposed, considering the deformability of articular cartilage. Notable findings include the squeeze-film mechanism, an idea about lubricant retention between surfaces, and concepts like boosted lubrication, and weeping theory. These models consider factors like cartilage tissue porosity and interstitial fluid pressure in supporting joint load and lubrication. Lastly, models such as boundary, hydration, biphasic and multimode lubrication were introduced representing each good lubrication property within a specific range of conditions [2, 9].

Boundary friction is largely independent of the underlying substrates and depends mostly on the physicochemical properties of the contacting boundary layers. Unlike fluid-film friction, where viscoelastic performance will depend on the mechanical properties of the substrate, such as permeability and stiffness. Also, it is worth noting that results showing friction independent of sliding velocity indicate predominant boundary lubrication, unlike fluid film where friction velocity depends on viscoelastic losses [1].

Fluid film lubrication

A thin fluid film ensures complete separation between the opposing surfaces during sliding. It is the first likely mechanism that comes into service when fully swelled cartilage is loaded. Recent models adjust prior hydrodynamic theory, to so-called biphasic model, composed of a porous-permeable matrix and water. Lubrication film between articulating surfaces arises when interstitial fluid is squeezed out from the cartilage under deformation [10, 11]. Interstitial fluid pressurization bears most of the contact load, while only a small fraction is passed on to the solid matrix. Athenian et al. [10] indicated that friction for biphasic models can be estimated by following the formula.

$$\mathrm{COF_{eff}} = \mathrm{COF_{eq}}\left[1 - (1-\varphi)\frac{\mathrm{W^p}}{\mathrm{W}}\right]$$

where COF_{eff} is the friction coefficient at the equilibrium state after interstitial fluid load support diminishes, COF_{eq} is the friction coefficient of solid-to-solid contact, φ is the fraction of the contact area of solid phase, W^p is the load support by fluid pressure, and W is total load pressure.

The formula gave a good layout for subsequent numerical models of biphasic lubrication and describing experimental behavior, Figure 2-5, where initially small friction, supported by high fluid support, increases as the fluid support rate slowly fades away. This is an important finding made earlier by Krishnan et al. [7], who revealed a linear correlation between an increase in COF and a reduction of intestinal fluid pressurization after load was applied.

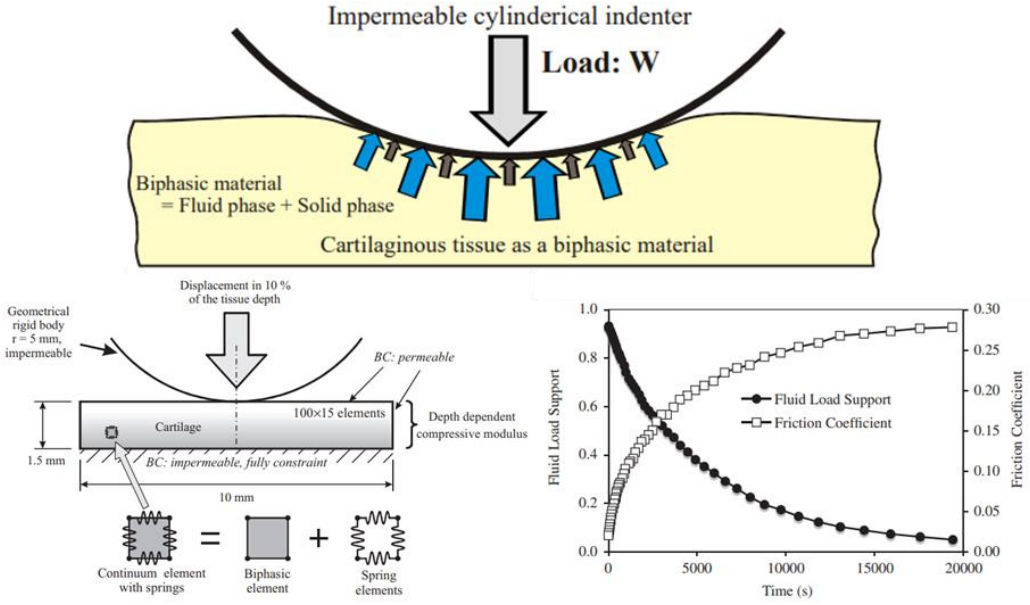

Figure 2-5 a) A biphasic material (blue arrow shows reaction force by interstitial fluid pressure, grey arrow shows reaction force by solid phase), b) Biphasic numerical model proposed by Sakai et al. [12], c) Correlation between fluid load support and COF, from the moment after loading [10].

Sakai et al. [12] introduced a finite element (FE) biphasic model which allowed us to have an inside look at interstitial fluid flow, stress distribution, and deformation in cartilage under different constitutive parameters. This model subsequently served as an inspiration for later studies [13–15], examining the effect of biphasic lubrication of either articular or artificial cartilage.

In the case of reciprocating compression and unloading, as occurs during walking, the biphasic model demonstrates that cartilage can rehydrate its internal fluid and maintain low friction through the periodic outflow and inflow of fluid driven by pressure gradients, which help sustain high interstitial fluid pressure, Figure 2-6 a) [11].

Moore et al. [16] showed that cartilage can recover interstitial fluid even without unloading, which cannot be explained with the biphasic model. They indicated that cartilage could reach partial rehydration of its internal fluid through sliding, creating hydrodynamic pressure forcing fluid inflow, Figure 2-6 b).

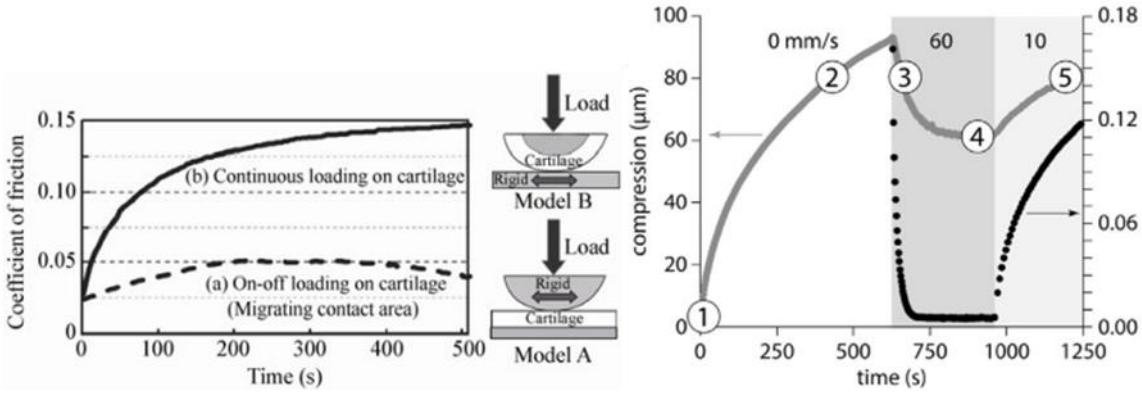

Figure 2-6: a) Friction response on cartilage after on-off loading and continuous loading. [11], b) Tribological rehydration (without unloading loading): (1) initial deformation and maximal fluid load support, (2) internal fluid slowly depletes causing higher solid load support, (3) setting a relative motion causes elastohydrodynamic build-up and fluid film is drawn into the contact surface. (4) dynamic motion balances the fluid outflow = force equilibrium, (5) slower relative motion interrupt the equilibrium state and deformation squeezes the interstitial fluid out [16].

Boundary lubrication

When the fluid flow lubrication declines and high compressive pressure does not allow cartilage to rehydrate and maintain surface separation, a partial or complete molecular contact between the surfaces can be established. To understand how superior lubrication might work under these otherwise severe conditions we need to identify the characteristic structures and molecular composition of boundary layers forming at the superficial layer. It is also important to note that boundary lubrication is largely independent of the material's bulk properties, except in the superficial zone, where the boundary layers are located. This contrasts with fluid flow lubrication, where interstitial fluid pressure is driven by the deformation of the underlying substrate [1, 2].

The main molecules detected to form boundary layers are HA, aggrecans, lubricin, and PLs, either alone or in combination. [2]

HA was previously seen as the molecule responsible for the lubricity of SF. HA itself has been revealed as a poor boundary lubricant, showing better lubrication in combination with other molecules (aggrecan, lubricin, PLs) linked to HA, this is briefly discussed later. However, HA, as a long-liner polymer, can contribute to shear-thinning behavior, maintaining high viscosity at low-shear rates and water-like viscosity at high shear rates. Such behavior may contribute to better wear protection at high contact loads.

Similarly to HA, neither lubricin (PRG4) can sustain low friction at pressures higher than few atmospheres. The precise lubrication mechanism of lubricin has not been fully elucidated yet. It is also believed lubricin has multiple functions, including protection of chondrocytes. [1]

Phospholipids (PLs), each composed of two hydrophobic tails and one hydrophobic head – named as phosphatidylcholines (PCs), can be found in both SF and cartilage. These molecules are believed to play a crucial role in maintaining low friction. Two models of its function have been proposed. One suggests a principle similar boundary layers of surfactants, a mechanism used in machine tribology, where the hydrophobic tails are sticking out and rubbing past each other. Such mechanism showed COF ≈ 0.05 – 0.1 which is much higher than in cartilage and therefore would not appear to be correct. Another one suggests a role in the hydration lubrication mechanism, where hydrophobic headgroups slide past each other. This mechanism reduces friction to values comparable to cartilage (0.001) at low pressures [1, 17].

Additionally, some works also noted that by using PCs bilayers (DPPC), or/and HA, a relatively low friction and higher load can be obtained. [1]

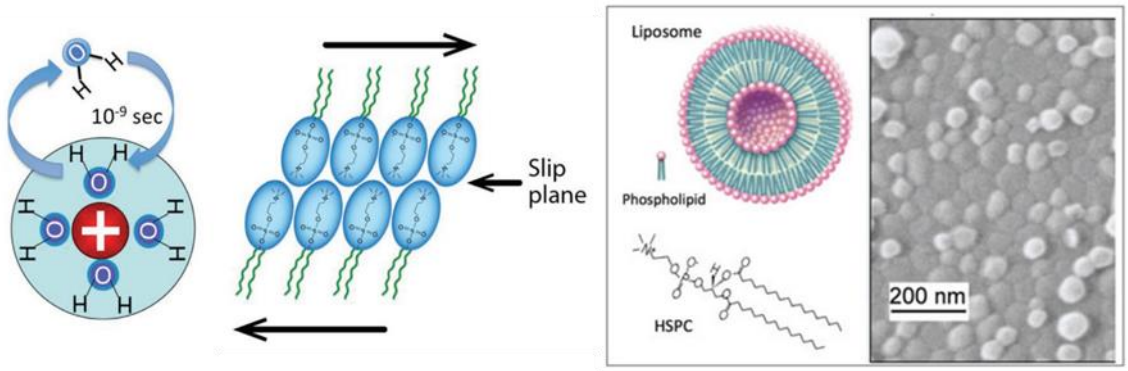

Figure 2-7: a) Left: Hydrated shell composed of hydrated ion surrounded by water dipoles; Right: grouping of PCs layer, where the shear plane is between the headgroups [1], b) A dense layer of liposomes adsorbed on the mica surface. [17]

Hydration lubrication

In 2002, a concept called hydration lubrication was introduced based on surface force balance (SFB) measurements. The mechanism suggests a boundary lubrication process in aqueous media, where hydrated ions trapped between surfaces slide past each other and provide easy shear lubricant supporting large stresses. Hydrated ions (hydration shells), Figure 2-7 a), consisting of ions and closely/strongly attached water dipoles around. Strong bonding to ion provides large load support without water dipole being squeezed out and very fast exchange of bonded dipole for free dipole, providing relaxation and fluidity during shear. [1, 2, 17]

Ikeuchi [18] defined hydration lubrication as “water lubrication of surface layer with hydrophilic polymers fixed to the surface” and indicated the common properties of hydrated surface as follows: As two bodies come into contact, pressure increases in the surface layer, generating a repulsive force between them, with the majority of the applied load being supported by water. During sliding motion, the water molecules experience shear under low stress, while the polymers remain fixed to the surface [8, 18].

In biological lubrication, the heads of PC lipids, acting as hydration shells, were found to be highly hydrated with 15-20 water molecules. This makes PCs possibly a very effective lubricant element. But other components of cartilage matrix and SF (HA, protein, aggrecan, lubricin) are partially hydrophilic/hydrophobic as well and may form hydrated groups, reviewed in detail by Klein et. al. [17], which are likely to contribute to hydrated lubrication [1, 2, 17].

DPPC or liposomes could act as an effective boundary lubricant exhibiting friction down to 10^{-4} at pressure over 200 atm. These values align with the superior lubricity observed in living joints. This was shown in an experiment where liposomes were adsorbed on a mica surface, Figure 2-7 b). The effectiveness of hydrated groups on lubricity, in general, depends on properties such as the nature of the charge (e.g. negatively charged ions are less hydrated, thus less effective) or ion-water binding force, resulting in different load-carrying capabilities. [1, 2, 17]

2.2.4 Effect Of Synovia Constituents

Under severe operating conditions, where the effectiveness of biphasic lubrication is reduced and molecular contact is established, the role of the adsorbed film comes to help with surface lubrication. SF is composed mostly of constituents included in the superficial layer – HA, lubricin, proteins (albumin, γ-globulin, and phospholipids).

The existence of proteins, especially γ-globulin, appears to be essential for the formation and maintenance of the adsorbed layer. γ-globulin is adsorbed at the surface and forms a durable layer protecting the underlying layers from wear. The second important protein is albumin, which forms a layer with weak shear strength. Both proteins, at the appropriate content, form a synergistic layer in which friction and wear are reduced due to forming easy shear layers, Figure 2-8. [19]

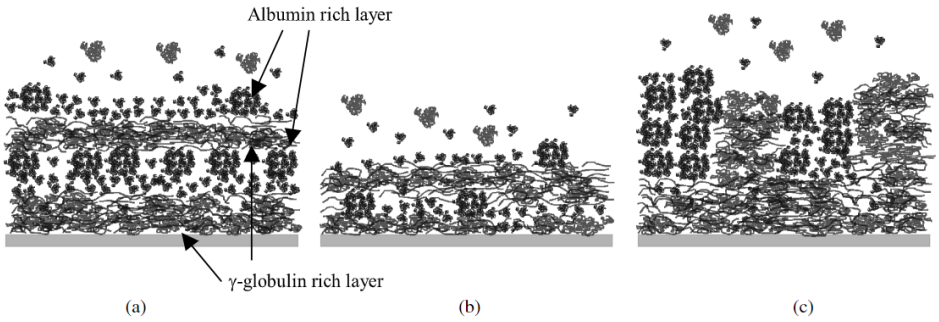

Figure 2-8: Adsorbed albumin and γ-globulin layers on surface. a) Laminated protein film, which resulted in wear reduction. b) Protein film with a little wear reduction. c) A film with incorrect amount of proteins resulting in increase of wear [19]

The origin of the different behavior of the two proteins lies primarily in their structures, which are responsible for their different adsorption properties. γ-globulin is predominantly composed of a β-sheet structure, while albumin is from the α-helix. [20]

Proteins can adsorb on the surface both in frictional motion and in the case of mere immersion. Hyaluronic acid (HA), however, is dominantly adsorbed only during motion. HA forms a gel-like film on the surface, which helps to reduce friction. The adsorption of HA on the friction surface can be increased by interaction with γ-globulin, the two components exhibiting attractive forces, whereas there are repulsive forces between albumin and HA. Since HA has a higher viscosity, it results in faster lubricant film formation when added to the lubricant [21]. PCs are dispersed in the lubricant as liposomes. PCs form multi-laminar layers with low shear resistance, consequently reducing shear resistance but sometimes disrupt layer adhesion [22].

In addition to the function of the individual components of the SF described above, the content and the relative proportion of the individual components are of major importance. For example, too high albumin content may lead to peeling of the film boundary layer [21]. If the phospholipid concentration is too high, the desired distribution of liposomes will not occur, which may result in higher adhesive wear. [22] However, at appropriate concentrations, a significant decrease in friction and wear can occur, as shown in Figure 2-9, showing a comparison of the magnitude of friction when using lubricants with one SF constituent, or their combinations [8].

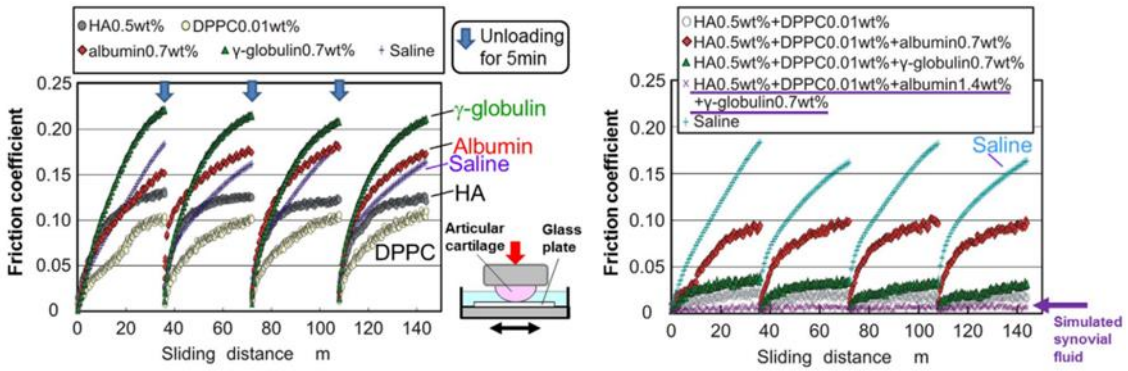

Figure 2-9: a) Influence of single synovia constituent on friction. b) Influence of multiple synovia constituents combined on friction. Results were conducted on the reciprocating friction test [8].

2.2.5 Lubrication Synergy In Cartilage Lubrication

PC lipids have been observed to interact with HA, as indicated by various investigations. Studies using friction force microscopy (FFM) and surface force balance (SFB) proposed that PCs, in combination with HA may end up forming strong boundary layers at the cartilage surface, contributing to friction as low as 10^{-3} even at pressures exceeding 100 atm, which is close to articular joins performance. Those promising results were shown on surfaces ensuring good attachment and deposition of the molecules (e.g. mica), hoping to mimic *in vivo* cartilage behavior under boundary lubrication, Figure 2-10 [1].

As mentioned, HA is a long, linear and flexible molecule. The likely reason why HA may contribute forming a stronger boundary layer is by making multiple contacts with an adsorbing interface, thus enabling some molecules to better adhere and accumulate on the surface. Such connections may occur with components like lubricin, a molecule known to be present both in the superficial zone and attached to the surface, contributing to the formation of a strong interface attachment or making complexes with PC lipids, exposing their hydrated head groups performing low shear friction. Also, linking aggrecan molecules with HA improves boundary lubrication, however, only at a pressure lower than 12 atm, Figure 2-11 [2].

Thus, the assumption that HA helps other SF components, notably PCs to adhere to surfaces, and serve as a building component rather than actively acting in friction reduction makes it quite important.

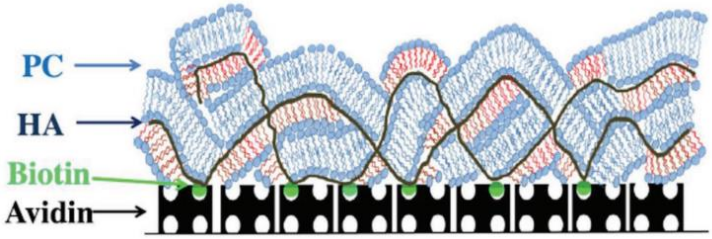

Figure 2-10: Schema of HA/PCs boundary layer attached on mica surface. Good molecular attachment is ensured by avidin-biotin chemistry [1].

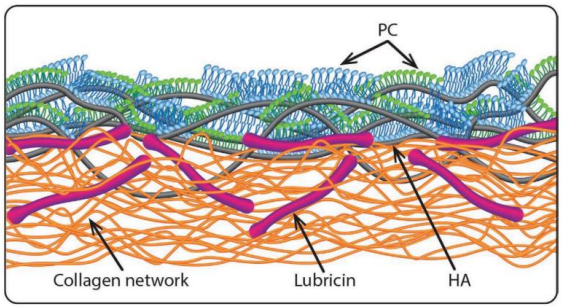

Figure 2-11: Schematic description of the molecular constitution of the superficial layer. HA, present within the superficial zone as well as protruding outside allows components such as PCs to adhere better onto the surface [1].

Under more severe operation conditions, such as after long-standing or slow movement in heavy loading, the effectiveness of fluid load support diminishes, and some local direct contacts occur between rubbing cartilage surfaces, the role of boundary lubrication mechanisms comes to play a role [8].

The adsorbed film is expected to become effective as the first solid-like barrier to maintain low friction and protect the surface. This adsorbed layer consists of synovia constituents described above. The surface structure underlaying the adsorbed film is called gel-line layer consisting of primarily of non-collagenous proteoglycan layer, acting as a low shearing layer, Figure 2-12. The gel-like layer works as a fail-safe, a protective barrier. If collagenous tissue comes into contact with an opposing surface, it is accompanied by a friction increase. If the surface of this gel layer is damaged, the chondrocytes are expected to produce and supply proteoglycan to this layer to repair. Other molecules, such as HA, seem to be supplied by SF [8].

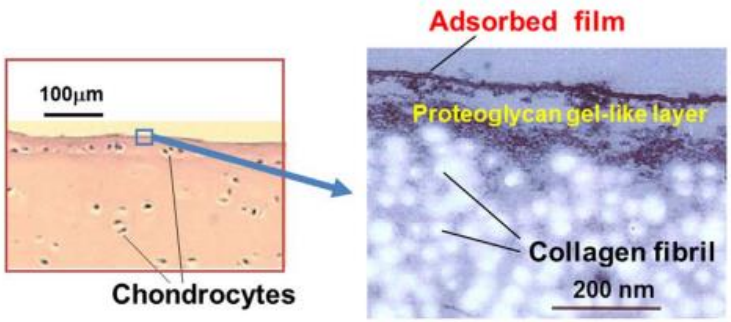

Figure 2-12: a) Cross-section of articular cartilage surface. b) An image of collagen/gel-like layer interface [8].

In natural synovial joints, many lubrication regimes become effective depending on the severity of operating conditions. Overall lubrication performance is then a result of the adaptive multimode mechanism, depicted in Figure 2-13 b), showing how individual regimes might act. The effectiveness of each lubrication regime is controlled by the operating parameters, well-known from the Stribeck curve, Figure 2-13 a) [8]:

$$\frac{\text{lubrication viscosity} \times \text{sliding speed}}{\text{load}}$$

Murakami et al. [8] summed up the expected sequence of each regime, see Figure 2-13. It is indicated that the hydration lubrication might be present over a wide range of boundary lubrication and overlap with other lubrication regimes. An important conclusion is that various regimes can act simultaneously/synergistically and ensure a robust boundary corresponding to changes in operating conditions. [8]

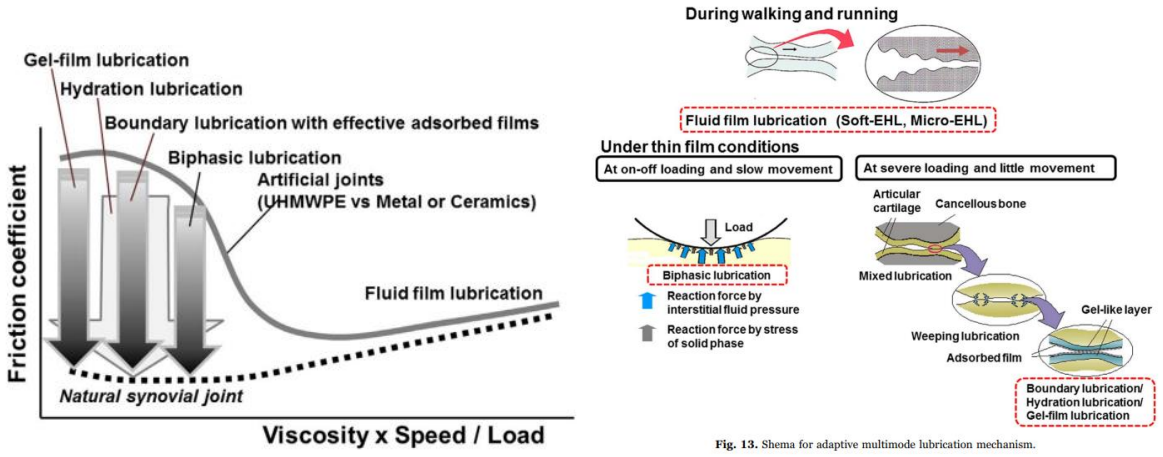

Figure 2-13: a) Stribeck curve for adaptive multimode lubrication, b) Schema of adaptive multimode lubrication mechanism.

2.3 Hydrogel development

A material that displays a basic property similar to articular cartilage is a biphasic material consisting of water and a solid phase called hydrogel. Both articular cartilage and hydrogel could retain interstitial water within its matrix and release it under deformation. This is a very fundamental condition of superior cartilage lubricity; however, it is not sufficient. Therefore, it is crucial to develop hydrogel following current knowledge of cartilage lubrication, such as its structure corresponding with fluid flow and superficial adsorption performance of SF as well as SF composition effects.

Articular cartilage is mainly composed of cross-linked collagen fibrils, proteoglycan, and aggrecan macromolecules. Similarly, hydrogel in a composition of cross-linked hydrophilic polymer chains solved in water. Friction force cannot be described with a standard Stribeck curve like for solid sliding surfaces, as chemical structure and its response to friction conditions are different. Most importantly, friction in hydrogel can reach friction as low as 10^{-4} under favorable conditions [23].

An important step in understanding gels has been made by Gong et al. [23, 24]. In those studies, a repulsion-adsorption friction model was proposed, introducing frictional stress dependence on sliding velocity, see Figure 2-14 a).

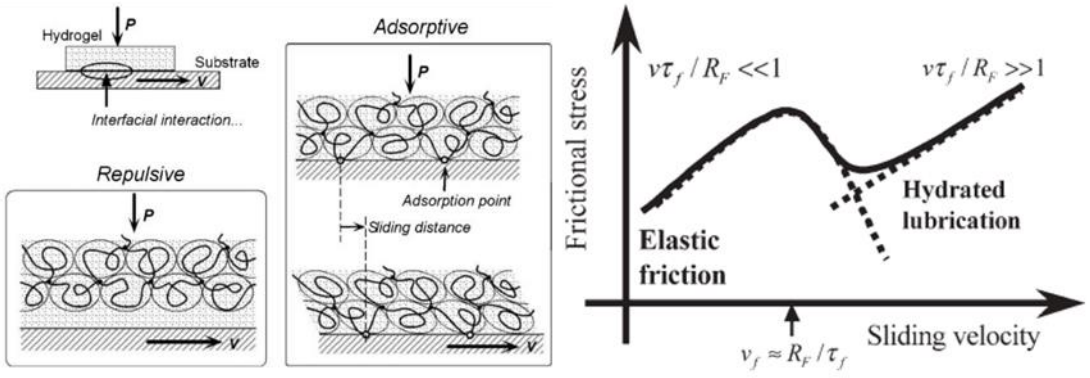

Figure 2-14: a) Schematic illustration of the repulsion-adsorption model for the friction of gel on a solid substrate. b) “Stribeck curve” adapted for repulsion-adsorption model considering behavior of gel materials [23].

The authors outlined two hydrogel-to-substrate responses: repulsive and attractive. In the repulsive scenario, friction arises from the hydrated polymer chains at the interface, and it should be proportional to the sliding velocity, similar to the behavior observed in HD lubrication on the Stribeck curve. The attractive case includes two mechanisms; firstly, for a low speed, see Figure 2-14 b), elastic friction appears as a result of adsorbing polymer chains. Those polymer chains are stretching up with higher sliding velocity, which corresponds with an increase of friction force up until "a peak" where the velocity is too high that polymer chains do not have enough time to form a bonding with opposing surface, lubrication than switches to hydrated lubrication. Hydrated lubrication leads to lower friction than elastic friction, as there is only a fluid viscosity, which increases the friction. Gels typically experience attractive behavior, on a smooth glass, is poly(2-acrylamido-2-methylpropanesulfonic acid (PAMPS) or PVA. Repulsive behavior can be seen at PNaAMPS (PAMPS with sodium salt).

A hydrogel that is being investigated extensively and is believed to have great potential to serve as artificial cartilage is PVA, due to its great biocompatibility, chemical stability, and ability to be tailored [25].

The first studies related to PVA hydrogel came out in the 1990's and laid out an important finding in biocompatibility and mechanical properties. These findings were then compared to UHMWPE which is commonly used in joint replacements. PVA was observed to have a superior shock-absorbency but challenging attachment to the underlying bone. Water content was observed to be ideal around the content of natural cartilage (80 %) for maintaining low friction, however, the strength with this much water is somewhat low, on the contrary, for lower water content, the strength increases but lubrication performance is getting worse. In any case, low wear resistance prevails to be the main issue [26–28].

2.3.1 Materials of PVA

PVA hydrogel hugely depends on cross-linking temperature conditions affecting microstructure and overall performance. This allows us to tailor material with various structures and properties.

The preparation of PVA hydrogel involves the dissolution of PVA powder in water and stirring to gain a homogenous solution. This is followed by the cross-linking process discussed further below. Besides cross-linking method, factors such as polymer molecular weight, polymerization degree, and water concentration in the initial solution significantly affect the resultant behavior.

The first method used already in 1990's in research studies is freeze-thawing (FT), which involves repeated freezing at -20 °C and thawing at 4 °C for several times to ensure maximal cross-liking. This method creates a soft, opaque while-looking matter. Another method used in research is cast-drying (CD), the PVA solution is left in at temperature and humidity-controlled environment for cross-linking [29]. This results in transparent gel with higher stiffness.

These two strategies result in different mechanical responses. FT presents material with non-homogenous and porous structure and amorphous zones. This is accompanied by high permeability and high-water content of ~85 %. On the contrary, CD displays a rather homogenous structure and less porous structure, with permeability about two orders of magnitude lower (at a similar level to natural cartilage) [13]. As we can see on AFM images in Figure 2-15, the topography of PVA varies a lot in the cross-linking process. This provides CD gel with maintaining high interstitial fluid pressure for a longer period of time, as the water flows out more slowly. Nevertheless, FT gel enhances the adsorbed film formation and provides superior lubrication properties under SF due to its rougher and porous structure. This implicates decrease in friction and surface protection. [13, 25, 30] However, wear resistance is considered the main prevailing issue despite the relatively low friction (~0.005-0.01) achieved either by the CD method or by FT under SF lubrication, Figure 2-16 b).

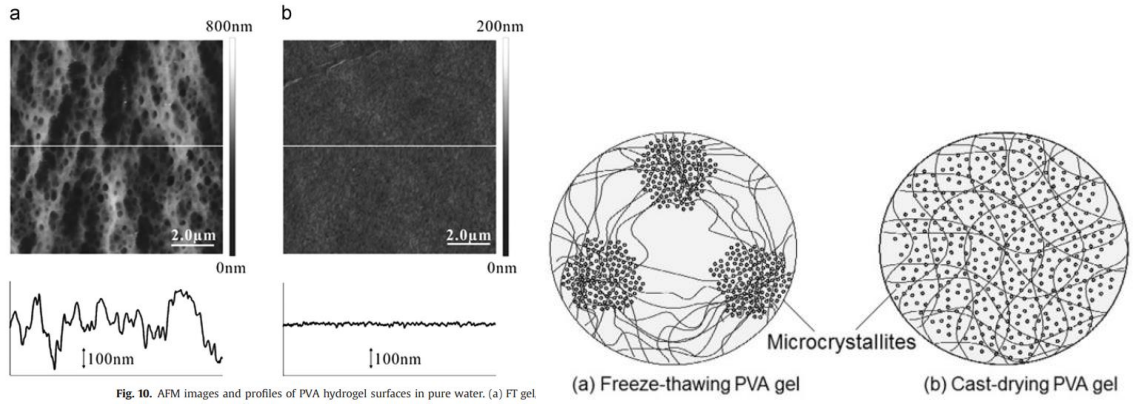

Fig. 10. AFM images and profiles of PVA hydrogel surfaces in pure water. (a) FT gel.

Figure 2-15: Left) AFM images and roughness of PVA hydrogel surfaces in pure water a) FT, b) CD. Right) Illustration of a) non-homogeneous structure of FT gel, b) homogeneous structure of CD gel. [13, 15]

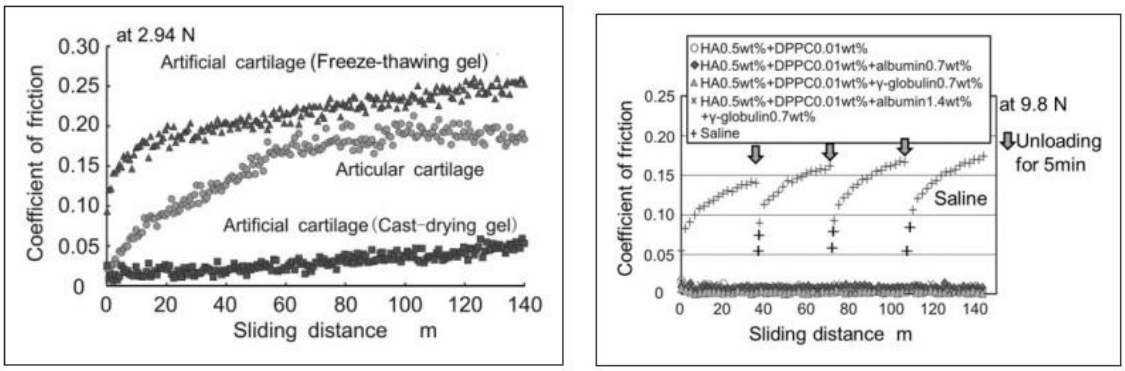

Figure 2-16: a) Friction performance of various hydrogels and separated articular cartilage against glass plate in saline. b) Effect of combination of synovia constituents on frictional behavior. FT hydrogel against the glass plate. [13]

Subsequently, a laminar (LM) FT on CD gel developed first by [31] has been introduced. This LM gel was observed by Yarimitsu et al. [30, 32] to have extremely low friction (0.003) and low wear. An important factor here was the drying process. Under accurate drying temperature and humidity control, a thin layer of protruded molecular chains with the optimum extent of cross-linking might be formed and have a hydration lubrication-like effect.

Despite these promising indicators, introduced hydrogels show good performance only at mild conditions with contact pressure lower than 0.5 MPa, which is far below expected conditions in clinical use.

Yarimitsu and Sawae [33] introduced cross-linked composite hydrogel (CP) combining FT process as well as high and low-temperature drying process. The CP's microcrystalline structure is both partially homogeneous and heterogeneous. An important role here is the high-temperature drying, which promotes higher wear resistance while exhibiting low friction of 0.01 via microsatellite growth and strengthening the crosslinking network. Furthermore, it was investigated that with longer high-temperature drying time, the structure loses its water absorption as the microcrystalline grows larger. This results in high elastic modulus. Short, high temperature drying supported heterogeneous structures with higher permeability. The authors noted that in order to maintain biphasic lubrication it is important that the internal fluid is not squeezed out from the matrix easily. Therefore, neither short drying (resembling FT structure) nor long drying where gel becomes too brittle, are ideal. An ideal match of desired properties was found at gels CP06 and CP12, showing minimal wear patterns and friction (0.01) while reciprocating friction test at 10 N loading.

Hydrogel structural properties change over time, as Murakami et al. [34] found out on aged PVA FT gel, submerged for 6 years in the physiological solution that its permeability decreased. This effectively impacts the biphasic lubrication of FT gel, as the water is pushed out of the matrix slowly, and interstitial fluid pressurization fades more gradually. However, ageing is accompanied by gradual hardening, which might prevent some further applications.

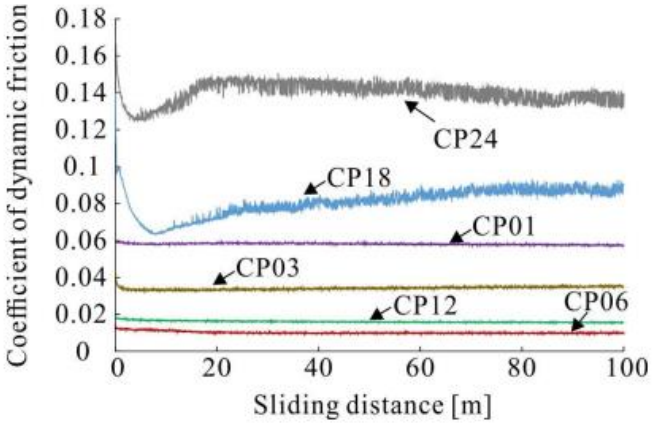

Figure 2-17: Different PVA CP gels displaying different COF. Reciprocating friction test. [33]

2.3.2 Cartilage-like hydrogel structure

PVA hydrogel showed it has a capability to achieve COF < 0.01 under a favorable condition. Nevertheles, such a level is still about a one-order magnitude higher than expected at articular cartilage. Another way to enhance the lubrication mechanism and possibly allow higher load pressure is using a reinforcing structure supporting a water-carrying matrix.

We already know that articular cartilage consists of collagen fibrils oriented differently in-depth, superficial layer, and transition zone. The highest collagen content is represented in the upper layer and decreases with depth, unlike proteoglycan bonding with water, whose highest concentration is at the depth. Compressive modulus is at articular cartilage, increasing with depth as well. We also know that the mechanical properties of cartilage are anisotropic, and the tangential stiffness is higher than in the compressive direction, forcing the interstitial fluid to flow toward the surface. Finally, the superficial zone interwoven with a dense collagen network is very thin but resilient.

Sakai et al. [35] tested horizontal fiber reinforcement of FT hydrogel, and proposed a fiber-layer arrangement with one and two layers. Results verified both experimentally and numerically showed that the friction reduction for a single-layer, placed into the superficial zone, was about 50 % and 20 % for double-layer compared to FT gel without any fibers.

Shirazi et al. [36] and Sakai el. al [37] investigated the role of vertical fibrils network. Shirazi found that deep vertical fibrils play an important role in the transient period after loading. During this period a matrix stiffness is increased and preserves the subchondral zone from overloading. This role diminishes over time and at slower rates. Sakai tested experimentally the frictional response of vertical fibrils on FT gel. Fibrils went throughout the entire depth with only a thin casted FT superficial layer to achieve a smooth surface. The experiments showed that the fibber model reduced friction.

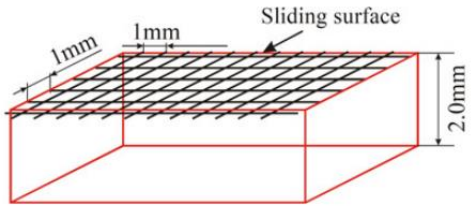

Figure 2-18: Horizontal fiber-reinforcement of FT hydrogel. [35]

Regarding the superficial layer, Fujie et al. [14] verified the importance of low tangential permeability on frictional property. In the numerical model, the tangential permeability was set to 1/10 of compressive direction up to a depth of 0.1 mm. Friction decrease was visible throughout the entire testing, but the most significant decrease was at the start-up zone. In another study, Fujie et al. [38] tested the effect of collagen-induced residual stress frictional performance. Results showed that residual stress induced rehydration due to negative pressure created behind the contact area, thus supporting biphasic lubrication. Also, they pointed out that a higher elastic modulus of fibrils influences friction performance negatively, mostly due to small contact deformation. The optimal residual stress was estimated to be 1 % by using the numerical model proposed by Sakai.

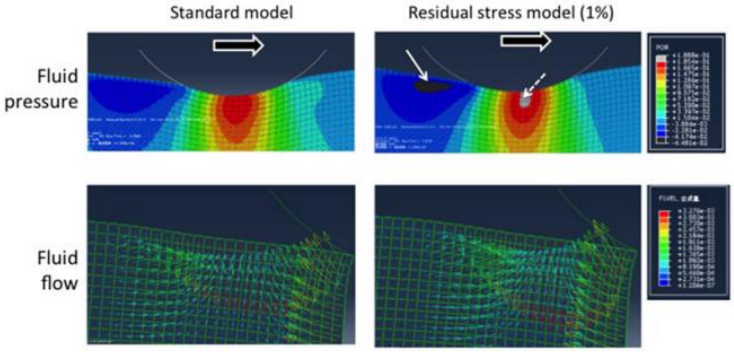

Figure 2-19: Numerical analysis showing fluid pressure and fluid flow distribution at sliding speed of 1 mm/s. [38]

Some studies were not only limited to pure PVA gel and introduced double network (DN) hydrogels. Ma et al. [39] tested a blend of hydrogels PVA and poly (vinyl pyrrolidone) (PVP) prepared by repeated FT method. PVP is another hydrogel commonly used in some other biomedical applications. Results showed that PVA/PVP hydrogel exhibited better mechanical properties due to stronger inter-chain hydrogen bonding than pure PVA and viscoelastic behavior very similar to articular cartilage. Lubrication performance was improved at any tested content of PVP. When the PVP content was of 1 % PVP matrix strength was greatly improved, whereas at 15 % PVP friction was the lowest, accompanied by a softer matrix than pure PVA.

Another study from Arakaki et al. [40] investigated PAMPS/PDMAAm DN hydrogel in both *in vivo* and *ex vivo* on rabbit knee. Specimens surgically implanted in the knee of a living rabbit showed only a mild irregularity in counter articular cartilage after 12 weeks. The ex vivo frictional test showed lower friction DN gel-to-cartilage contact than for cartilage-to-cartilage contact. The authors, however, point out contact pressure was unknown because of the difficulty of determining the real-time contact area. DN gel had an ultimate compressive stress of 3.1 MPa, despite the 94 % water content. For comparison, articular cartilage is exposed to 3-5 MPa during walking in the hip and knee joint

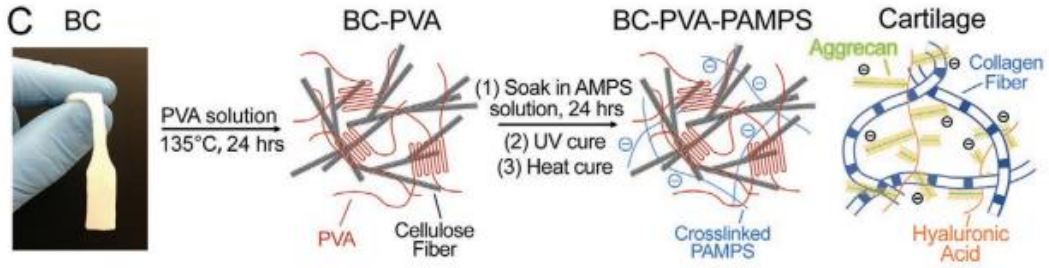

Figure 2-20: Illustration of BC-PVA-PAMPS hydrogel fabrication process. [41]

In a recent study, Yang et al. [41] reported potentially revolutionary double network hydrogel PVA-PAMPS hydrogel infiltrated with bacterial cellulose (BC) nanofiber. This hydrogel exhibits the same strength as articular cartilage – 44 times more wear resistance with 45 % lower friction than at cartilage and equivalent fatigue strength. Authors discuss this outstanding performance with used additives that provided artificial cartilage with desired properties: BC gave matrix collagen-like strength, PVA viscoelastic properties, and PAMPS had a similar role to aggrecan. Additionally, all these materials are biocompatible.

In a subsequent study, Zhao et al. [42] introduced BC-PVA hydrogel, which possesses a mechanical strength of 1.8 times higher than articular cartilage. This is attributed to greater crystallization provided by the FT method and annealing process, ensuring lower water content. Wear resistance was observed to be even greater than in articular cartilage exhibiting the same friction after one million cycles. Additionally, the study reported the first hydrogel-to-metal attachment exceeding the shear strength of a cartilage to bone, by using adhesive, a clamp, and freeze-dried BC to the metal

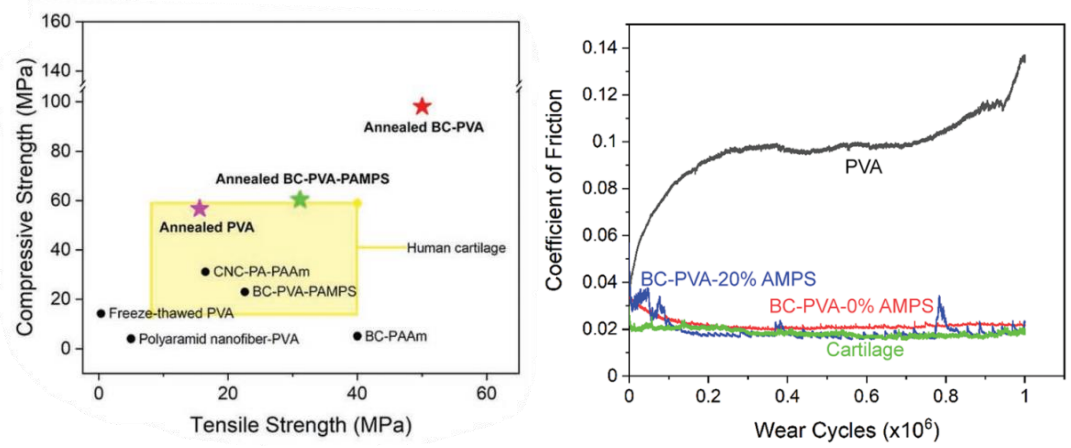

Figure 2-21: a) ,b) [41]

2.3.3 Low-shear bio-inspired superficial layer

Creating a superior lubricating performance requires hydrogel to have a high-level surface hydration. Hydrogels having a decent hydration level usually lack load-bearing capacity, leading to severe deformation. In contrast, proposed high-strength hydrogels reinforced by the DN network experience low hydration levels, which negatively influences COF. Several recent studies introduced a layered hydrogel consisting of high-strength bulk hydrogel with a thin hydrated hydrogel layer mimicking the cartilage superficial surface.

Hydrogel surface structure depends on the material it was molded against – resulting in either more compliant or stiffer material. Using polyacryalmide hydrogels against polystyrene mold Johnson and Dunn have observed a gradient-density surface with a low dense brushy layer capable of quick re-uptake when out of contact [43]. Rong et al. [44] introduced a bilayer material consisting of hydrophobic polymer brushes grafted into a stiff hydrogel substrate. Such synergy with aqueous lubrication allowed great long-term tribological performance under 10 MPa contact pressure. Similarly, Yu et al. [45] introduced low-friction "hydrogel skin" capable of being applied on arbitrary polymers with arbitrary surfaces, however their research focused primarily on other medical applications. Wie et al. [46] found a very promising tribological behavior when depositing elastic hydrogel and soft polymer brush layer onto hard PEEK material, seeing no obvious wear after long-lasting friction test. Lastly, a scallion leaf-inspired layered hydrogel was proposed by Liu et al. [47]. Experiments revealed ultra-low friction (0.006) under up to 2.4 MPa contact pressure.

All the experiments showing a superior lubricating behavior have been shown only on a microscopic scale, not representing the actual conformal cartilage-like contact or movement.

2.4 Summary of key findings

2.4.1 Articular cartilage

Articular cartilages we pose in our bodies can be thought of as superior bearing with great tribological performance. Up until this date, no satisfactory mechanism of its function has been replicated on a macroscale as the explanation lies in complex synergic cooperation of multiple lubricating mechanisms [10, 48, 49].

Natural cartilage consists dominantly of water (≈ 70 %), a well-structured matrix of collagenous fibrils, and proteoglycan molecules [50]. From a tribological point of view, this helps the cartilage to dump sudden impacts and water release under deformation – acting a bit of as a hydrostatic bearing. The mechanism behavior is called biphasic lubrication [51]. After the water within the cartilage is depleted (due to an inactivity and constant load) close contact molecular interaction becomes a major factor to keep low friction. The superficial cartilage layer contains sophisticated molecular structures likely responsible for its superior lubrication performance [48, 52]. Recent publications point out that the main influential molecule, among others, is phospholipid, promoting the creation of easy shear and highly resilient layers. Such a mechanism called hydration lubrication is theoretically capable of friction even lower than 10^{-4} [17, 48].

Most of the proposed lubricating mechanisms of articular cartilage proposed to date work efficiently within a limited range of conditions and are isolated from the others. Whereas real lubrication is believed to work synergically with various overlapping mechanisms working together to maintain not only extremely low friction but also high wear and load resistance [8].

2.4.2 Hydrogel material

Articular cartilage can be thought of as a two-phase state tissue dominantly based on water. In analogy with natural cartilage, hydrogel material consists dominantly of water and polymer structure, making it a promising candidate for inheriting some key lubricating mechanisms.

The tribology of hydrogel materials cannot be viewed in the same way as solid materials. Due to their higher compliance and high water content (60 - 80 %), the standard Stribeck curve describing the frictional behavior of the solids is not accurate and is supplemented by the repulsion-adsorption friction model [24, 53]. Like in articular cartilage, biphasic lubrication is well described in hydrogels, making it an effective cartilage substitute for on-off loading (e.g. walking), allowing full film separation [10, 16]. In contrast, hydrogel performance at boundary lubrication is poor, exhibiting significant surface damage. The likely reason is that synovial constituents do not form such an effective protective layer as they do in articular cartilage – making this a substantial issue to be examined [19, 21, 49]. PVA hydrogel is a promising material for synthetic cartilage, as it is biocompatible and chemically stable, and its properties can be easily tailored to scientific research. Hydrogel's basic mechanical properties (e.g. PVA) are considerably lower than in the case of natural cartilage. Recent research has shown that it can be effectively reinforced by crosslinking cellulose fibers mimicking structures of articular cartilage [41, 42].

The main objective of hydrogel research is to effectively transfer, and mimic properties found in articular cartilage. This seems to be a long-run issue requiring a comprehensive understanding of *in-vivo* cartilage functioning. The current research activities are thus divided into the description of effective hydrogel reinforcement capable of withstanding cartilage-level stresses and the recreation of an effective boundary layer protecting the surface from damage.

2.5 Knowledge gap and research opportunity

The development of cartilage-like hydrogel material is based on research on the lubricating performance (superficial layer) and effective reinforcement of hydrogel matrix (bulk properties) using mostly either microscale evaluation (e.g. surface force balance) [17] or conventional reciprocating tests [22]. Tribological experiments which have been performed in this regard have focused on either one of those fields (e.g. reaching the lowest friction possible, or the highest wear resistance), where the lubrication regime was mostly mixed or full-film, imitating walking conditions. An understanding of how those two factors might be connected to form the desired outcome is rather missing. While it is currently believed that comprehending boundary lubrication is the key to developing an efficient and long-term working cartilage replacement, only a few studies have focused on this topic. It is known that SF constituents firmly adhere to cartilage surface, forming a protective layer, such features have been observed restrictively on hydrogel materials, giving mixed results.

Thus, clarification of solid-solid interaction as well as stiffness evaluation might bring a new insight into hydrogel's lubricating capabilities and shed light on a deficit of SF protective layer.

3 PROBLEM ANALYSIS AND AIM OF THE WORK

3.1 Problem analysis and aim of the work

Despite the superior performance of articular cartilage over a human lifetime. A potential issue disabling its function is something human society deals with on a common basis. The present cartilage replacements clinically used suffer from excessive wear and their lifespan is thus limited. Creation of a cartilage-like material and mimicking its lubrication capable of overcoming the obstacles issued in the chapters above, outlined in Figure 3-1, humankind would have a powerful tool to not only help millions of people to move again but also have a superior lubricating mechanism capable of reduction of energy loss in overall machine industry.

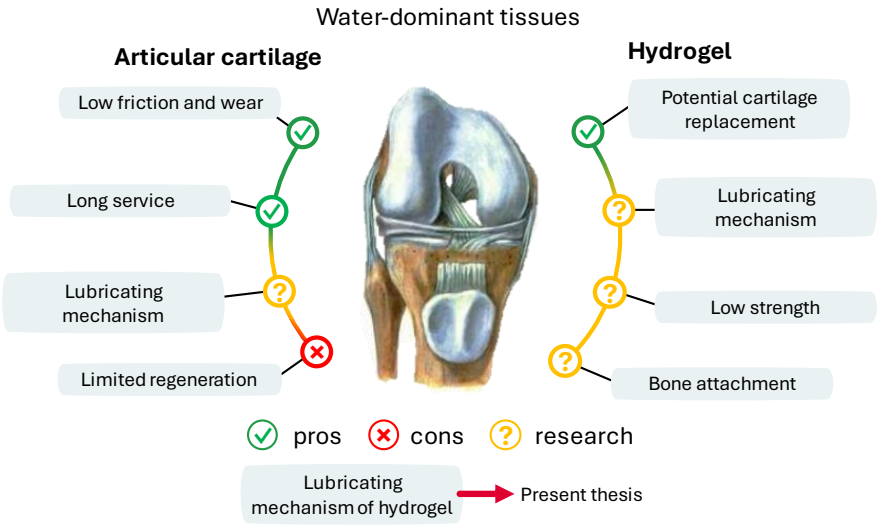

Figure 3-1: An illustrative description of problem analysis. Green color: long-term achievement, Yellow color: issues a need to be overcome, Red color: Issues that cannot be prevented.

The scope of this thesis concerns the lubricating mechanism issue outlined in Figure 3-1. The research done on this topic indicates the three main fields that the focus shall be paid on a broader scope, see Figure 3-2. The main focus of this work is the tribological assessment of the influence of different hydrogel stiffness and the elucidation of the boundary lubricating mechanism. The need for such research lays in a consequence of an imitation of cartilage properties (Figure 3-2), in which the material stiffness is influenced, and broader the knowledge of the elastic boundary friction while lubricating insufficiency. The influence of SF constituents is due to its complexity simplified to only a protein constituent. The work is further divided into two separate parts. The 1st experimental part aims to assess the hydrogel material at boundary lubrication. The 2nd part extracted the two best-performing PVA materials from the 1st part and compared them with poly(2-hydroxyethyl methacrylate) (pHEMA) hydrogels on the reciprocating test.

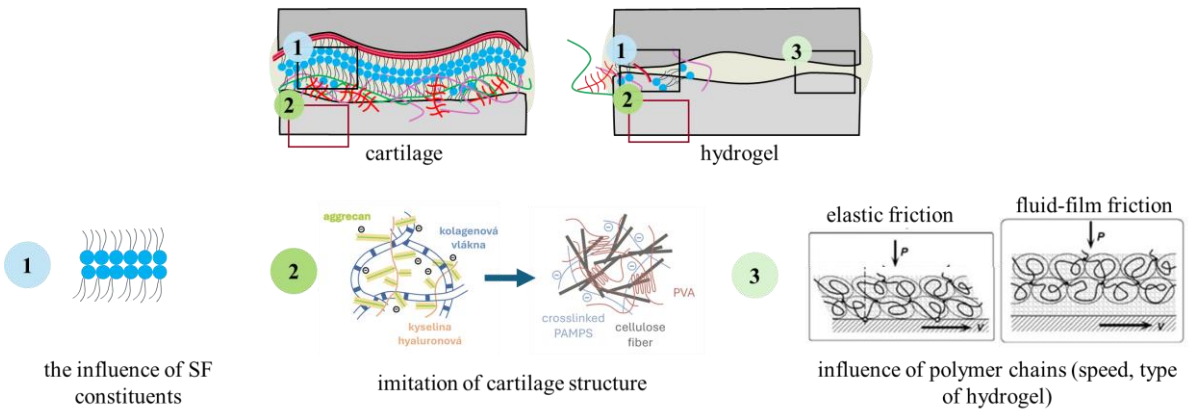

Figure 3-2: Conclusion of cartilage-like material research. Topics 1-2 are interlined with cartilage research, topic 3 seeks a unique hydrogel property.

3.2 Research questions and hypotheses

Based on the conclusions of conducted research a general question of "*How does boundary lubrication of hydrogel look like?*" was raised. Four questions and hypotheses were given to identify measurable objectives and results. The first three Q&Hs come from the 1st experimental part. The 4th Q&H comes from the 2nd experimental part.

1st Question: How do different PVA hydrogel stiffnesses affect the amount of wear?

1st Hypothesis: The compliant hydrogel resists wear better due to better contact conformability. Uncross-linked PVA chains on the surface serve as a wear-reducing barrier.

Explanation: Higher-stiffness PVA hydrogels, with lower permeability, support sustained biphasic lubrication but may perform unsatisfactorily in boundary lubrication due to limited conformal contact and rehydration. Conversely, compliant (soft) PVA hydrogels with better conformal contact and enhanced polymer chain adhesion can mitigate wear through reduced ploughing friction, instead of relying on elastic stretching of polymer chains. The softer hydrogels' microcrystalline structure allows for increased adhesion, promoting energy dissipation through elasticity rather than surface scratches.

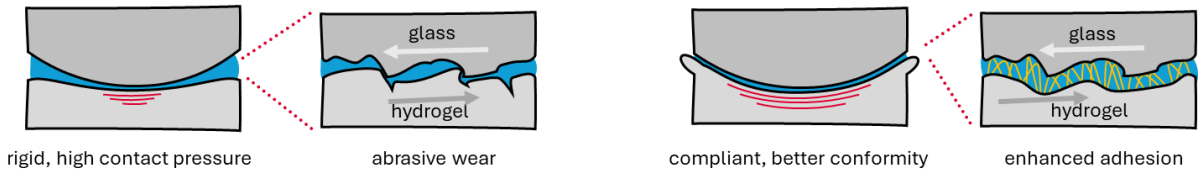

Figure 3-3: An Illustration of the 1st hypothesis.

2nd Question: How does toughness affect the formation of a protective protein layer?

2nd Hypothesis: The boundary protein layer adsorbs better onto a tough hydrogel.

Explanation: The protective boundary layer (easy shear and wear resistance) formed onto the cartilage surface cannot be easily mimicked at hydrogel material - the incorporated SF molecules form other agglomerates than desired, and the resultant layer is unstable. Different stiffness might be partially responsible for imperfect adsorption of a lubricating layer.

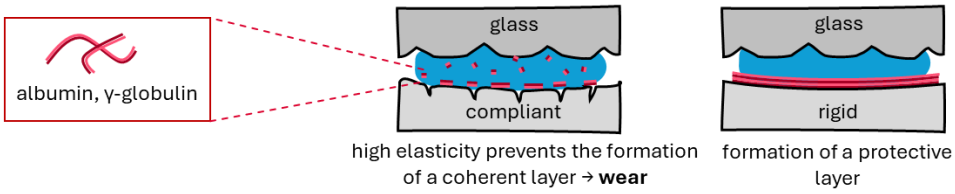

Figure 3-4: An Illustration of the 2nd hypothesis.

3rd Question: What kind of lubricating mechanism is responsible for excessive wear of hydrogels?

3rd Hypothesis: The transitioning zone (between elastic and hydration lubrication) plays a crucial role in contributing to wear.

Explanation: Based on the knowledge of the repulsion-adsorption model introduced by Gong et al. [23] it is now known that the frictional force of PVA hydrogels against solid glass substrate is dominantly adhesive, having its origin in the elastic deformation of the polymer chains adsorbed to the substrate. By pre-experimental loading of PVA hydrogel (to diminish the internal fluid contribution to lubrication) and subsequent measurement of frictional-speed dependence, we could replicate the proposed lubrication behavior and further evaluate our observations with a focus on wear.

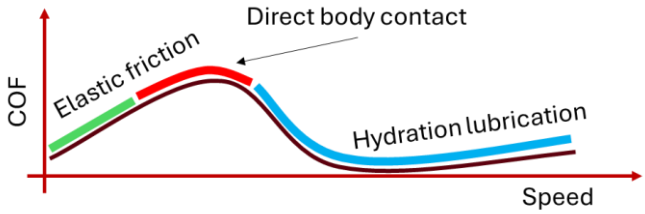

Figure 3-5: An Illustration of the 3rd hypothesis.

4th Question: Which of the two PVA hydrogels (LM, CP06) will have less wear in the presence of biphasic lubrication?

4th Hypothesis: CP06 will better resist wear due to the more sophisticated cross-linking of the polymer chains. A smaller cross-linking density of LM will not affect the predicted low COF.

Explanation: Two low-friction PVA hydrogels were tested for performance comparison. Due to the multiple-stage cross-linking of CP06, the structure obtains both stiffness and hydration-charged surface needed for long-term wear resistivity. PVA LM's upper layer consists of a single cross-linking stage at low temperatures, creating a well-hydrated surface but stiffness insufficiency.

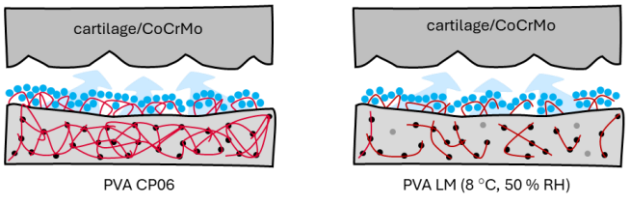

Figure 3-6: An Illustration of the 4th hypothesis. Note: PVA LM has only the upper CD layer illustrated.

4 MATERIALS AND METHODS

4.1 Work layout

The thesis has been divided into two separate parts. 1st part deals with boundary lubrication of PVA hydrogel samples – in which five PVA samples with different stiffness were manufactured and tested. The 2nd part involves a comparison of different hydrogel materials (PVA and pHEMA) – where two PVA samples (performing the best in the 1st part) were selected for comparison with best performing pHEMA samples (based on the parallelly ongoing research carried out at BUT institutions). As this thesis strictly focused on PVA material, experiments with pHEMA samples were conducted simultaneously (same experimental conditions) as part of Bc. Jan Gregora's master thesis, however, their differences were discussed.

Each part involves different devices used in the experiments. The 1st part was conducted during the author's internship at Kyushu University in 2023. The 2nd one was performed at Brno University of Technology (BUT) in 2025.

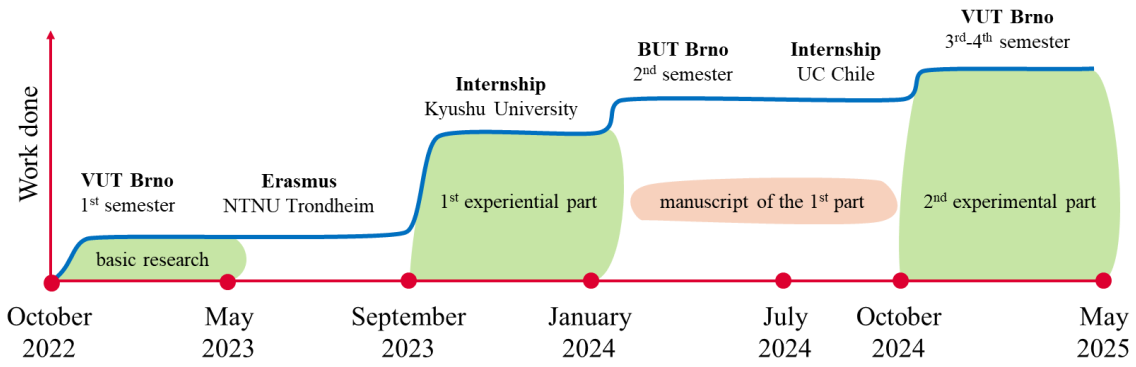

Figure 4-1: Work layout throughout the master's studies.

4.2 Methodology

This thesis is classified as relational research work as its ambition is to bring a new perspective to boundary lubrication of PVA hydrogel materials as well as describe the effect of the material properties (e.g. stiffness, adhesion) on wear resistance and stability of the lubricating layer.

To verify the hypothesis introduced in the previous chapter, several PVA hydrogels with different manufacturing processes were made and subsequently examined on a rheometer for their tribological performance and viscoelastic properties. Best-performing hydrogels were further evaluated on reciprocating tests and compared with pHEMA hydrogel. The main parts of this chapter are illustrated in the Figure 4-2.

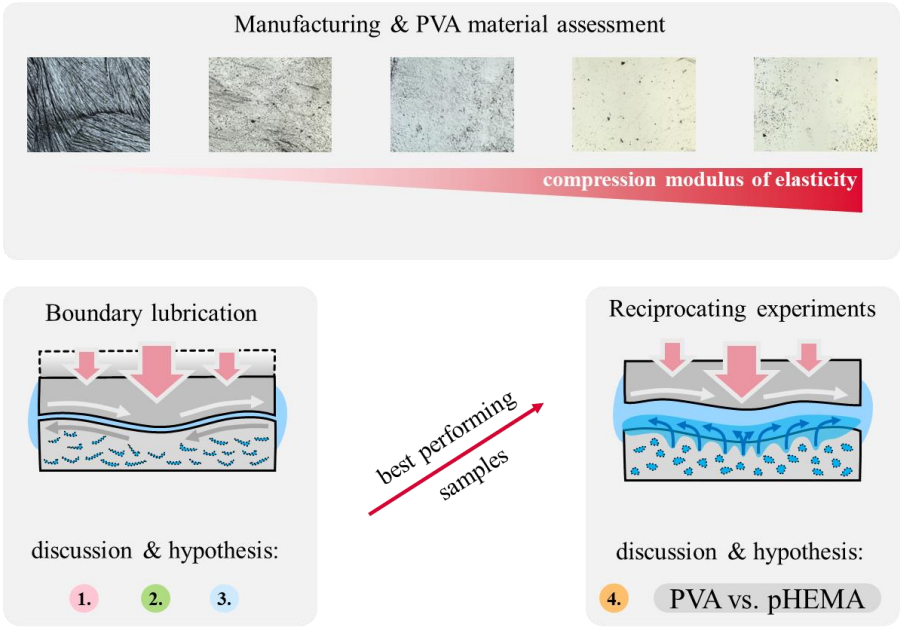

Figure 4-2: An illustration of material and experimental methods.

4.3 Materials

Materials and manufacturing processes listed in this chapter were learned and applied in the 1st experimental part (Kyushu University, 2023). Best-performing materials (PVA CP06, PVA LM) were subsequently manufactured using the equivalent conditions and recipe for the 2nd experimental part, conducted at Brno University of Technology.

4.3.1 Preparation of PVA hydrogel

For the frictional tests conducted on the rheometer, five types of PVA gels with identical chemical composition were prepared. Variations in overall physical properties (stiffness, porosity, microcrystalline structure) were driven by different climatic conditions controlled in a heat-controlled chamber (SH-662, Espec, Osaka, Japan).

Laboratory equipment needed:

Two glass bottles, two glass jars, a magnetic stirring device with embedded heating, two magnetic stirring bars, and four laboratory slides, distilled water (optional: thermal probe, aluminum foil, laboratory spoon).

1. Two portions of 22.5 g of PVA powder and two portions of 127.5 g of distilled water were prepared. (Note: PVA specifications: polymerization degree: 1700, saponification degree: 98-99 mol%, Kuraray Co., Ltd.)
2. The weighted portions of distilled water were poured into the two glass bottles and put to stir (ca. 500 rpm).
3. While stirring, a weighed PVA power is slowly poured into the distilled water. Slow pouring prevents the creation of an undesired powder agglomerate. After powder pouring is completed, each of the two solutions contains 22.5 g of PVA + 127.5 g of distilled water (= 150 g). The bottles are then capped and the solution is left to stir for at least 10 minutes to homogenize.
4. Meanwhile, two jars were prepared (inner diameter must be enough to accommodate a glass bottle + ca. 1 cm; height was equal to or slightly bigger than a glass bottle). Four lab slides were placed on the bottom (by two) of a jar – to prevent overheating of PVA later on.
5. After homogenizing the stirring of PVA, glass bottles were placed in the prepared jars. The jars were then filled with water (ca. 1 cm above the PVA solution level) and covered with an aluminium foil.
6. Prepared jars (with the bottles inside) were put back onto the stirring pad, and the temperature was set to 160 °C – the temperature needed to sustain temperature at PVA solution within a range of 90 °C to 95 °C (alternatively, the temperature can be monitored with a thermal probe). The stirring revolutions were decreased to ca. 200-300 rpm. Note: As the PVA solution starts to react, viscosity increases and the stirring bar slows down or even stops moving. To keep it in motion it is necessary to gradually (ca. first 30 minutes after the temperature range is reached) decrease the revolution down to 60-80 rpm.
7. The solution was left to stir at the temperature range (90 °C to 95 °C) for 2-3 hours to achieve a homogeneous (transparent) solution.
8. The solution was cooled for 2 hours to room temperature while the stirring (ca. 120 rpm) was continued.
9. The stirring process of the PVA solution was then completed. Usually, a dense film layer develops onto the PVA's surface, such layer shall be removed before casting into a form.
10. A 30 g of the finished PVA solution was poured into each of six polystyrene dishes (9 cm in diameter).
11. Any bubbles formed during the casting of the solution were carefully removed using a pipette. The resultant casted PVA should be glass transparent.

The basic preparation of the PVA solution remains the same regardless of the type of hydrogel being produced.

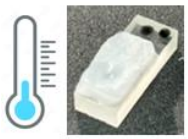

Freeze-thawing cycle (FT)
-20°C for 8 hours
+4°C for 16 hours

Cast-drying cycle (CD)
Temperature and humidity control
E.g., +60°C and 80%RH, until water content drops below 12%

Figure 4-3: Illustration of Freeze-thawing and Cast-drying method.

4.3.2 Freeze-thawing (FT) preparation process

… follow-up to step 11 (preparation of PVA hydrogel)

1. The polystyrene dishes were sealed using tape to prevent water or moisture from getting in and out of the sealed solution.
2. The dishes were inserted into the heat-controlled chamber.
3. Each FT cycle consisted of exposure to -20 °C for 8 hours, followed by 4 °C for 16 hours. The whole FT process involved four such cycles.
4. After the crosslinking process was finished (4 days), the dishes were removed from the heat-controlled chamber, and each PVA gel was removed from the bowl and placed separately into 1 liter of pure water (to facilitate osmosis). The PVA gels were left to swell for 3 days. (remembering which side was at the top and the bottom)
5. After swelling was completed, the hydrogel was ready for slicing and experiments. The bottom side of the hydrogel (the bottom side adhering to the bowl) was used as the sliding surface (as the bottom surface had better surface quality).

4.3.3 Cast-drying (CD) preparation process

… follow-up to step 11 (preparation of PVA hydrogel)

1. The bows were partially closed with a lid, leaving them open ca. 2 cm, and the lid was secured to the bowl by tape. The dishes were inserted into a heat-controlled chamber, ensuring the open side was covered against the fan inside the chamber.
2. The humidity-controlled chamber was set to 60 °C and 80 %RH, and the dishes were left under these conditions for 3 days.

$$4.5\ \text{g} = 30\ \text{g} \,.\, 0.15$$

$$100.\frac{x - 4{,}5}{x} < 12\%$$

3. Afterward, the dried PVA film was weighed, and the water content was calculated assuming 15 % of the original weight of 30 g is solid. If the water content was less than 12 %, the drying process was considered completed and proceeded to the next step. Note: It is important to mark or remember which side of the dried PVA gel was at the bottom of the bowl.
4. Each gel from a bow was placed into 1 liter of pure water and left to swell for 3 days.

5. After the swelling process, the PVA gel was ready to be used. The bottom side of the hydrogel was the sliding surface having a smoother surface.

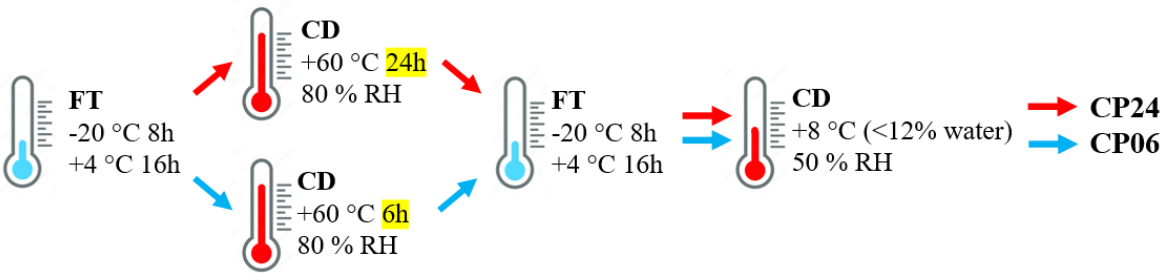

Figure 4-4: Schema of the CP method.

4.3.4 CP24 preparation process

… follow-up to step 11 (preparation of PVA hydrogel)

Note: The CP process includes both the FT method and the CD method as follows (FT → CD → FT→ CD).

1. For the 1st FT process, the polystyrene dishes were sealed using tape to prevent water from getting in or out.
2. The dishes were inserted into the heat-controlled chamber.
3. A single FT cycle was set (-20 °C for 8 hours → 4 °C for 16 hours).
4. The dishes were then removed from the heat-controlled chamber.
5. For the 1st CD method (high-temperature drying), the dishes were unsealed and partially left partially open (such as a standard CD process).
6. The dishes were inserted into the heat-controlled chamber, ensuring the open side was covered against the fan inside the chamber.
7. The humidity-controlled chamber was set to 60 °C and 80 % RH, and the dishes were left under these conditions for 24 hours. Note: The high-temperature drying predetermines the resultant CP properties. 24 hours of such drying results in CP24 hydrogel.
8. For the 2nd FT process, the polystyrene dishes were again sealed using tape to prevent water and moisture leakage. The dishes were inserted into the heat-controlled chamber.
9. A single cycle was set, following the same parameters as before (-20 °C for 8 hours, and 4 °C for 16 hours). The dishes were then taken out of the heat-controlled chamber.
10. For the 2nd CD process (low-temperature drying), the tape on the dishes was removed. The dishes were unsealed and partially left partially open (such as in the standard CD process).
11. The dishes were inserted into the heat-controlled chamber, ensuring the open side was covered against the fan inside the chamber.
12. The humidity-controlled chamber was set to 8 °C and 50 % RH, and the drying process continued until the water content in the dry film was reduced to a predetermined level of <12 % (ca. 4-5 days).
13. Each gel from a bow was placed into 1 liter of pure water and left to swell

for 3 days. Note: It is important to leave a mark on the side of the PVA film to distinguish which is the bottom one.

14. After the swelling process, the PVA gel was ready to be used. The bottom side of the hydrogel was used as the sliding surface.

4.3.5 CP06 preparation process

Note: The preparation process mirrors that of CP24, with the only distinction being the duration of the high-temperature drying in the 1st CP process, which is shortened from 24 hours to 6 hours (60 °C, 80 % RH, 6 hours).

4.3.6 Laminar gel (LM) preparation process

Note 1: LM gel consists of two layers: FT and CD.

Note 2: The following process describes the recipe used for the 1st experimental part. The 2nd experimental part was conducted at 8 °C, with 50 % RH condition at the 3rd step, and then dried for ca. 5 days.

1. The standard PVA solution was prepared, and the standard FT preparation process was followed. Four FT cycles were conducted.
2. Another layer of standard 150 g solution was poured onto the FT layer.
3. The CD preparation process was used, specifying the temperature (20 °C), relative humidity (50 % RH).
4. The drying process was continued until the water content in the dry film was reduced to a predetermined level of <12 %. This typically took approximately 3 days.
5. The dried PVA films were individually placed into 1-liter containers of water and left to swell for 3 days.
6. After the swelling process, the PVA gel was ready to be used. Unlike at the other manufactured PVA hydrogels. The sliding side was we upper one, not the one facing the bowl.

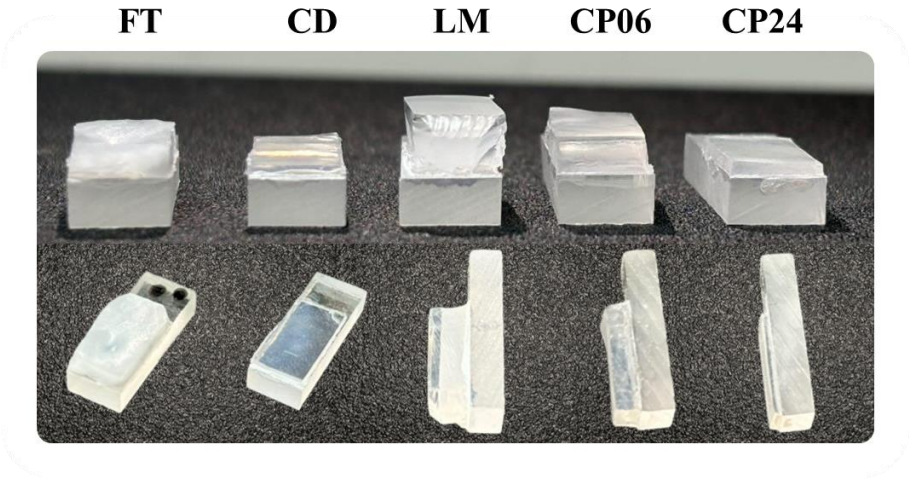

Figure 4-5: Manufactured PVA hydrogels used in experiments. From the left: PVA FT, PVA CD, PVA LM, PVA CP06, PVA CP24

4.4 Methods: the 1st experimental part

4.4.1 Friction and viscoelastic experiment (boundary lubrication)

Stress-controlled modular compact rheometer (MCR 302, Anton Paar, Graz, Austria) equipped with a combined motor transducer system can be used for all kinds of rheological investigations and material characterization operating in rotational and oscillatory modes.

In this thesis, the device was used for an investigation of the boundary lubrication effect of PVA hydrogels across various sliding velocities. The boundary lubrication effect was achieved by pre-experimental loading. The experimental setup included a tribo-cell (T-PTD 200, Anton Paar, Austria) with a ball-on-three-plate configuration arrangement, where the three PVA samples were positioned at an angular offset of 120° and tilted at 45° the vertical axis. To ensure a uniform distribution of normal force over the plate samples, a lateral spring integrated into the tribo-unit effectively reduced lateral shear. The measuring system, equipped with the ball-mounted shaft, was powered by a synchronous motor and supported by an air bearing.

Figure 4-6 illustrates the experimental configuration and measuring principle of both friction and viscoelastic experiments. For the friction measurement, a continuous rotation with gradual acceleration (0-max) and deceleration (max-0), was used, ranging from 10^{-5} to 10^{3} $mm.s^{-1}$. Each individual frictional data points were sampled at a constant velocity on a predetermined sliding distance – an illustrative outcome in Figure 4-6 c). The tested PVA samples were submerged in a phosphate-buffered saline (PBS) or protein solution (1.4 wt % albumin, 0.7 wt % γ-globulin) and loaded (5 N, or 10 N). The viscoelastic data were obtained by switching the motion to oscillation movement, where under a constant frequency (1 Hz) and 2 N loading, stress-strain dependance was measured. Individual data points were obtained by keeping the strain amplitude constant for a predetermined time. As a contacting counter-body a smooth glass ball (⌀ 12.7 mm) was used. Detailed information about the configuration setup is shown in Table 4-1. Tested PVA samples (6 x 10 mm) were affixed to a polycarbonate plate using a cyanoacrylate adhesive. The material used in the experiments with measured thickness and water content is displayed in Table 4-2.

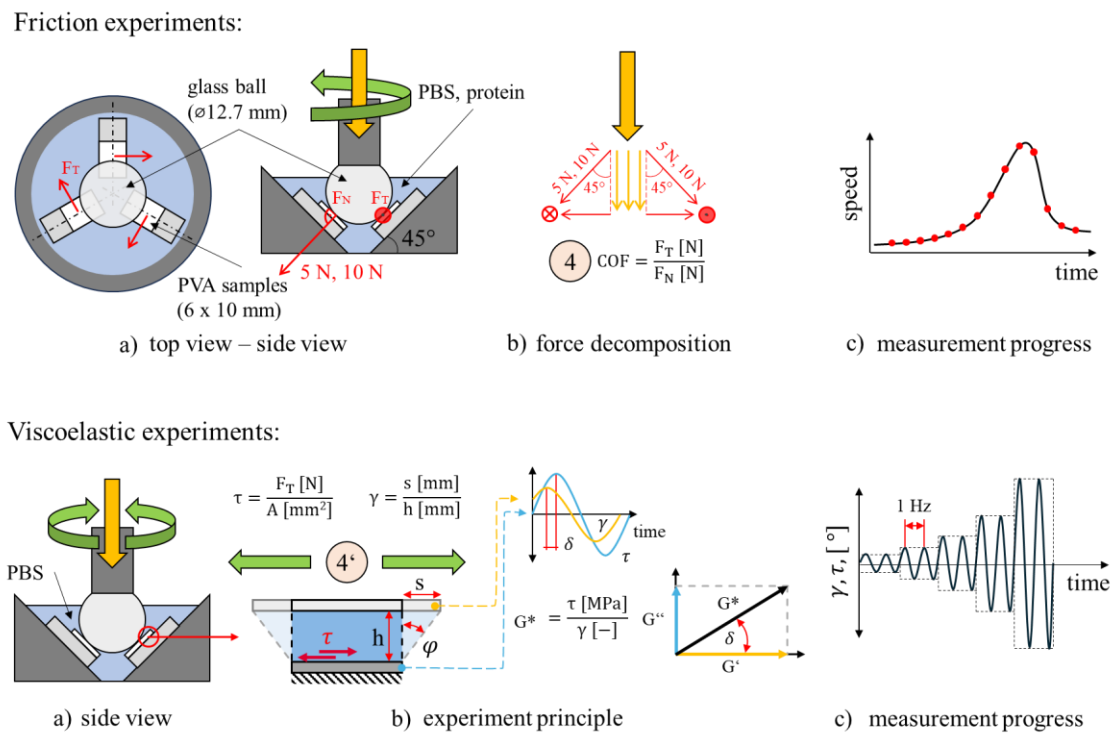

Figure 4-6: Friction experiments – a) a scheme of the experimental configuration, b) loading force (normal force) decomposition, c) An example of monitored COF-speed output; Viscoelastic experiments – a) A scheme of oscillation motion, b) the principle of the viscoelastic experiment, c) Data acquisition with controlled strain and constant frequency. Note: 4 and 4' refers to Figure 4-7.

Table 4-1: Rheometer experimental configuration for friction and viscoelastic experiments. Note: the protein solution consists of (1.4 wt% albumin, 0.7 wt% γ-globulin).

	Friction experiments	**Viscoelastic experiments**
Ball material	glass, ø12.7 mm	
Plate material	FT, CD, LM, CP24, CP06	
Temperature	25 °C	
Normal load	5, 10 N	2 N
Shear strain	–	(0.01, 1000) [%]
Speed range	(0.00001, 1000); (1000, 0.00001) [mm/s]	–
Lubricants	PBS, protein solution	PBS

Table 4-2: PVA samples used for testing with the rheometer.

	Tested samples				
PVA hydrogel	**FT**	**CD**	**LM**	**CP24**	**CP06**
Fabrication process	FT	CD	laminar FT/CD	FT-CD-FT-CD	FT-CD-FT-CD
Thickness [mm]	2	1	4	1.7	2.5
Water content [%]	~85	~75	~73	~60	~73

The experimental procedure for measuring friction and viscoelastic properties, see Figure 4-7, consisted of preparatory and experimental phases. The preparatory phase aimed to reduce the amount of interstitial fluid incorporating at biphasic lubrication. The interstitial fluid was reduced by 30 min (15 min for viscoelastic tests) of static loading of the housed PVA samples (the same force as used in the experimental phase). After the creep deformation stage was completed, a 10 sec unloading followed by 60 sec static loading was executed. The experimental phase followed immediately after the preceding phase. The frictional series consisted of three repetitions in the follow-up order: 1-2-3-4-2-3-4-2-3-4, where the first 4th step consisted as a run-in phase. In total, three frictional series were performed to provide sufficient statistical repeatability. As for the viscoelastic tests, measurement was carried up in this order: 1-2-3-4, with two series performed.

Figure 4-8 shows an illustration of biphasic lubrication reduction after the load is applied. Initially, high interstitial fluid pressure (contributing to low friction at reciprocating experiments) gradually decreases to a quasi-equilibrium state, where loading and reaction forces are in equilibrium. After the preparatory phase was completed, friction or viscoelastic tests were initiated. Numbers 1-4 shown in the graph represent the individual steps in the preceding Figure 4-7.

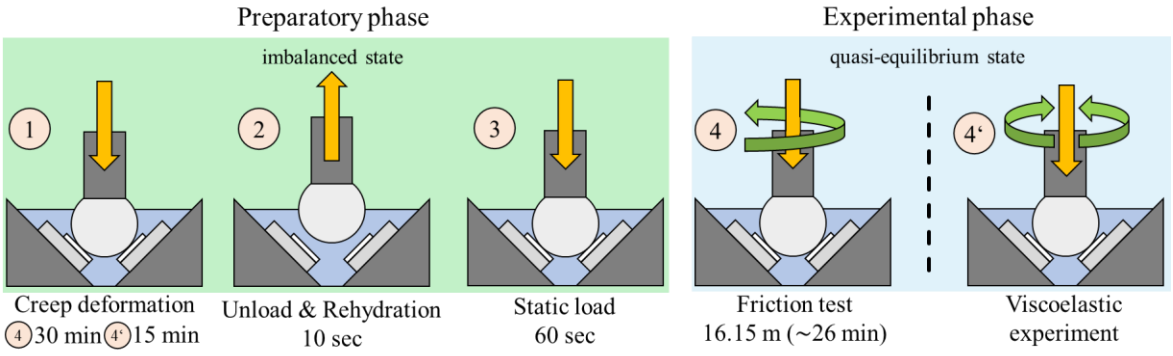

Figure 4-7: Experimental procedure for friction and viscoelastic measurements.

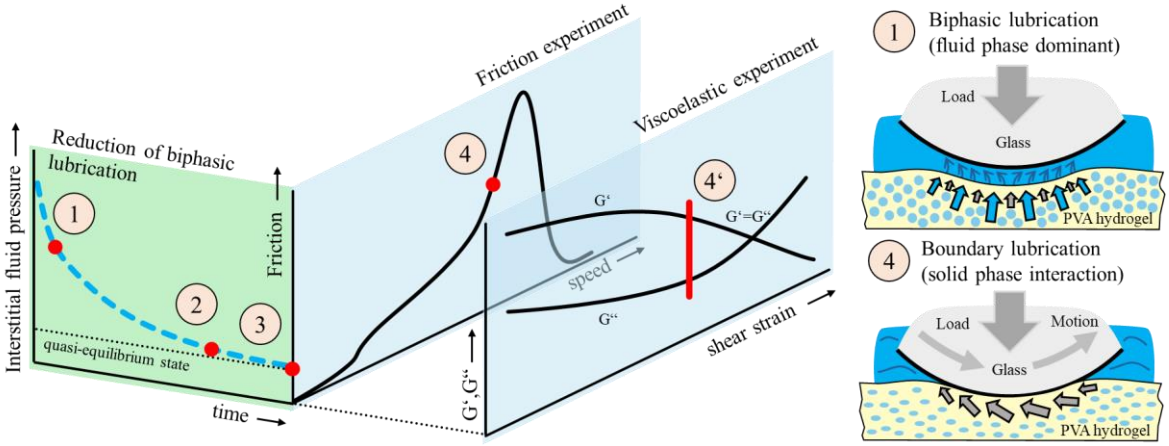

Figure 4-8: Left: An illustration of pre-experimental and experimental part. Right: Interstitial fluid contributes to low friction. Pre-experimental loading diminishes this effect and leaves solid-solid friction.

Figure 4-9 a) shows the real experimental data for (PVA CP06, lubricant: protein, load: 5 N). For the evaluation of friction responses, the initial run-in friction curve was excluded due to notably different responses compared to the subsequent sliding tests at the same set of PVA samples. The mentioned 3 experimental series yielded in (3+3+3 = 9) data sets. Thus, Figure 4-9 a) is a result of (2+2+2) data sets. An example of a data set including run-in phase (Average 1) is shown in Figure 4-9 b), where the Average 1 means an average of (1+1+1) run-in friction. As observed, run-in friction visibly deviates from the Average 2 and Average 3.

Viscoelastic tests is a result of two repetitions, see Figure 4-9 c). The resultant graph contains storage modulus (G’) and loss modulus (G”) as a function of shear strain. For a strain region, where G’ > G”, the material behavior is considered as solid-state dominant, and as fluid-state dominant if G” > G’.

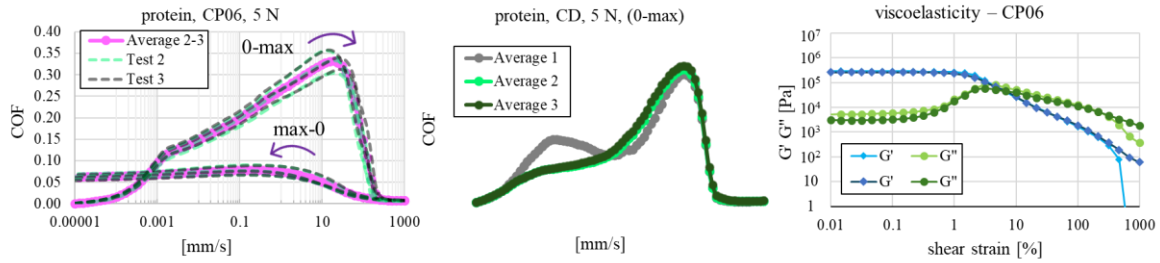

Figure 4-9: a) frictional measurement of (protein, CP06, 5 N). The upper (0-max) curves are a result of an acceleration measurement, the bottom curves (max-0) are a results of deceleration measurement. Average 2-3 corresponds to Test 2 and Test 3 results of the 3 series. b) frictional measurement of (protein, CD, 5 N, (0-max). Average 1 (run-in curve), Average 2, and Average 3 is a result of the 3 series testing. c) Viscoelasticity measurement for CP06.

4.4.2 Laser scanning microscope

A laser scanning microscope (LSM, VK-X260K, Keyence, Japan) is an advanced tool for high-accuracy non-contact measurement analysis of surfaces capable of measuring 3D profile and roughness parameters. The laser microscope was used for the observation of PVA hydrogel surfaces. Both worn and virgin samples were observed. Virgin samples served as a reference. The collected data served as background for the frictional data.

Worn surfaces were observed at different locations, see Figure 4-10. For one selected worn surface, the whole contacting area (A) and central area (C) with 10 x magnification were taken. C image further served for surface evaluation (Ra, Rz). Additionally, a boundary area and magnified C zone (50 x, 150 x) were scanned – however not included in the final assessment. Every experimental configuration generated 9 worn PVA samples, of which 5 were selected for the observation.

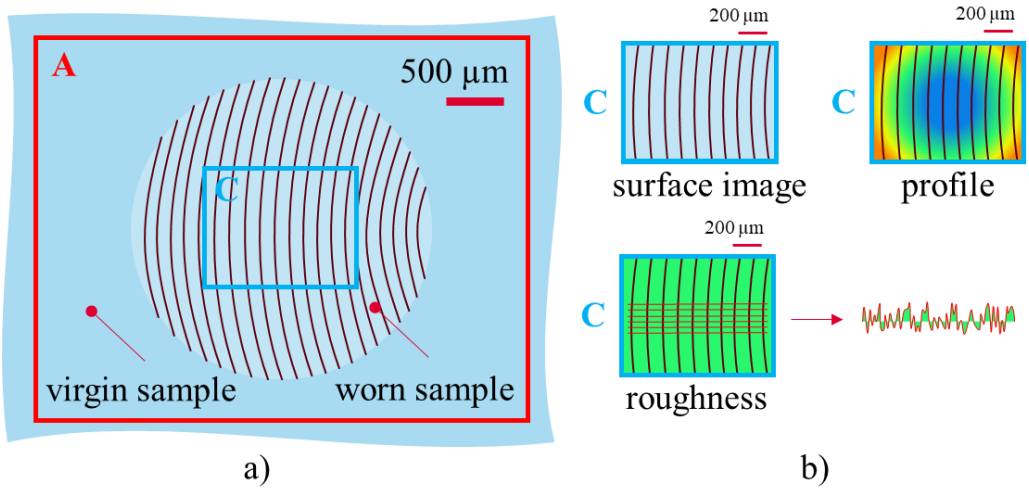

Figure 4-10: a) The image setup taken for every tested PVA hydrogel. b) A “C” central surface image, surface profile, and surface roughness

4.4.3 Compression test

For calculations of the Hertz contact of the tested PVA samples, an elasticity modulus for each sample had to be obtained. Due to the non-uniform thickness and waviness of samples, a tensile experiment appeared too difficult. Instead, a compression test was performed, see Figure 4-11. The measuring setup was configured to the compression speed of 10 $mm.s^{-1}$. The elastic modulus was calculated between 10 % and 20 % strain.

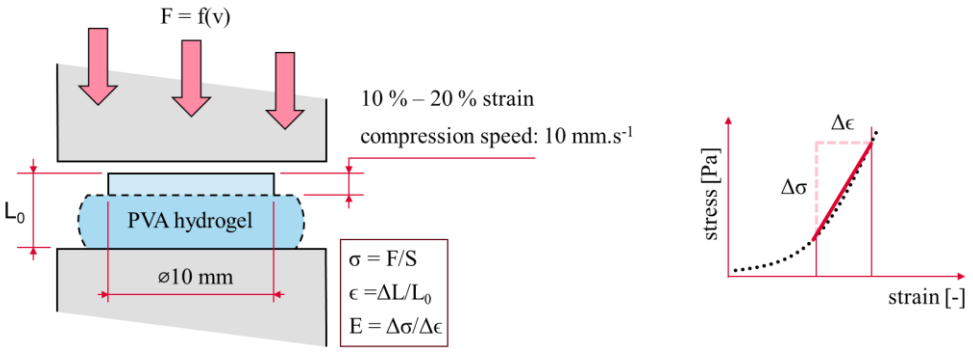

Figure 4-11: An illustration of compression test. left – compression test, right – calculation of an elastic modulus.

4.5 Methods: the 2nd experimental part

4.5.1 Friction experiment (reciprocal tests)

A commercial tribometer device, Bruker UMT TriboLAB, was used for reciprocal experiments, where unlike at the rheometer MCR302, a biphasic lubrication is included. The tribometer is capable of conducting friction experiments within a wide range of test configurations. For the purpose of this research, a pin-on-plate (CoCrMo-on-PVA) and (cartilage-on-PVA) was utilized. Detailed experimental conditions are listed in Table 4-3. The friction is evaluated via a module equipped with a biaxial load cell mounted on a sensor with a load capacity of 50 N for both axis. The reciprocating motion is induced by a slider mounted to the load cell. The slider provides a linear motion (constant motion), using a stepped motor, see Figure 4-12. To ensure valid results, friction tests were repeated five times, while wear tests were repeated three times. The lubrication during reciprocal experiments is expected to be biphasic, whereas at the MCR302 rheometer (where the sliding area does not change), it is expected to work in the boundary lubrication regime.

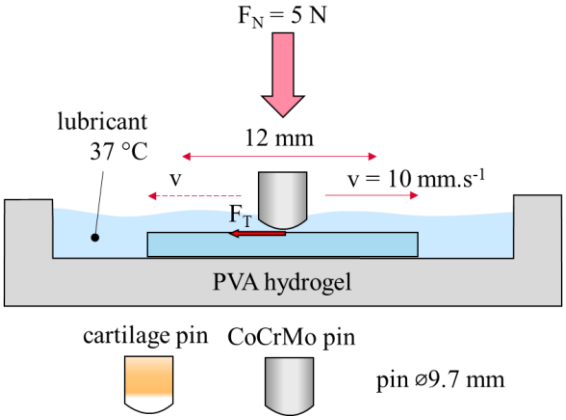

Figure 4-12: Tribometer experimental set up.

Table 4-3: Tribometer experimental parameters.

	friction test	wear test
material	PVA (CP06, LM)	
load	5 N	
stroke	12 mm	
lubricant	synovial fluid	
speed	10 mm.s^{-1}	
pin	cartilage	CoCrMo
cycles	750	7500
(duration)	30 min	5 hours
repetition	5 times	3 times

Table 4-4: The composition of synovial fluid lubricant.

SF	albumin	γ-globulin	hyaluronic acid	phospholipids
[mg/ml]	20	3.6	2.5	0.15

4.5.2 Digital optical microscope

Optical microscopy (VHX, Keyence VHX 7000) enabled the capture of high-resolution images of PVA CP06, LM and pHEMA hydrogels. The primary reason for using a different microscope was due to the different workplace from the 1st experimental part.

Images of a virgin and worn sample were taken for wear assessment. To assure roughly the same scanning position, an imaginary crosshair was drawn using alcohol-based makers (ca. 10 mm apart) – black dots in Figure 4-13. For each sample, three areas within the crosshair were scanned. Each scan provided information about the surface topography (profile, surface roughness) as well as detailed surface image, see Figure 4-13.

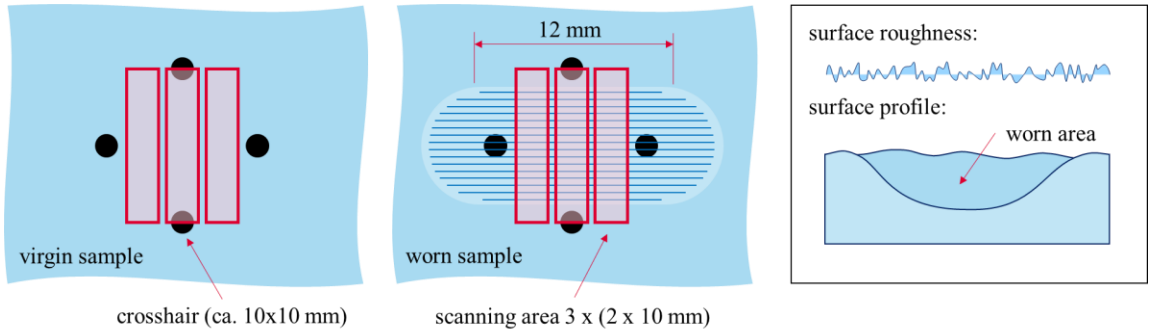

Figure 4-13: left: virgin sample, middle: worn sample, right: obtained data from scanned areas.

4.6 Tested predictions

For testing the 1st hypothesis, a detailed set of images by LSM was taken, as described in the methods. The amount of wear of each sample was observed and put in correlation with the measured material properties (modulus of elasticity, contact pressure). Surface parameters were also compared. The influence of PVA polymer chains is discussed via frictional data. The prediction is verified when compliant hydrogels exhibit generally lower about of surface wear.

Similarly, like the 1st hypothesis, the 2nd hypothesis is assessed primarily by LSM images. To verify the tested prediction, the amount of wear shall be smaller on PVA samples with a lower modulus of elasticity.

The 3rd hypothesis is assessed primarily with frictional data, where different frictional areas across the speed range were indicated. The observed frictional data will be discussed in relation to previous predictions.

During reciprocating frictional tests, the hydrogel will have time to rehydrate. Thus, biphasic lubrication will be maintained, keeping friction at a very low value. The 4th hypothesis is verified when the PVA LM sample reveals a higher amount of wear than PVA CP06 during 5-hours lasting wear test.

5 RESULTS

As the standard PVA solution underwent different climatic conditions (temperature, humidity), the resultant surface profile and material properties were strongly influenced at first glance. Therefore, an evaluation of basic material properties was carried out, serving as a basis for discussion over the frictional experiments. Figure 5-1 indicates the visible differences of the PVA surfaces – lower manufacturing temperatures (e.g. FT, CP06, LM) resulted in a softer material and a rougher surface, contrary to the CD, and CP24 with dominantly higher temperatures while manufacturing.

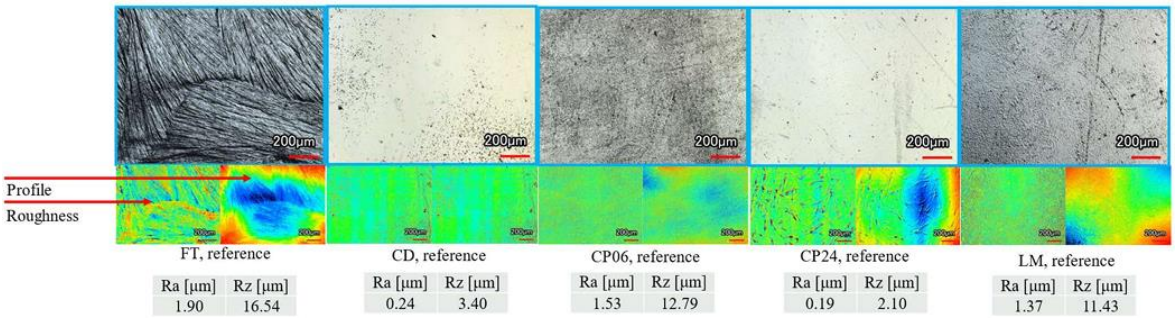

Figure 5-1: Unworn (virgin) PVA samples after manufacturing observed by LSM.

5.1 Viscoelastic and material properties of PVA samples

Oscillatory and compression experiments allowed a rough estimate of basic material properties, allowing qualitative comparison between tested samples.

The first thing standing out in the results of viscoelastic properties is the dominance of G' over G" at low strain (0.01 – 10%) for all PVA samples, see Figure 5-2. Ratio G'/G" gradually decreases with increasing shear strain until reaching cross-over points, where G" outweighs G'. This indicates that most of the biphasic lubrication is successfully filtered out during pre-experimental loading. PVA samples (LM, CP06) having cross-over points (at 4.6 % and 6.8 %, respectively) at the lowest strain suggests it might secondarily hydrate the contact surface at major overloading. Other PVA samples have their cross-over points as follows: CP24 = 10 %, CD = 14.6 %, FT = 100 %. The magnitude of G', G" of PVA samples ranges between $9x10^5$ Pa – $1.7x10^4$ and $2.4x10^4$ – $2.5x10^2$ Pa (at low shear) for G' and G" respectively, with its values in respective decreasing order: CD, CP24, CP06, LM, and FT. Apart from PVA FT with the lowest moduli, all samples are grouped within a small range. Such results point out very different stiffness of FT as compared to the rest of the PVA hydrogel.

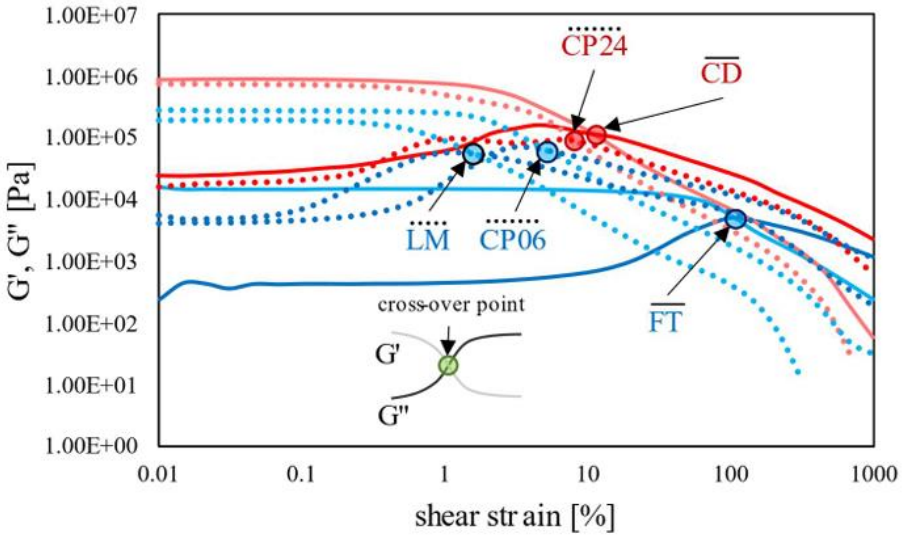

Figure 5-2: Viscoelastic behavior of PVA hydrogel samples.

Additionally, a compression test (between 10 % – 20 % strain) has been conducted and compression elastic modulus was obtained. Using the contact Hertz theory based on [54] contact pressure of 5 N and 10 N loading was calculated. Poisson's ratio was assumed 0.45 for all PVA samples, as it was difficult to measure by compression test.

$$a = \sqrt[4]{\frac{4}{3}.\frac{F.R.b}{E}.14.\frac{(1-2\nu)^2\,(1-\nu^2)}{(1-\nu)^2}}$$

$$\delta = R - \sqrt{R^2 - a^2}$$

$$p_{max} = \frac{(1-\nu)^2}{1-2\nu}.\frac{E}{1-\nu^2}.\frac{a^2}{2.R.b}$$

$$S = 2.\pi.R^2\left(1 - \frac{R-\delta}{R}\right)$$

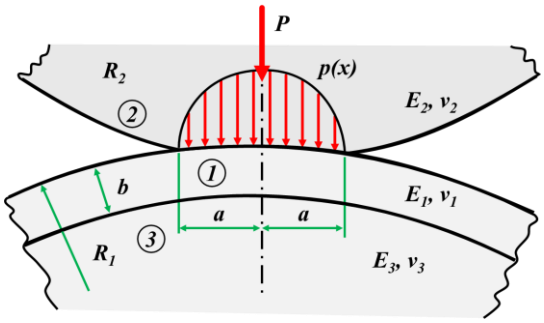

Figure 5-3: Hertzian contact model for layered solids, plates and shells whose properties differ from the substrate. left – formulas used, right – an illustration of layered solids model [54]

Where the parameter a stand for contact radius, δ for contact deformation, p_{max} for maximal Hertzian pressure, and S for contact area. Other parameters describe the following (F = normal load, R = ball radius, b = sample thickness, E = modulus of elasticity). Based on the calculations of E (Table 5-1), the individual PVA samples were categorized into two compliant (FT, CP06, LM) and rigid (CD, CP24) category. The categories will further serve for a better understanding of the presented results.

Table 5-1: Theoretical contact pressure.

	FT	CD	CP06	CP24	LM	
E	0.08	2.51	0.51	1.43	0.63	[MPa]
			Calculations 5 N loading			
p_{max}	0.19	1.54	0.44	0.89	0.39	[MPa]
S	58.21	6.56	23.92	11.45	27.38	[mm^2]
			Calculations 10 N loading			
p_{max}	0.27	2.18	0.62	1.26	0.55	[MPa]
S	88.24	9.33	34.59	16.36	39.74	[mm^2]

5.2 Results Description of Individual PVA Samples

This chapter summarizes the results of the 1st experimental part involving boundary lubricating.

5.2.1 PVA FT hydrogel

Frictional data shows similar trends in frictional response at different velocities. Starting with acceleration (0-max) results, initially low friction (~0.001) gradually increases to its maximum (0.25 – 0.35) at a speed of around 20-40 mm/s. From there, the friction becomes a decline trajectory until it reaches the maximum experimental speed of 1000 mm/s. A completely different trend is observed when speed gradually decreases (max-0). Friction at max-0 does not follow the same pattern as for 0-max. Instead, friction rises to around 1/3 of 0-max maximum, after that, the friction gradually reduces to 0.02 – 0.06 at a speed close to 0 mm/s, see Figure 5-4.

As seen in Figure 5-4, the friction value is strongly dependent on the lubricant and load used in the experiment. The protein solution keeps friction always at substantially higher values than PBS does. Overall, the lowest friction is observed for 5 N and PBS lubricant, contrary the highest is seen for 5 N and protein solution (10 N + protein solution was not conducted). The friction force is analogous with friction (F_T/F_N, F_N = constant) for most observations, however at 10 N loading, the friction force is the highest even though the friction behavior did not show increased response.

As for LSM observations, PVA FT samples showed great plastic deformation, making profile evaluation difficult to perform. Figure 5-5 depicts not only the images of the worn-out sample, but the roughness and profile image as well. Even though some visible stretches are visible, the unsuitable mechanical properties ruled the FT material out of further consideration for possible articular cartilage tissues.

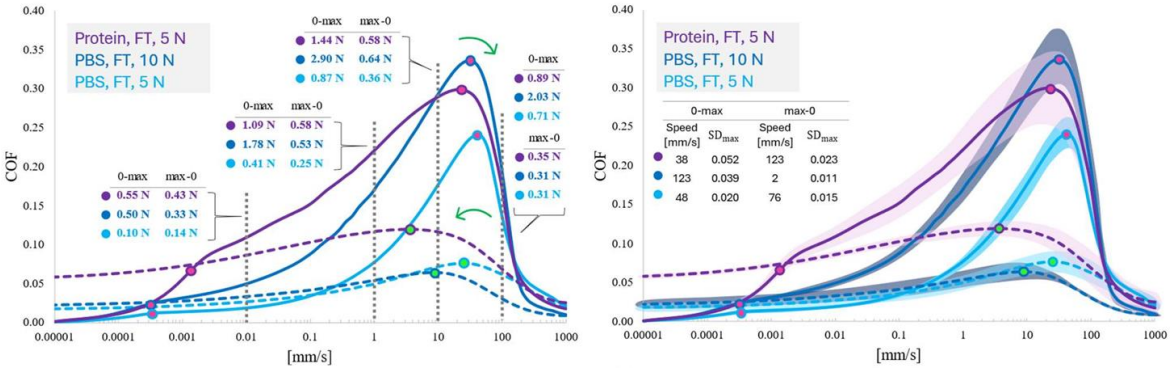

Figure 5-4: left: Averaged frictional data of PVA FT and indicated frictional force at velocities of 0.01, 1, 10, and 100 mm/s. right: Standard deviation (SD) of frictional data.

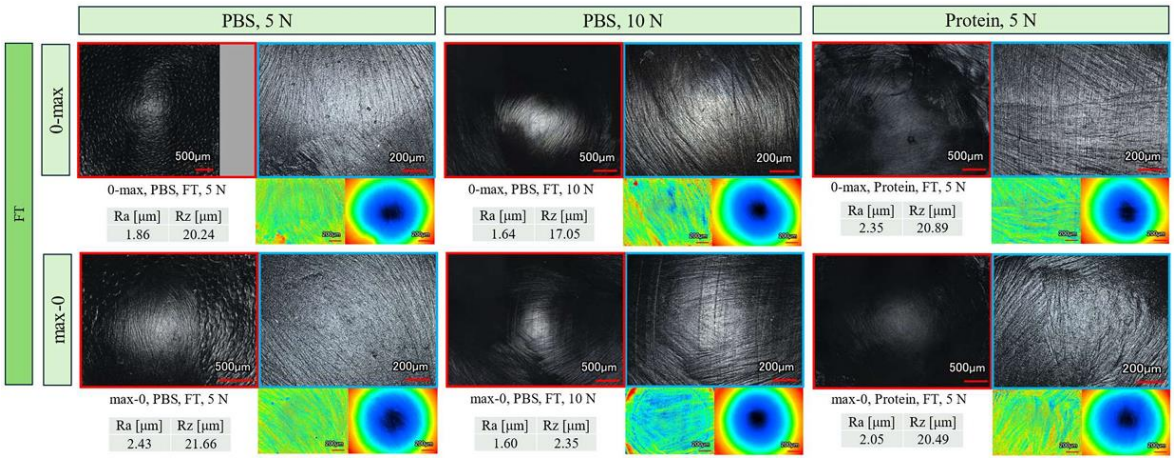

Figure 5-5: LSM images of worn PVA FT samples.

5.2.2 PVA CD hydrogel

Contrary to PVA FT, showing poor mechanical properties, PVA CD was calculated to have the highest elastic modulus and contract pressure. Frictional behavior is observed to have similar trends as FT across the 0-max and max-0 speed ranges. However, the maximum friction peak is lower and ranges between 0.2 – 0.26 and 0.04 – 0.07, respectively, see Figure 5-6.

Visible scratches are seen at any PVA CD sample, Figure 5-7, within the worn-out area (diameter of ~2.6 mm). The surface roughness has increased, compared to a virgin sample, different loading or lubricant had no impact on different roughness. Interestingly, the major difference is observed even compared to 0-max and max-0 experiments. Samples being exposed to gradually increasing speed were observed to have much fewer wear scratches than with decreasing (max-0) speed. Furthermore, as Figure 5-6 shows, less wear is attributed to higher friction and severe wear to smaller friction.

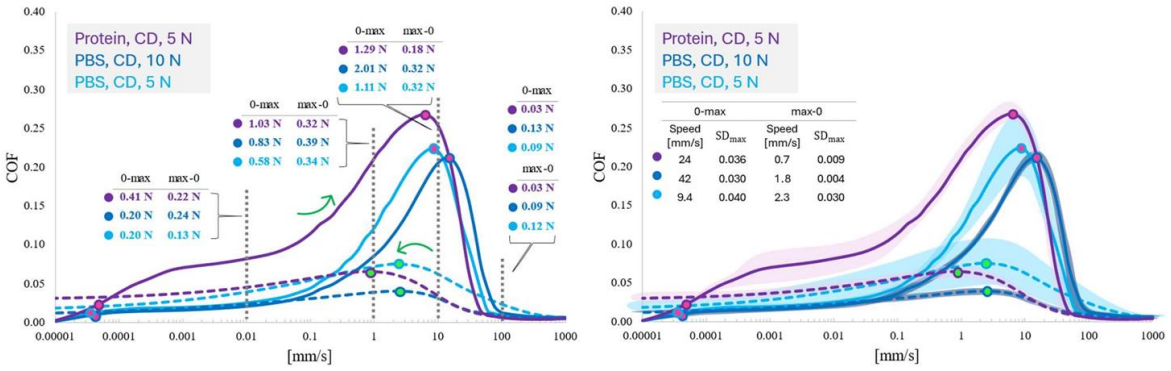

Figure 5-6: left: Averaged frictional data of PVA CD and indicated frictional force at velocities of 0.01, 1, 10, and 100 mm/s. right: Standard deviation (SD) of frictional data.

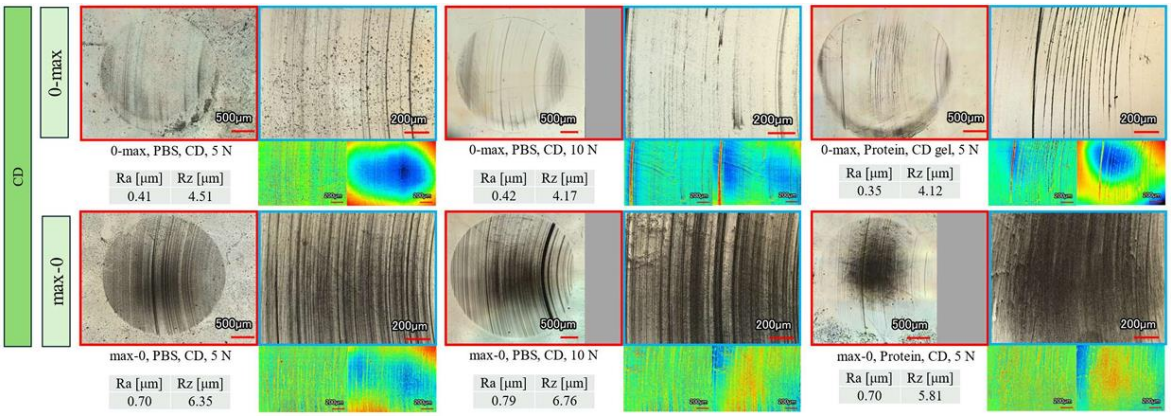

Figure 5-7: LSM images of worn PVA CD samples.

5.2.3 PVA CP06 hydrogel

Frictional peaks (0.25 – 0.35) at PVA CP06 are roughly about the same level as for PVA FT (higher than at PVA CD). What stands out here is the frictional course and values when protein solution is used. Until around 0.001 mm/s, friction grows with a concave pattern; after that, a small convex course is indicated, followed by a linear growth, see Figure 5-8. Such a pattern was observed only for 0-max results, although the protein solution greatly increased friction for max-0 as well. As for PVA CD, higher loading resulted in a little bit higher friction for PVA CP06.

Interestingly, CP06 did not show a significant scratch at the sliding area, nor was the roughness majorly influenced. A visible exception is seen for the configuration of 0-max, 5 N, protein lubricant leaving the surface heavily scratched, see Figure 5-9. However, due to the initially rough surface, increased roughness of the worn area was not indicated. The contact zone was estimated to have a diameter of ~5.2 mm.

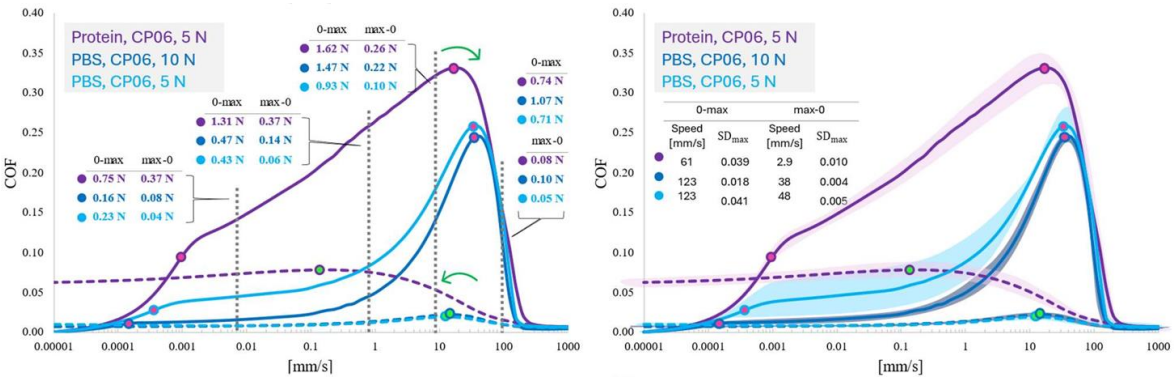

Figure 5-8: left: Averaged frictional data of PVA CP06 and indicated frictional force at velocities of 0.01, 1, 10, and 100 mm/s. right: Standard deviation (SD) of frictional data.

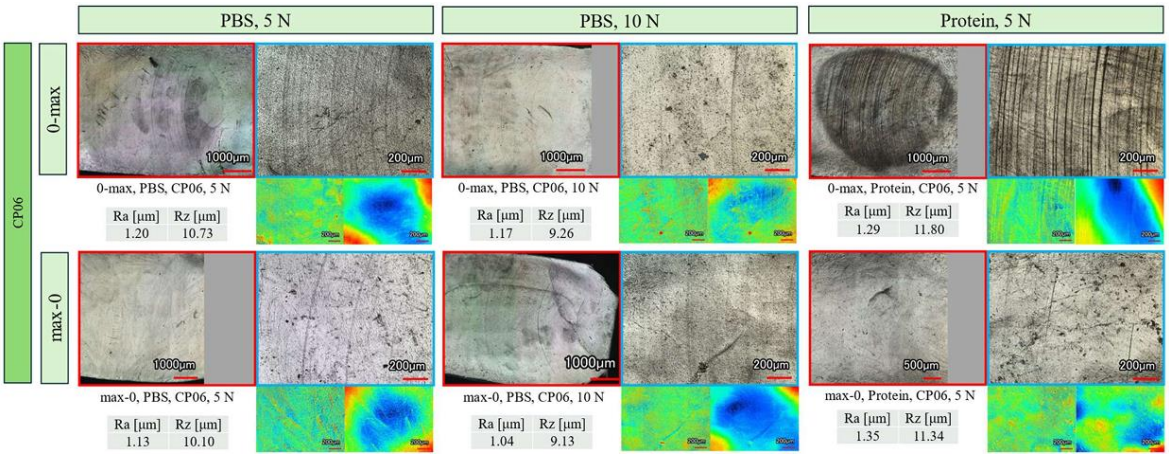

Figure 5-9: LSM images of worn PVA CP06 samples.

5.2.4 PVA CP24 hydrogel

If leaving CP06 at high-temperature drying process for 24 hours (instead of 6 hours), we get CP24. Such difference leaves the PVA sample with very similar properties to PVA CD. Friction values and pattern over the whole speed range are almost identical – CP24 appears to be less sensitive to different loading and seemingly smaller SD, Figure 5-10.

Analogously, with observations of CD, CP24 exhibit visible scratches and a rougher surface after the friction experiment, as well as severe surface damage at max-0 too, see Figure 5-11. Even though the elastic modulus of CP24 is half of CD's, it is still about 3 times higher than CP06 (having minimal surface damage).

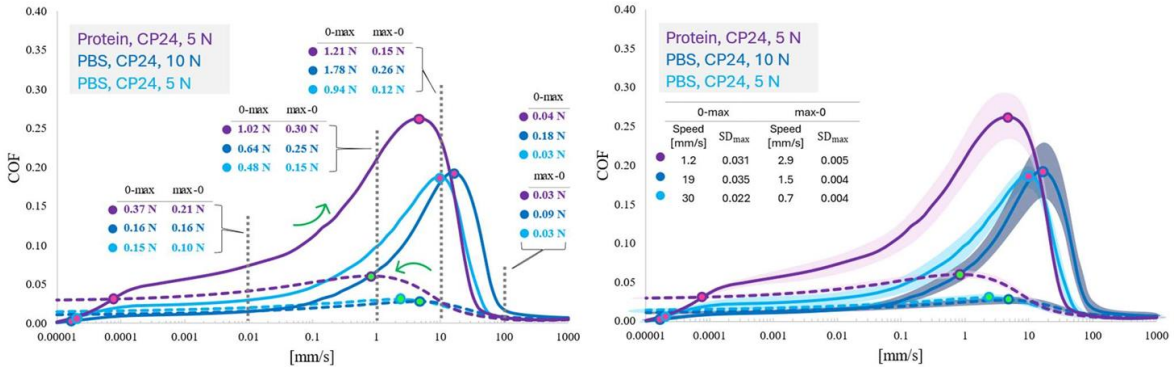

Figure 5-10: left: Averaged frictional data of PVA CP24 and indicated frictional force at velocities of 0.01, 1, 10, and 100 mm/s. right: Standard deviation (SD) of frictional data.

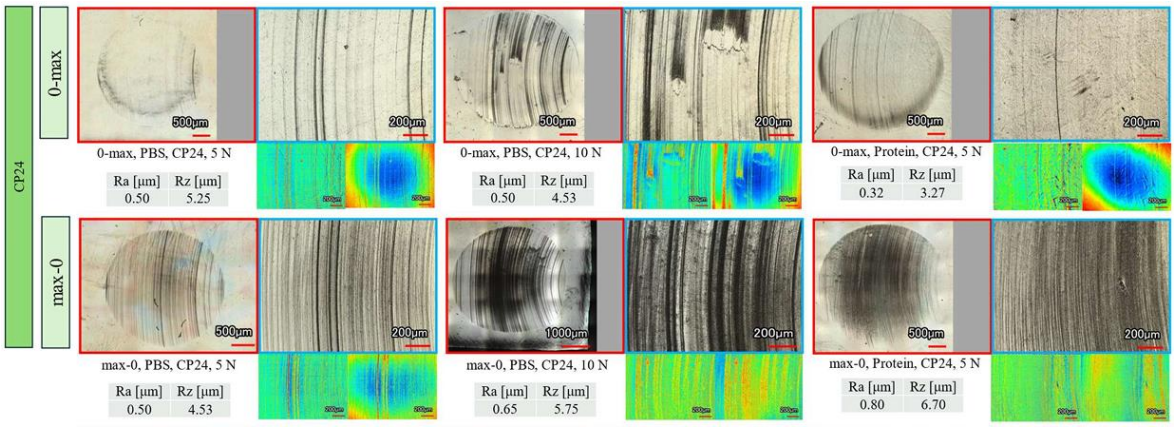

Figure 5-11: LSM images of worn PVA CP24 samples.

5.2.5 PVA LM hydrogel

Laminar hydrogel consisting of the bottom FT and upper CD layer follows up the same frictional trajectory as at the previous PVA samples. The maximal peak of friction coefficient at 0-max is around 0.20 – 0.30, at max-0, friction remains below 0.05. The frictional curve of 10 N load slightly exceeds the friction of 5 N load. The highest friction remains for samples with a protein solution, as for all other hydrogels.

Figure 5-13 shows a worn-out area of laminar hydrogel. Despite the images showing a visible contact area, scratches are insignificant. For some samples (e.g. when protein lubricant is used), there are no visible scratches at all. Unlike PVA samples with high elastic modulus (CD, CP24), there is no difference between the worn area at 0-max and max-0 experiments.

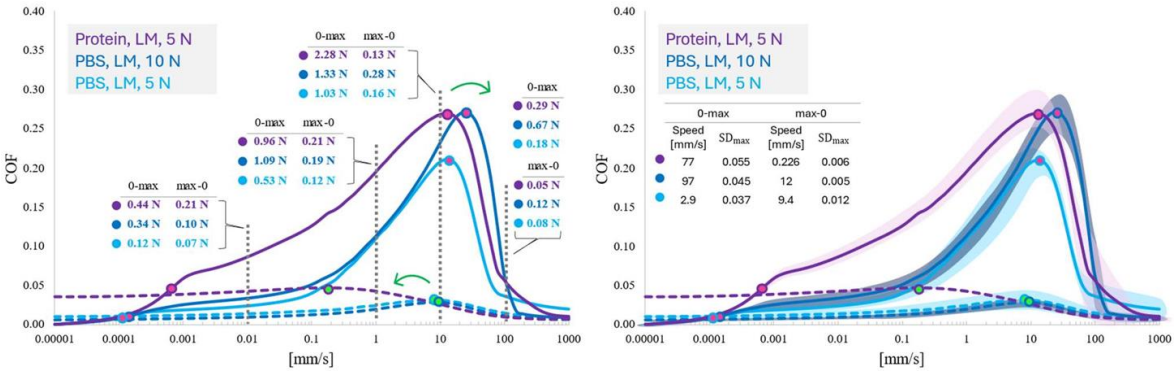

Figure 5-12: left: Averaged frictional data of PVA LM and indicated frictional force at velocities of 0.01, 1, 10, and 100 mm/s. right: Standard deviation (SD) of frictional data.

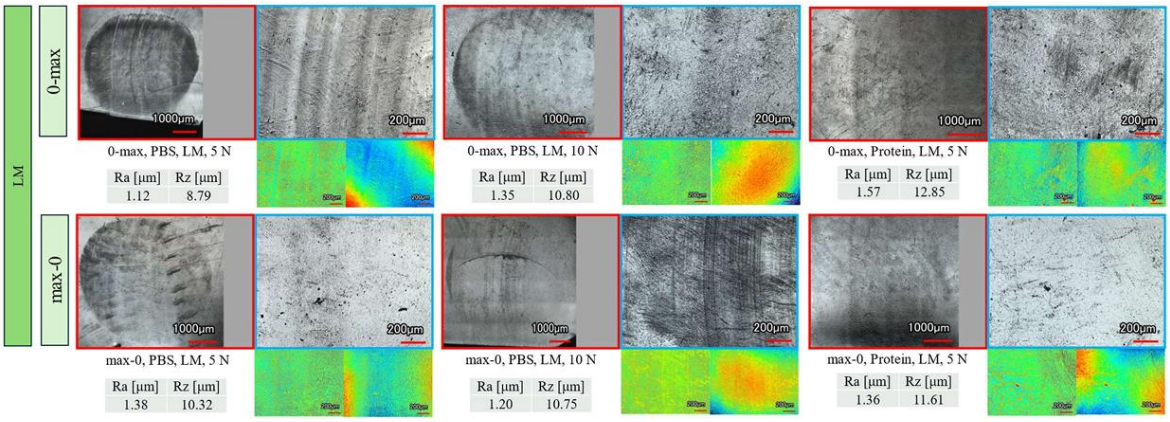

Figure 5-13: LSM images of worn PVA LM samples.

5.3 General Trends in Friction and Wear Across the Speed Range

5.3.1 Run-in Phase

As already explained in Figure 4-9, the first frictional result of each series was excluded from the detailed frictional evaluation due to different curve patterns, compared to the steady behavior of the second and third frictional results. Figure 5-14 illustrates how the first (run-in) pattern resulted. With some exceptions, the run-in phase can be divided into a category of compliant and rigid PVA samples. The run-in test exhibits a lower friction at the low-speed region before the COF peak, with a COF difference of 0 – 0.04 (depending on the PVA type). For compliant hydrogels, a COF peak at low-speed region appeared with 0.02 – 0.06 COF increase. Frictional data obtained with decreasing speed exhibited visible run-in curve deviation as well, however at a much smaller scale, therefore not discussed. The exception disrupting the illustrated scheme was observed for (the CP24, 5 N, protein, 0-max) configuration, where the curve followed the "compliant hydrogel pattern"; however other experiments with protein and PBS lubricant kept the proposed pattern.

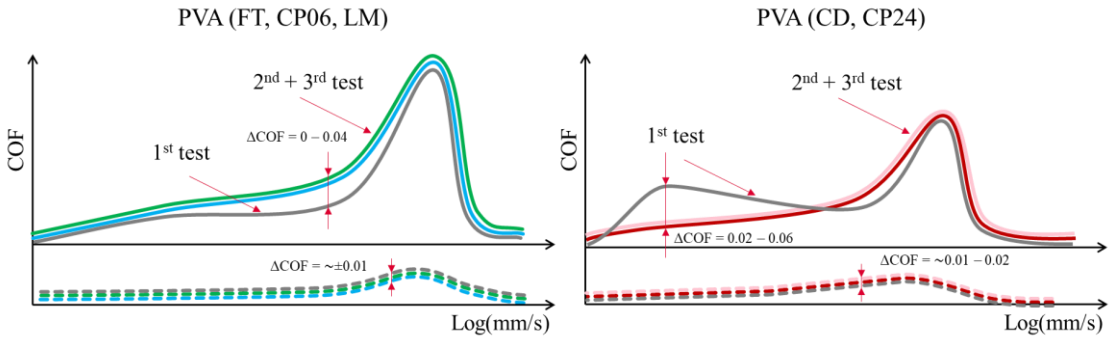

Figure 5-14: An illustration of a different 1st test (run-in) and 2nd, 3rd test trajectory. Left: Compliant PVA samples, Right: Rigid PVA samples.

5.3.2 General Trends in Friction Behavior

Tested PVA samples exhibit some similar behavioral patterns, which can be conveniently used for overview description and categorization of individual samples.

As observed above, frictional responses at different speeds are different depending on whether the speed gradually increases (0-max) or decreases (max-0). Increasing speed results in steeply increasing friction at low shear velocities of 10-30 mm/s. Beyond that, the coefficient of friction continuously decreases up to 1000 mm/s. On the other hand, if the initial speed was 1000 mm/s and subsequently decreased, friction was at least 1/3 smaller than for 0-max. Additionally, some recurring frictional patterns are observed. Looking closely at the frictional data, most of the data follows up a concave trajectory, however in some areas, the trajectory changes to convex. For further evaluation, the first inflex point at low speed and stationary point (maximum value) of each sample was recorded in Table 5-2 and indicated as colorful dots in frictional graphs.

Table 5-2: left: Transition points (TPs) of COF-mm/s curve. 1st TP (inflex point), 2nd TP (maximum value), right: Standard deviation of the TPs.

			$10^{-4}\ mm/s$			$10^{-5}\ mm/s$			$10^{-5}\ mm/s$			$10^{-6}\ mm/s$	
			FT	**CP06**	**LM**	**CD**	**CP24**		**FT**	**CP06**	**LM**	**CD**	**CP24**
0-max	1st TP	PBS, 5 N	2.9	2.9	1.6	0	2.5		4.6	14.3	5.0	0	4.1
		PBS, 10 N	1.9	1.5	2.1	0	0		2.4	5.9	4.8	0	0
		Protein, 5 N	16.4	9.5	7.8	9.2	6		27.1	11	8.5	18.2	6.4
	2nd TP	PBS, 5 N	38.2	35.6	13.2	7.9	9.4		0	3.7	2.6	1.2	0
		PBS, 10 N	31.7	41.6	24.0	14.0	15.0		9.5	4.7	4.6	1.5	0
		Protein, 5 N	21.0	18.8	15.0	6.4	4.8		4.2	4.4	0	0.7	0.9
			FT	**CP06**	**LM**	**CD**	**CP24**	1 mm/s	**FT**	**CP06**	**LM**	**CD**	**CP24**
max-0	2nd TP	PBS, 5 N	24.0	15.1	7.7	2.2	2.4		4.6	6.4	1.8	0.2	0.3
		PBS, 10 N	8.8	15.3	8.8	2.3	4.6		2.5	2.9	0.9	0	1
		Protein, 5 N	3.8	0.2	0.2	0.8	0.9		2.6	0.1	0.1	0.2	0.2

1 mm/s

A general frictional behavior observed was plotted in Figure 5-15. Based on aspects like the position of TPs, or modulus of elasticity, introduced PVA samples were sorted into two categories: rigid (CD, CP24) and compliant (FT, CP06, LM). Figure 5-15 a) shows how the two categories vary in frictional responses. The compliant category of hydrogels shows overly high COF, and TPs are located at higher velocities. On the contrary, for rigid hydrogels, friction was observed to be smaller and TPs happened at lower velocities. Figure 5-15 b) separates the influence of individual PVA samples and focuses only on how the separate experimental components (loading, lubricant) influence the frictional behavior. On average, the COF was lower at a 10 N load than at a 5 N load, as expected. Protein lubricant always contributed to higher values of COF and prolonged the trajectory change (see TPs) at low shear. In contrast, 2nd TP was shifted to slightly smaller velocities. Friction force was proportional to the presented COF values – an exception was captured at PVA FT where the increased F_T could relate to heavy plastic deformation seen at the FT samples, Figure 5-15 c).

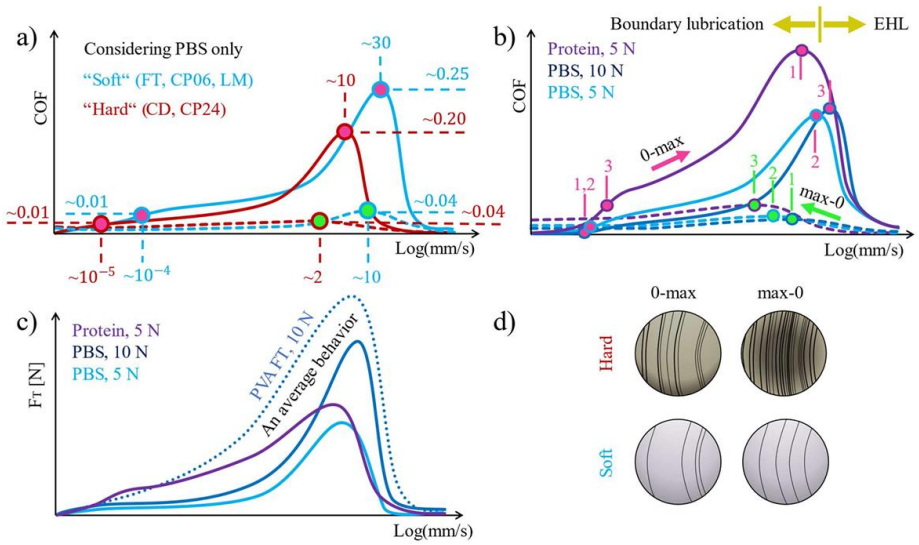

Figure 5-15: An observed general behaviors of a) rigid and compliant PVA hydrogel, b) load (5 N, 10 N) and lubricants (PBS, protein), c) friction force (FT), d) Observed PVA surface damage after friction test.

5.3.3 Wear Analysis of PVA samples

Over the testing of various PVA samples at different speed rates (0-max, max-0), several wear patterns were repeatedly observed. Importantly, no significant/persuasive change in the wear track was observed under different loading conditions or lubricants. Although some changes in irregular patterns (e.g. different wear rates) were spotted, their repeatability was poor, and therefore excluded from further evaluation.

As mentioned earlier, all samples could be sorted into compliant or rigid categories. Similarly, as both categories differed with COF or modulus of elasticity, they exhibited different wear damage as well. Figure 5-16 a) illustrates that PVA FT failed to withstand the applied load, resulting in permanent plastic deformation. Other compliant representatives have proven to be both load- and wear-resistant, where the contact area was often impossible to distinguish from non-worn surfaces. Roughness at the contact area has improved (more at max-0), see Figure 5-16 b). Rigid hydrogels (CD, CP24) have notably more wear scratches. Interestingly, at max-0, scratches were excessively more severe than for 0-max, and roughness increased accordingly.

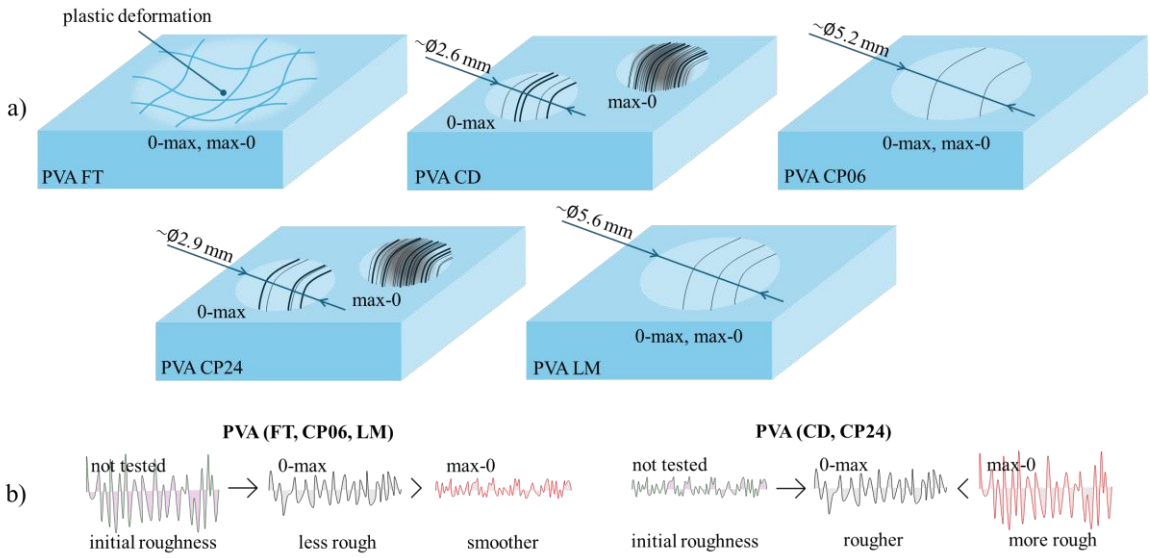

Figure 5-16: Significant wear behavior for tested PVA samples. a) An illustration of observed wear tracks. b) Illustrative roughness changes at different rate speed rate.

Table 5-3 evaluates the measured roughness, which was referred to in Figure 5-16 b). Unlike in the case of compliant samples, where the roughness of the contact area decreases after the friction tests, rigid hydrogels, having initially very smooth surfaces, exhibited increased roughness by at least 2 folds.

Table 5-3: Roughness evaluation for tested PVA samples.

$Ra_{average(5)}$, (SD_{Ra})

FT	CD	CP06	CP24	LM
		not tested		
2.33, (0.87)	0.24, (0.18)	1.53, (0.38)	0.19 (0.05)	1.37 (0.21)
		0-max, **5 N**, PBS		
1.86, (0.20)	0.41, (0.11)	1.20, (0.34)	0.44, (0.25)	1.12, (0.28)
		max-0, **5 N**, PBS		
1.64, (0.24)	0.70, (0.25)	1.13, (0.40)	0.50, (0.11)	1.38, (0.31)
		0-max, **10 N**, PBS		
2.43, (0.54)	0.42, (0.20)	1.17, (0.40)	0.50, (0.07)	1.30, (0.18)
		max-0, **10 N**, PBS		
1.60, (0.19)	0.79, (0.14)	1.04, (0.20)	0.65, (0.09)	1.20, (0.39)
		0-max, 5 N, **protein**		
2.35, (0.36)	0.35, (0.10)	1.29, (0.14)	0.32, (0.05)	1.57, (0.42)
		max-0, 10 N, **protein**		
2.05, (0.24)	0.79, (0.19)	1.35, (0.18)	0.93, (0.32)	1.36, (0.53)

5.4 Results description of pHEMA and PVA samples

This chapter summarizes the results of the 2nd experimental part, describing the results of the selected PVA samples (PVA CP06, PVA LM) – the selection is explained is Discussion chapter. The results of pHEMA samples are included in the thesis of Bc. Jan Gregora. The comparison of those two different hydrogel materials is discussed in the follow-up chapter.

5.4.1 PVA CP06 hydrogel

Reciprocating friction tests of the PVA CP06 have shown a friction at extremely low levels (0.006 – 0.016). Figure 5-17 left, displays the frictional results with cartilage pin. Throughout the 1800 sec (30 min) testing, the friction was kept constant with a very low average deviation, starting with COF 0.0071 (SD: 0.0010) and finishing with COF 0.0063 (SD: 0.0005). The lowest COF (0.0054) was measured when very smooth counter surfaces were slid.

Sliding experiments with a cartilage pin exhibited no visible wear. Therefore, a CoCrMo pin with an artificially increased roughness to 530 nm was used. The five-hour (18000 sec) wear test results are shown in Figure 5-17 right and Figure 5-18. The COF curve had an increasing trend with an average COF value 0.0114 (SD: 0.0027) at the start and 0.0164 (SD: 0.0054) at the end of the test. While at the experiments with cartilage pin no wear appeared, CoCrMo left a visible scratch, see Figure 5-18 left. A comparison of worn and non-tested samples is shown in Figure 5-18 right. The computed area loss ranged from 0.17 to 0.27 mm^2. Due to the natural hydrogel drying while the area was scanned, calculated area loss might not be caused only due to the wear but shape change at scanning too. Each 2 x 10 mm area took 10 – 30 min to scan. The width of the worn area is around 6 mm (note: ⌀9.7 mm pin).

The surface smoothness and flatness of a hydrogel were difficult to separate. A small surface shape imperfection had a visible impact on the result value of COF value. The COF pattern shown in Figure 5-17 displays only the results of best-performed samples.

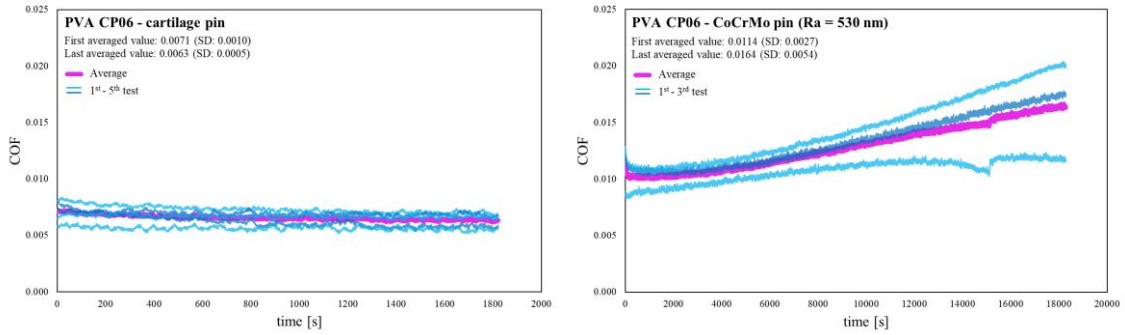

Figure 5-17: The results of the reciprocating friction test of PVA CP06 – cartilage (left) and PVA LM – cartilage (right)

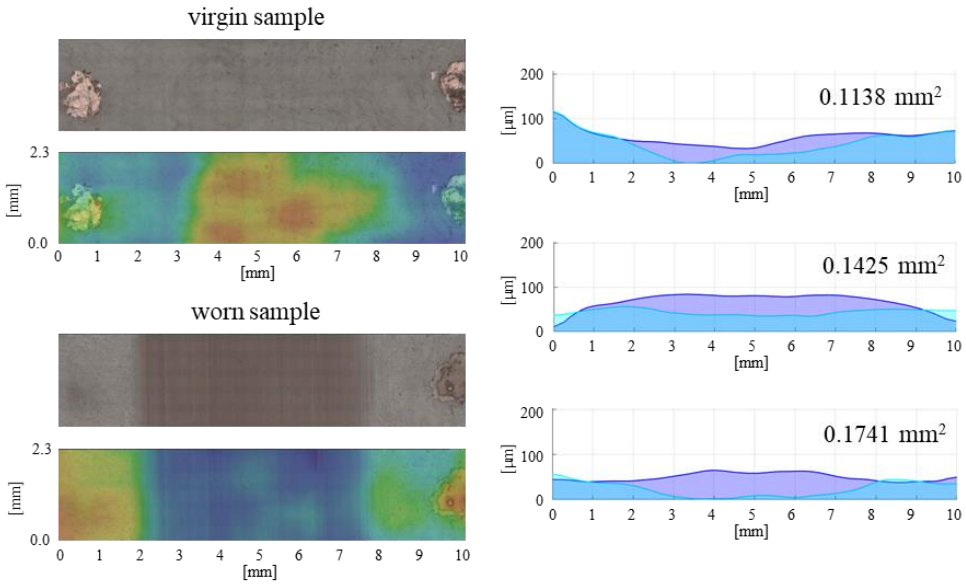

Figure 5-18: Observations done by VHX. left – Scanned area of a virgin and worn PVA CP06 sample, right – Surface profiles of a virgin/worn sample and calculated volume loss.

5.4.2 PVA LM hydrogel

Compared to PVA CP06 – cartilage results, the COF values were kept slightly higher (start: 0.0090 (SD: 0.0006), end: 0.0081 (SD: 0.0006)) and similarly constant over the 30 min testing, see Figure 5-19 left. Unlike the results with CP06, PVA LM samples against cartilage pin exhibited few distinct scratches on the otherwise virgin-like surface.

Increasing friction during the 5 hours of testing was observed when a roughened CoCrMo pin slid against PVA LM. Averaged COF of 0.0134 (SD: 0.0013) at the beginning of and 0.0151 (SD: 0.0016) at the end was observed, Figure 5-19 right. The initial fluctuation at one of the COF datasets was likely caused by some impurities or a different SF lubricant batch used during measurement. The comparison of worn and non-tested areas is shown in Figure 5-20 left. As for the CP06, the CoCrMo pin left a visible scratch on the surface. The estimated area loss after the sliding was between 0.20 – 0.30 mm^2; however, the shape change while surface scanning is likely different from CP06 due to a laminar FT/CD arrangement. An example of a combination of drying deviation and manufactured caused curved cross-section is seen in Figure 5-20 top-right – the sample was used for the friction test because of its longitudinal smoothness (essential for low friction). The transverse wear track is around 7 mm wide.

As for the CP06, the friction of the PVA LM sample was greatly influenced by its shape. The results displayed in Figure 5-19 represent samples with a smooth longitudinal profile. By the presented observation of the two PVA samples, it cannot be clearly distinguished which surface exhibited severe wear damage. Thus, same wear rate of the two samples was considered for further evaluation.

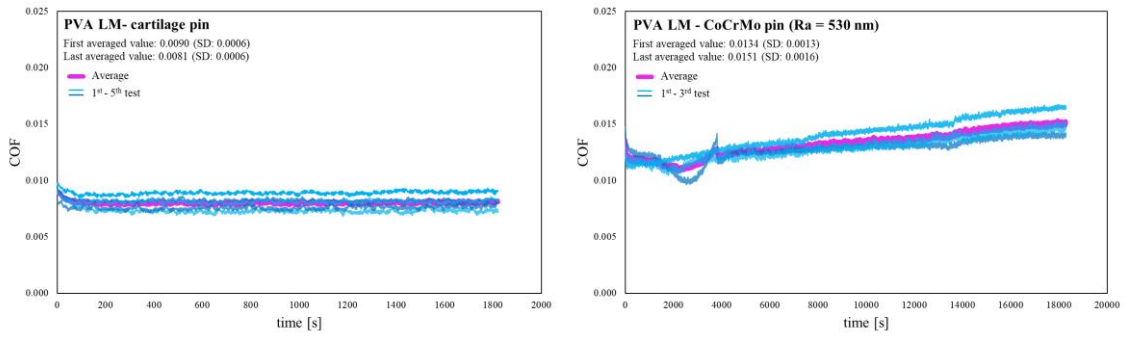

Figure 5-19: The results of the reciprocating friction test of PVA LM – cartilage (left) and PVA LM – cartilage (right)

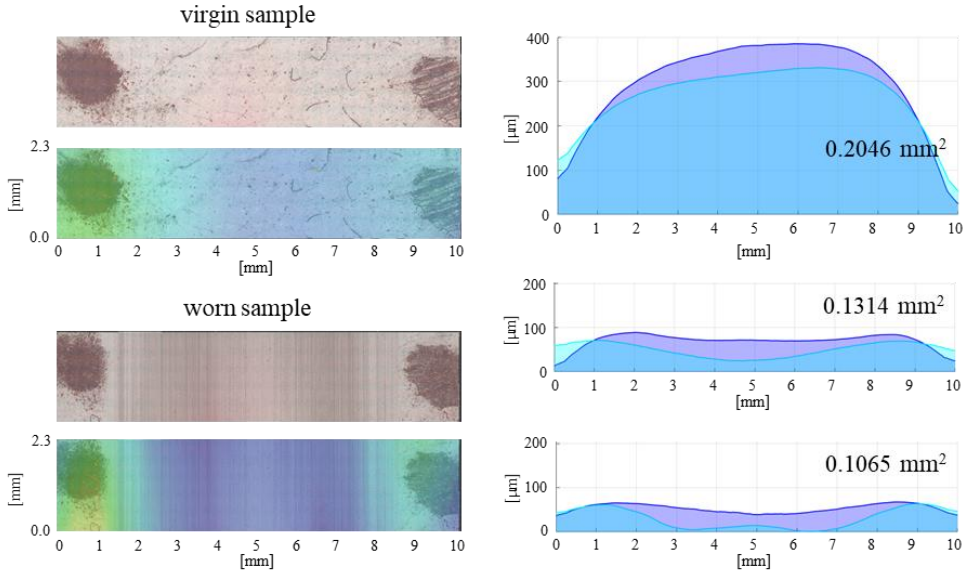

Figure 5-20: Observations done by VHX. left – Scanned area of a virgin and worn PVA LM sample, right – Surface profiles of a virgin/worn sample and volume loss.

6 DISCUSSION

6.1 An overview of the experiments and research remarks

The present thesis consisted of two experimental units. A tribological investigation (1st experimental part) was conducted to evaluate the influence of varying stiffness on wear, alongside an effort to deepen the understanding of lubrication mechanisms in hydrogels. Subsequently, long-term wear tests (2nd experimental part) of the selected PVA samples were utilized and compared with the results of pHEMA hydrogel. This complex work aimed to evaluate PVA hydrogel material potentially eligible for cartilage implants and outline the properties needed for further cartilage-like material development.

For clear arrangement of the work, four questions and hypotheses were laid out. 1st – 3rd hypothesis concerns the 1st experimental part, the 4th hypothesis the long-term wear test, involving different experimental set-up.

An important knowledge outcome of the 1st part of the thesis lays on the foundations of the knowledge of the polymer chains believed to play an important part in hydrogel lubrication. Gong et al. [23] proposed an adhesion-repulsion lubrication model for hydrogel materials,discussing the relationship between friction and polymer brush properties (e.g. length, cross-linking density, adhesion, etc.). The study also commented that the PVA hydrogel has a weak attractive interaction (by adhesive dangling chains) with a glass surface – consequently increasing friction. Yarimitsu et al. [32] reported on the PVA LM hydrogel's manufacturing conditions for creating an optimal extent of protruding PVA polymers contributing to the creation of a wear-resistant hydration layer. Also, reporting that low and excessive cross-linking results in wear progression. Miao et al [55] studied a conformation of polymer brushes under shear. It was found that polymer brushes tilt and stretch along the direction of the hydrodynamic flow. Based on that and some other studies [43, 56] concerning behavior of polymer chains under shear, a novel boundary lubricating mechanism was proposed involving the influence of uncross-linked polymer chains dispersed on the hydrogel's surface.

6.2 Evaluation of the effect of different stiffness on wear

The determination of the influence of different hydrogel stiffness on wear, as a response to different manufacturing conditions, was in accordance with the proposed 1st hypothesis and in the contraction with the 2nd hypothesis. The experimental conditions of the 1st and 2nd hypotheses remained the same, emphasising the protein lubricant at 2nd hypothesis.

More rigid PVA hydrogels (CD, CP24) were confirmed to exhibit a higher wear rate than the compliant samples (CP06, LM, FT). The spinning glass ball always imprinted a visible sliding area into the rigid samples with scratches. Such damage was hard to spot at the compliant materials, leaving the surface with only a few scratch lines or intact. No clear boundary of the contacting surface was observed for CP06, which was partially visible for LM. An interesting finding was observed when comparing the accelerating and decelerating experiments for the rigid surfaces. The surface damage created during decelerating tests was much more severe than that for the accelerating case, Figure 6-1.

The probable cause of such behavior, as well as enhanced adhesion reducing a ploughing wear, is discussed within the boundary lubricating mechanism in the following subchapters.

Figure 6-1: Selected worn PVA samples for 1st hypothesis evaluation, left – PVA CP24, right – CP06

The stiffness response on wear when protein solution was present in the contact was contrary to the 2nd hypothesis – no additional surface protection for rigid samples was observed with protein lubricant. The protein solution tends to support the observations noticed in the experiments with PBS lubricant – sometimes inducing higher wear at rigid samples and reducing it for compliant materials, with the exception of (CP06, 0-max), as commented in the Limitation chapter.

According to the 2nd hypothesis, the rigid surfaces were supposed to be better protected against excessive wear due to the formation of a boundary protein layer. The LSM images showed no such result. As Figure 6-2 illustrates on the selected samples, no wear decrease was observed when protein was used instead of PBS lubricant. The prediction was based on the findings made by [20, 57] discussing adequate albumin and γ-globulin content to form such a layer. Compliant materials were anticipated to increase wear due to higher elasticity disrupting the film formation. The layer is believed not to have formed at either surface. Instead, the proteins likely formed the agglomerates which did not adhere to the surface, thus not influencing the wear. As the graphs in chapter 5.2 show, protein solution increased the COF at all PVA samples. That is due to the rise in adhesion of the overall sliding interface when protein was present. Such adhesion does not promote the polymer chain adhesion believed to be responsible for surface protection. The probable reason why the protective layer was not formed is due to a different experimental configuration used in the studies (reciprocating tests) [19, 57, 58] reporting such an effect and the present thesis (spinning ball on the stationary contact).

As observed, the protein solution had no clear influence on the wear. The hypothesis should be extended to determine the influence of SF's constituents and SF itself. Furthermore, a Fourier-transform infrared spectroscopy (FT-IR) shall be used to determine the protein absorbance on the hydrogel surfaces. FT-IR microspectroscopy device (Nicolet iN10 IR, Thermofisher, USA) was used in the thesis for such determination. However, no reliable data were obtained (due to an inappropriate measuring method), therefore, they were excluded from the thesis.

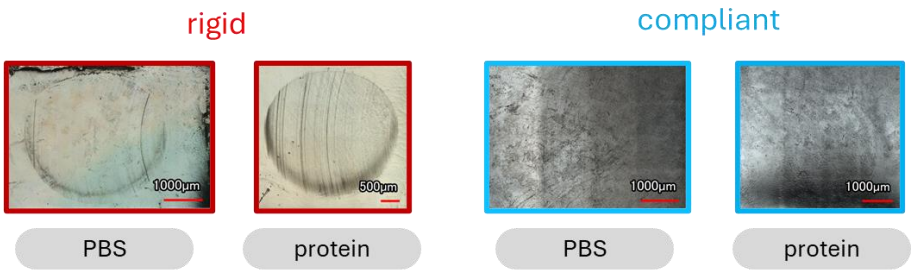

Figure 6-2: Selected worn PVA samples for 2nd hypothesis evaluation.

Moreover, the impact of higher load (10 N vs. 5 N) on the COF and wear was assessed. As Figure 5-16 b), c) shows, a 10 N load induced a lower COF for the low-speed region (until COF peak). The lower friction, compared to 5 N testing, is due to residual interstitial fluid pressure from the pre-experimental phase, where probably more time is needed to fully diminish the biphasic effect [7, 10, 13]. Interestingly, the wear rate appears to be more severe at rigid hydrogels and has no effect on compliant materials. PVA FT was excluded from wear assessment due to substantial plastic deformation, transmitting the load directly to the PVA's substrate material.

6.3 Identification of the lubricating regimes on the boundary Stribeck curve

The frictional data obtained with reduced biphasic lubrication exhibited a common course for all PVA samples. The differences lay in the different positions of the T.S.'s (e.g. different position of COF peak). The common COF course at the changing velocity was introduced in Figure 5-16. If the frictional data were shifted at the COF axis (y-axis) into a logarithm scale, the graphs revealed areas where the course of COF changes its trend, such a shift is illustrated in Figure 6-3.

Figure 6-3 shows a trend in COF for the rigid and compliant categories for increasing and decreasing velocity tests. The frictional course at increasing test can be divided into three regions – very low speed (< 10^{-4} mm.s^{-1}), low speed (< 30 mm.s^{-1}) and high speed (> 30 mm.s^{-1}). In the very low speed region, the friction increases linearly. The linearity might correspond to elastic stretching of protruding uncross-linked polymer chains dispersed on the PVA surface [23], therefore, the friction is labeled as adhesion dominant. Concurrently, rigid hydrogels show none or limited linearity to only a < 10^{-5} mm.s^{-1}, low surface density of the uncross-linked polymers. The low-speed area appears non-linear and rises until the COF's maximum value. Such a pattern is associated with dominant abrasion friction, where surface asperities are in direct contact. After the COF's peak, friction suddenly decreases. This behavior is probably caused by the elastohydrodynamic (EHL) effect, providing partial and later full surface separation. Based on these assumptions, the frictional pattern of decreasing friction is after the start (1000 mm.s^{-1}), attributed to the EHL regime, followed by abrasion friction after the COF's peak. Since no linearity is observed in the very-low speed region, no adhesion dominant area is anticipated. Figure 6-3 b) shows different inclinations of the tested PVA samples at a very low speed region. It is assumed that the lower the inclination, the higher the polymer adhesion.

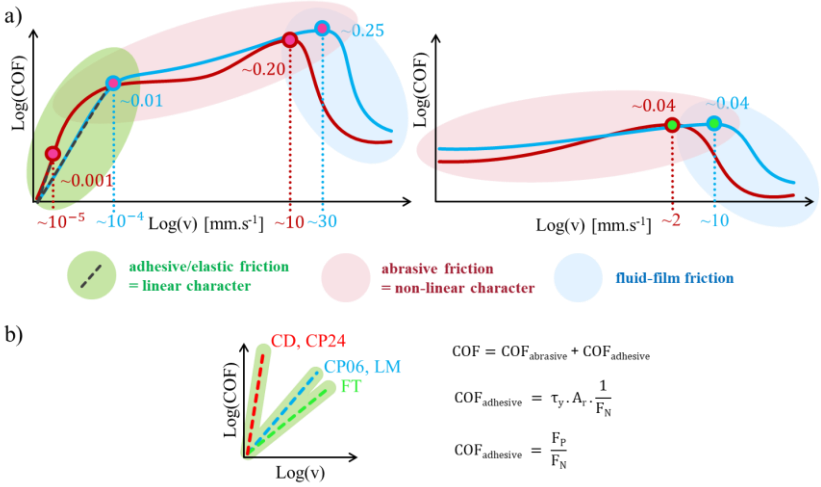

Figure 6-3: Logarithmic illustration of Figure 5-16 – rigid PVA category (red), compliant PVA category (blue). a) classification of lubricating regions with dominant frictional components. b) linear inclination of PVA samples at very low speed. Basic frictional equations illustrating its variables (τ_y, F_P) and constants (F_N, A_r) – where τ_y stands for yield strength, F_P ploughing force, F_N normal force, A_r real contact area. Note: The τ_y is anticipated as the variable responsible for the linear character, whereas F_P for non-linar COF growth.

Based on the assumptions made in Figure 6-3, a boundary lubricating mechanism emphasising the lubricating influence of dangling polymer chains was introduced.

In relation to the regions introduced at Figure 6-3, the frictional patterns in Figure 6-4 are sorted into: static adhesion – where the COF increase was linear, dynamic adhesion – with dominant abrasion friction, and EHL lubrication. The patterns are applied similarly in reverse motion. Convex areas are understood as a zone where one lubricating mechanism is active, whereas the dark concave areas are recognized as transitions between each regime.

When the friction is initiated at a low speed, low friction is believed to be caused due to dangling polymer chains adhering onto the opposing sliding surface, Figure 6-4 a). The sliding surfaces are then separated due to the polymer elastic stretching [55]. The low speed ($0 – 10^{-4}$ mm.s^{-1}) consequently provides enough time for polymer relaxation and adhering again after excessive stretch and detach [23]. After the sliding velocity is shifted to the dynamic adhesion ($10^{-4} – 30$ mm.s^{-1}) the polymer adhesion is reduced as the time to re-adhesion is limited. Lack of adhered polymers results in direct body contact – inducing wear as the roughness plough through the body. The sudden fall of COF at high-speed region is explained by the hydrodynamic effect, where the spinning ball creates an EHL wedge, consequently providing surface separation.

The reason for low friction when decelerating motion might be due to a forced rehydration [16] while in the EHL regime, see Figure 6-4 b). The fluid pressure partially rehydrates the hydrogel's pores and increases interstitial fluid pressure, which is originally in equilibrium with the applied load from the pre-experimental phase. The rehydrated surface induces secondary biphasic lubrication, causing the COF to decrease as the speed gradually decreases. The secondary biphasic lubrication provides partial fluid load support and a little surface separation.

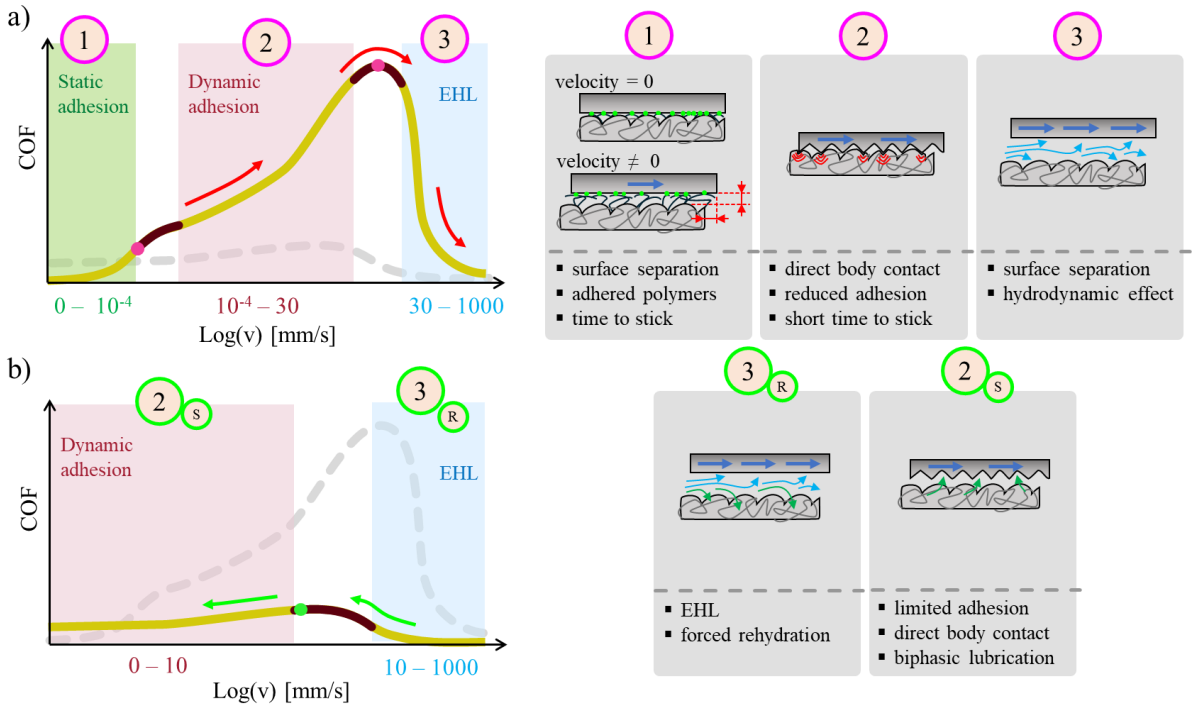

Figure 6-4: Boundary lubricating mechanism. a) accelerating speed, b) decelerating speed

In connection with the just introduced mechanism (Figure 6-4) an alternative explanation justifying the different COF pattern for 0-max and max-0 motion is introduced in Figure 6-5. The major COF difference is seen at tangled polymer chain structure [55, 56], causing resistance to motion as the asperities of the opposing surface plough through during movement. Tangled structure at low speed causing COF to grow as the asperities slide past and stretch and tilt the tangled polymers. When the motion shifts to high speed (EHL), the polymer brush is expected to untangle and align with the direction of movement. Such polymer arrangements diminish the resistance to movement; thus, the COF remains low and does not increase outside of the EHL. Moreover, the resistance decrease is expected to bring the sliding asperities close to the surface, causing wear. Thus, tangled polymers are also expected to protect the surfaces from excessive wear.

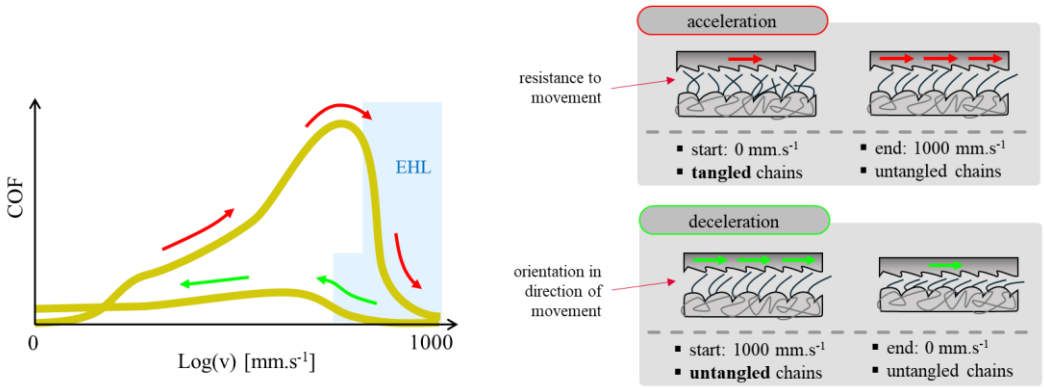

Figure 6-5: Stretch and tilt polymer brush.

6.4 The lubricating mechanism in the context of the results

The proposed lubricating mechanism should correspond with the observed results and explain the measured data. It should also provide enough reasoning for answering a question related to the 3rd hypothesis.

Looking back at the common course of COF at Figure 5-15 a), the following important observations are made. Rigid hydrogels exhibit lower friction, and their COF peak (2nd T.P.) is at a lower velocity than for compliant materials. However, lower apparent COF results of rigid materials are accompanied by higher wear rates. Moreover, a significant wear increase at the deceleration tests for rigid materials, where COF remained very low and for compliant materials left very little damage, is rather curious and suggests a particular mechanism shift on the sliding superficial surface.

The apparent change in the COF peak position among PVA samples is due to the different elasticity of each material. Compliant materials have a smaller EHL region, as the smaller contact pressure creates a weaker hydrodynamic wedge at the interface. Proteins and lower load further prolong the EHL area into a small speed region.

The resultant behavior, typical for each introduced PVA sample, differs due to a different physiological property given by different environment (temperature, humidity, time) while cross-linking. Besides the dominant water component, the solid phase composes of molecular chains and micro-crystallites – a bonding point of molecular chains [59]. If the resultant structure is rather stochastic (non-homogeneous) [13], mechanical properties are poor, any homogenous pattern within the structure thus improves its strength. Such stochastic structures are found at PVA FT, where, due to low fabricating temperatures (-20 °C, -4 °C) microcrystalline are grouped together and connected with long tangled polymer chains (Figure 6-6), the structure exhibits large plastic deformation, as the results showed. Exposure to higher temperature (60 °C, 80 °RH), hydrogels' (PVA CD, CP24) structure contains tight-stretch polymers – stiffening the whole structure. Longer time exposure at high temperatures (e.g. PVA CD) also makes micro-crystallites grow in size and in numbers providing, higher structure homogenization – further increasing the structure's strength (

Table 5-1). Consequently the water content and swelling ratio are reduced. As both extreme approaches do not provide the surface with the wear-resistance needed, their combination, such as PVA CP06, LM, proved to be the way. The crosslinking process was developed by Yarimitsu et al. [32, 33], where the process apparently allows for decent structure stiffness, yet the polymers remain less stretched and more tangled. Uncross-linked, tangled polymers are then expected to protrude onto the hydrogel's surface and form a wear-resistant layer working in accordance with the proposed lubricating mechanism.

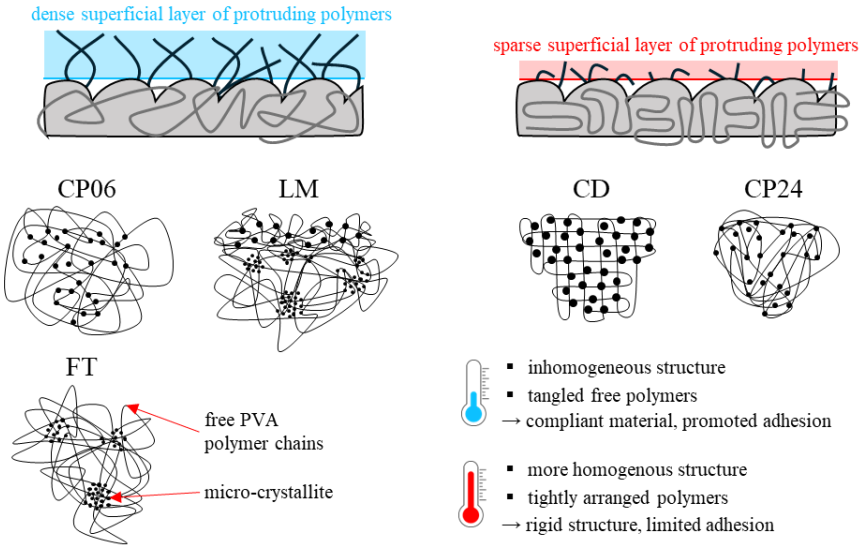

Figure 6-6: A proposed structure of PVA samples.

The 3rd hypothesis suspects that the wear is caused by the transition zone between elastic friction and hydration (EHL) lubrication. General data says PVA CP06 and LM exhibit low wear no matter the conditions, whereas PVA CP24 and CD exhibit wear under any conditions. The superior property driving the wear-resistance is believed to lie in the extent of cross-linking polymers protruding into the superficial surface. An optimal cross-linking provides a dense layer of the polymer brush-like structure, promoting elastic friction, and tangled polymers hinder direct body contact. High level of cross-linking results in the sparse brush-like layer, although fewer adhesive protrusions result in less COF, the layer is unable to effectively separate the surfaces or induce EHL rehydration. This theory corresponds with the results gained. Rigid hydrogels with a high extent of cross-linking exhibit wear at every configuration, especially with decreasing speed, where lack of elastic adhesion and untangled oriented polymers are unable to separate sliding surfaces. The speed region where those two mechanisms are disabled for both rigid and compliant materials is at the dynamic adhesion – which corresponds with the proposed hypothesis.

Since further testing to support the hypothesis could not be carried out (see the Limitations section), the run-in phase results (Figure 5-14) may serve as partial evidence. During this phase, an increased COF was observed in the dynamic adhesion region for rigid PVA samples, indicating run-in wear. Also, compared with virgin samples, rigid hydrogels showed increased roughness, whereas at compliant materials, roughness tends to decrease – possibly indicating a gradual loss of the protruding polymers.

6.5 Long-term wear tests of the selected PVA and their comparison with pHEMA material

As mentioned earlier, the 2nd experimental part merges the knowledge of PVA materials shared with Prof Yoshinori Sawae's research group (Kyushu University, Japan) and Jan Gregora's thesis dealing with pHEMA materials, based on cooperation with Lucy Vojtová's research group (CEITEC, Czechia). For the creation of a scientific publication, the two master's theses were merged and their experimental methods unified.

To compare PVA samples with pHEMA (air) and pHEMA (N_2), the two best-performing PVA samples, CP06 and PVA LM, identified in the 1st experimental part, were selected. Regarding the corresponding 4th hypothesis formulated for the separate PVA sample testing, it was predicted that CP06 would exhibit less wear than LM due to its multi-stage cross-linking, which provides higher strength. In contrast, the less crosslinked LM was expected to maintain a low COF, due to its well-hydrated surface formed by a dense polymer brush. The protruding polymers are not expected to play a surface-protective role in biphasic lubrication, as they do in boundary lubrication. Instead, only abrasive and viscous friction are anticipated. Moreover, the polymer chain radius is in the order of tens of nanometers [23], whereas the roughened CoCrMo pin has a surface roughness of Ra = 530 nm, which would easily penetrate and disrupt the boundary brush layer, see Figure 6-7.

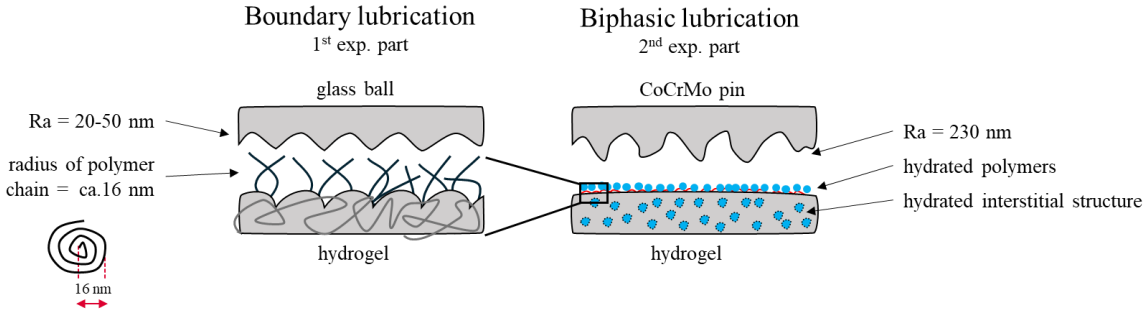

Figure 6-7: Illustrative comparison between boundary and biphasic lubrication and body interactions. Radius of polymers taken from Gong et al. [23].

The predicted low COF of PVA LM was maintained at a level comparable to that of CP06, consistent with findings previously reported by Yarimitsu et al. [32, 33]. Experimental results confirmed that both PVA samples exhibited similarly low COF values, demonstrating nearly superlubricating behavior (≤ 0.01) against both cartilage and roughened CoCrMo counter surfaces (see Figure 6-8). This observation is in good agreement with earlier studies on the same PVA materials [30, 32, 33]. The expected higher wear of LM hydrogel (as compared to CP06) was not confirmed, as it appeared to be more or less the same. The surfaces seem to be worn evenly, VHX data tends to support such observation, see Figure 6-9 (PVA CP06) and (PVA LM). The likely reason for the similar results (contrary to the prediction) is that as long as the less complex crosslinking provides structure with decent strength and surface hydration (both from interstitial structure and hydrated polymers) biphasic lubrication performance is good. As Yarimitsu [30] and Sakai et al. [12] pointed out in the reciprocating test with PVA CD and LM, good performance comes from smaller micropores, maintaining high load support if rehydrated. If the surface is not properly rehydrated, a share of the solid load support on lubrication increases. In that matter, Yarimitsu et al. also indicated PVA LM has higher wear resistance than PVA CD due to a lack of surface hydration. Lack of surface hydration occurs at overly homogenized PVA CD and PVA CP24 – such findings were in confirmed at the 1st experimental part, (where interstitial fluid load support was diminished), leaving higher wear on CD and CP24, compared to less homogeneous samples.

Moreover, the PVA LM used for the reciprocating testing was fabricated under a lower temperature (8 °C, 50 %RH) than in the 1st experimental part (20 °C, 50 %RH) – the adjustment was based on a direct consultation with Dr. Seido Yarimitsu, when a manufacturing issue occurred. Lower temperature offers better material shape stability and better frictional properties [32].

PVA LM material, as one of the best-performing materials, sustains a major waste during production and subsequent smoothness selection. Since the material consists of two layers with different degrees of polymerization, the interlayer adhesion is difficult to guarantee. The upper (less cross-linked) layer is exposed to the cast-drying process, causing delamination and a bumpy surface. The complex CP06, consisting of only one layer, does not exhibit such issues. A manufacturing stability and very good frictional/wear performance make the PVA CP06 the best option for further development and fabrication process optimization.

It is important to state that the comparison of the worn areas (volume loss) showed ambiguous results – further elaborated in the Limitations chapter. Therefore, the 4th hypothesis cannot be supported by solid data, but rather on visual observations, which frankly are quite common for hydrogel assessment according to available literature.

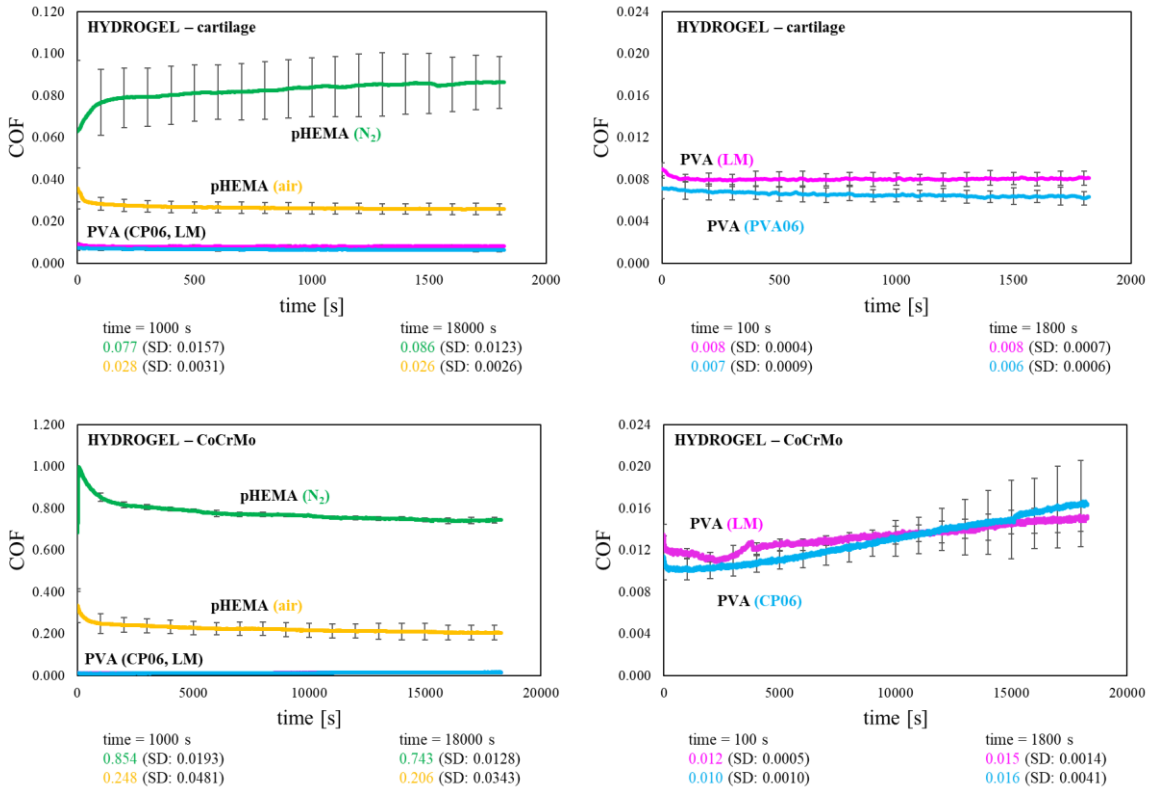

Figure 6-8: Friction comparison of reciprocating tests of PVA and pHEMA hydrogels a) sliding tests with cartilage pin, b) sliding tests with CoCrMo pin.

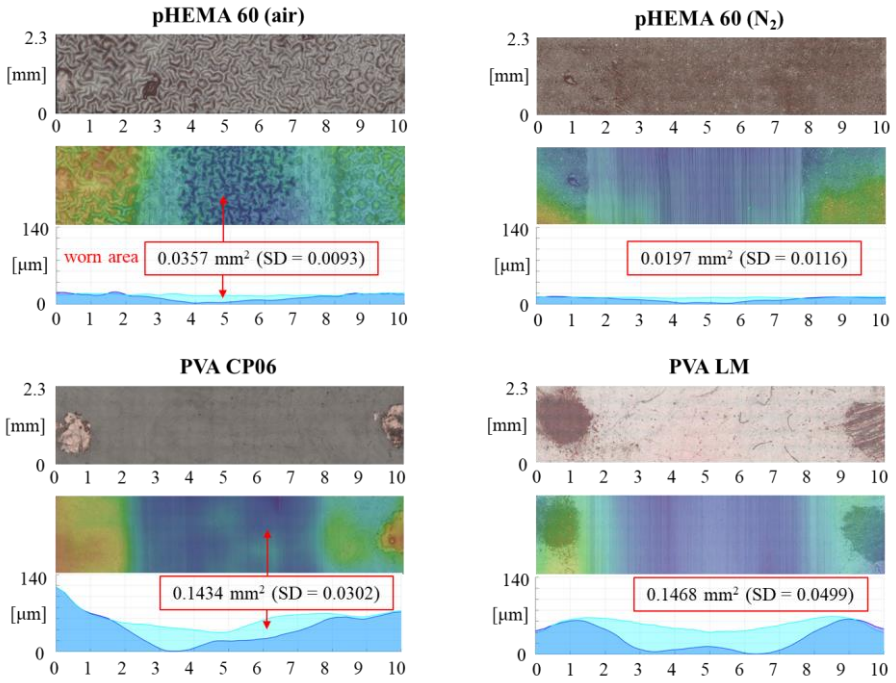

Figure 6-9: Selected images and their probable volume loss after wear test (VHX images).

A comparison of pHEMA and PVA materials unveiled the superiorly low COF (~0.010) of PVA-based materials and showed their insensitivity to the opposing sliding material. In contrast, pHEMA showed a strong COF dependence (by order of magnitude, N_2: 0.026/0.206 and air: 0.086/0.743) on whether the sliding material was cartilage or a roughened CoCrMo pin. Like for the PVA samples, where the manufacturing conditions had a major impact on resultant tribological properties, the pHEMA was greatly influenced by the ambient atmosphere during cross-linking, resulting in different surface topography, see Figure 6-9. The pHEMA 60 (air) crosslinked under an air environment resulted in a bumpy surface, whereas pHEMA 60 (N_2)'s surface (manufactured under nitrogen atmosphere) resulted in a smoothness comparable to PVA materials. Despite the high COF, the wear rate of pHEMA seems to be smaller (e.g., N_2: 0.036 < CP06: 0.143). A few studies testing pHEMA materials with similar sliding conditions were published [60, 61], of which Freeman et al. [61] conducted a series of experiments of pHEMA (with the same crosslinking method) indicating wear depth 0.02 to 1.32 mm depending on various conditions (e.g., crosslink density and load) after just 30 min. The wear indicated at pHEMA 60 (air), (N_2) showed wear depth ~0.01 mm against the roughened CoCrMo pin and after 5 hours of sliding.

hydrogel	E	Ra	water content	permeability
PVA CP06	0.51	1.53	73	$\sim 1.10^{-15}$
PVA LM	0.63	1.37	73	$\sim 1.10^{-15}$
pHEMA 60 (air)	0.93	6.68	61	$9.10^{-15} - 5.10^{-15}$
pHEMA 60 (N_2)	0.83	1.53	54	$2.10^{-14} - 3.10^{-14}$
units	[MPa]	[µm]	[%]	$[m^4.(Ns)^{-1}]$

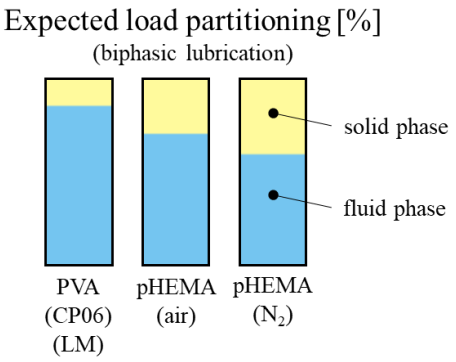

Figure 6-10: Comparison of properties influencing the tribological properties of hydrogels at reciprocal test. Note: Ra data comes from virgin samples, permeability of CP06 and LM are estimated based on [33, 34]. Expected load partitioning estimated according to [62].

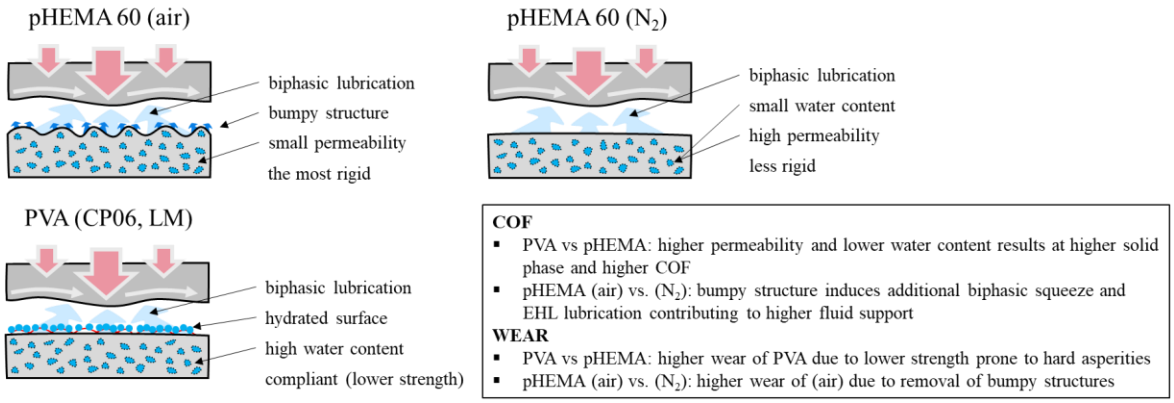

Figure 6-11: Explanation of long-term wear tests results with CoCrMo pin.

To conclude and explain the observed performance of the tested hydrogel samples, Figure 6-10 and Figure 6-11 were created. The difference between the presented PVA and pHEMA lays in the different water content. The 12 – 19 % difference in water content likely makes a significant difference in COF compared to pHEMA. The low COF of CP06 and LM is enhanced via well-hydrated polymer chains on the surface [32, 33]. Such surface hydration is possibly limited for pHEMA, similar to PVA CD, as mentioned earlier. pHEMA 60 (air)' intermediate COF is a result of not only a higher water content (pHEMA (N_2) had the lowest) but also the bumpy structure, inducing additional biphasic squeeze and EHL lubrication – behaving as a water reservoir. The highest COF at pHEMA (N_2) is a combination of high permeability and low water content, resulting in low fluid support share on lubrication [34, 62]. On the other hand, pHEMA (N_2) demonstrated the lowest measured wear, likely due to its initially smooth surface and adequate strength. In contrast, higher wear observed in low COF pHEMA (air) is likely attributed to the abrasion of bumpy protrusions. It is expected that once these protrusions are worn down, the wear rate will decrease, partly due to their higher strength compared to pHEMA (N_2). High wear of PVA might be due to either lower strength, making PVA more prone to hard asperities or due to an inappropriate wear measuring method (discussed in the Limitation).

In summary, the best performing materials – PVA materials and pHEMA 60 (air) – possessed higher water content and lower permeability (note: cartilage's permeability is 1.10^{-15} – 1.10^{-16} mm^4. $(Ns)^{-1}$). The synthesis of good mechanical properties and a resilient lubricating layer, combining strength, a highly hydrated, easy-shear layer and a permeable layer often appears contrary [44]**.** However, the presented results indicate that good lubricity could be retained at high-strength hydrogel if the CP06' and pHEMA (air)' fabrication parameters are further advanced.

The subsequent research could focus on the detailed description of the effect of SF while boundary lubrication with a special interest in polymer protrusions-SF constituents interaction for the development of resilient, easy shear cartilage-like boundary layer. Further improvement in PVA hydrogel fabrication concerning its shape stability is needed.

For the detailed results and discussion on the matter of pHEMA hydrogels, please refer to the thesis (written in the Czech language) of Jan Gregora submitted in 2025 [64].

6.6 Limitations

The present thesis assumes a certain simplification and assumption that should be emphasized and considered for further study concerning a similar topic. The original scope of the work was a simple evaluation and comparison of the five PVA samples for their tribological properties. Certain methods were proposed for such an evaluation. Further, as the results proved eligible for unveiling a more detailed material property, only a minor supplement testing verifying the novel insight was conducted due to the author's time-limited internship at Kyushu University. Frictional experiments were conducted at continuous rotation only, as it was the most convenient approach to measure COF-speed dependance, also aligning with the study of Gong et al. [23] and serving as a springboard for further investigations. To prove the accuracy of the proposed lubricating mechanism, frictional tests should be conducted within the dedicated range of the proposed lubricating mechanism (e.g. dynamic adhesion, or a specific velocity). Also, the continuous rotation does not correspond with the motion in articular cartilage. For further biotribological investigations, oscillatory motion would be more accurate.

A protein solution and PBS were used as lubricants. The absence of the SF or its constituents is needed for additional iteration of the proposed lubricating mechanism as well as hydrogel's stiffness response. The protein solution was used due to its abundance as a molecular constituent in SF. Also, for further biotribologal investigations, other than articulating glass should be considered, as the glass' elastic modulus is much higher than natural articulating surfaces (e.g. hydrogel – polyethylene, hydrogel – cartilage shall be examined). The glass material was used to mimic the adhesion-repulsion lubrication model proposed by the already mentioned study of Gong et al [23].

Regarding the results introduced, strong wear at (CP06, 0-max, protein) configuration, seemingly disrupting the proposed mechanism functioning, might be influenced by the different production batch used in the experiment, where possibly the different climatic conditions influenced the resultant material property. The particular configuration should therefore be remeasured.

A suitable wear measurement technique which anticipates hydrogel's natural drying and compensates for its shape deformation while scanning should be considered. The introduced surface scanning method at the comparative study of PVA and pHEMA materials, concerning surface scanning right after being taken out of water, was found inappropriate as each individual sample took a different time for surface scanning (due to wavy surfaces leading to variable depth of focus), consequently leading to uneven drying. The suggested improvement of the method used would be to unify the hydrogels' water content at a certain low level, using a climatic chamber. With a note that a simple surface image might inevitably be deformed.

At a glance, the PVA surfaces seem to be worn evenly, VHX data tends to support such observation, see Figure 6-9 (PVA CP06) and (PVA LM). However, it is believed that the volume loss method selected for the quantification of wear was inappropriate. During area scanning, the PVA hydrogels exhibit considerable drying, influencing the overall virgin/worn shape. Despite the author's best effort at careful sample selection, the samples were not perfectly flat in direction traverse to sliding. The uneven height strongly influenced the scanning time of each individual hydrogel sample, making it difficult to compare with each other. Improving ambient humidity to slow down sample air drying was considered impractical due to potential VHX damage and water precipitation onto the PVA sample. The PVA sample needs to remain free of water during scanning.

The quantification of the volume loss of hydrogel material in earlier studies is usually evaluated by a simple microscope image and wear scratch comparison [22, 32, 33, 58] or by scanning electron microscope (SEM) [25]. Other methods (e.g., weight loss [60] or contact profilometer [63]) were found inappropriate for the present investigation, due to the overall small wear damage to the tested samples and the issues related to high water content and drying. For any future consideration of volume loss/wear quantification, a different method shall be used.

7 CONCLUSION

The thesis investigated the tribological behavior of PVA hydrogels with varying stiffness and their potential application as cartilage replacement materials. The objective was to assess:

- the influence of different material stiffness on wear
- bring a new insight into boundary lubricating mechanisms

It was found that compliant PVA samples (e.g. CP06, LM) demonstrated superior wear resistance compared to stiffer variants (e.g. CP24, CD), aligning with the hypothesis that lower stiffness enhances surface protection via protruding polymer abundancy responsible for the abrasive wear decrease and better contact pressure distribution. Contrary to expectations, protein lubrication did not reduce wear in rigid samples, likely due to insufficient boundary layer formation under the given experimental conditions (stationary spinning ball against a hydrogel plate). Moreover, considering the manufacturing process, it was suggested that a single-layered hydrogel with tuned crosslinking conditions has better shape stability and more homogenous properties than laminar material, where its non-homogeneity and layer delamination remained a challenge.

A novel boundary lubricating mechanism was proposed, highlighting the role of dangling polymer chains in creating an adhesion-dominant regime at low speeds, transitioning into abrasion and elastohydrodynamic (EHL) lubrication. The findings support the hypothesis that wear is critical during the transition between low speed (static adhesion) and EHL regimes, especially for highly cross-linked samples with sparse surface polymers, see Figure 6-1 and Figure 6-6. The mechanism explains the observed superior wear resistance of PVA CP06 and LM: the shear force is borne by a dense brush of tangled polymers adhering to the opposing surface. Although adhesion decreases at higher speeds, wear remains low – either due to the dense tangled polymer network separating the sliding surfaces, or as a result of secondary biphasic lubrication combined with improved surface conformity when the structure is untangled by the shear (see Figure 6-4).

Further on, the study was extended to reciprocal experiments, with the objective of:

- assessing the PVA performance and wear rate after long-run 5-hours tests
- tribological comparison of PVA and pHEMA hydrogels

Long-term wear tests confirmed the exceptional lubricating performance of PVA CP06, LM hydrogels compared to pHEMA, showing extremely low COF of ~0.01 (Note: pHEMA 0.03-0.70) across cartilage and CoCrMo counterfaces. Regardless of the COF, pHEMA led to a lower wear rate (0.02 mm^2), compared to PVA hydrogels (0.14 mm^2) – attributed to their higher stiffness. However, challenges in wear quantification due to hydrogel dehydration were noted, revealing a fast dehydration of PVA and suggesting the need for improved methods in future studies. PVA CP06 and pHEMA 60 (air) performed the best, due to the fluid support reducing friction and wear (Note: pHEMA 60 (N_2)'s high permeability and low water content led to worse tribological performance, PVA LM´s difficult manufacturability clearly favors CP06).

Overall, the results underscored the importance of optimized cross-linking in developing hydrogel-based cartilage implants, balancing load-bearing capacity with surface lubrication properties.

The observations on the boundary lubrication mechanism from the 1st experiment part were accepted for publication in the Friction journal (April 3, 2025), in a manuscript titled A glance into the boundary lubrication mechanism of PVA hydrogel after the reduction of interstitial fluid pressurization.

Němeček D, Nečas D, Shinmori H, et al. A glance into the boundary lubrication mechanism of PVA hydrogel after the reduction of interstitial fluid pressurization. Friction, 2025, https://doi.org/10.26599/FRICT.2025.9441106

Additionally, a manuscript entitled Towards cartilage-mimicking hydrogels: Biotribological evaluation of pHEMA and PVA-based materials (the 2nd experimental part) was prepared throughout March–May 2025:

Nečas D, Němeček D, Gregora J, et al. Towards cartilage-mimicking hydrogels: Biotribological evaluation of pHEMA and PVA-based materials. Tribology International, 2025, [manuscript in preparation]

8 REFERENCES

[1] LIN W, KLEIN J. Recent Progress in Cartilage Lubrication. *Advanced Materials*. 2021. Available at: doi:10.1002/adma.202005513

[2] JAHN S, SEROR J, KLEIN J. Lubrication of Articular Cartilage. *Annual Review of Biomedical Engineering* . 2016. Available at: doi:10.1146/annurev-bioeng-081514-123305

[3] MOW VC, RATCLIFFE A, a POOLE AC. Cartilage and diarthrodial joints as paradigms for hierarchical materials and structures. *Biomaterials* [online]. 1992. Available at: doi:10.1016/0142-9612(92)90001-5

[4] KORHONEN RK, WONG M, AROKOSKI J, LINDGREN R, HELMINEN HJ, HUNZIKER EB, JURVELIN JS. Importance of the superficial tissue layer for the indentation stiffness of articular cartilage. *Medical Engineering and Physics*. 2002. Available at: doi:10.1016/S1350-4533(01)00123-0

[5] REYNAUD B, QUINN TM. Anisotropic hydraulic permeability in compressed articular cartilage. *Journal of Biomechanics*. 2006. Available at: doi:10.1016/j.jbiomech.2004.10.015

[6] DESROCHERS J, AMREIN MW, MATYAS JR. Viscoelasticity of the articular cartilage surface in early osteoarthritis. *Osteoarthritis and Cartilage*. 2012. Available at: doi:10.1016/j.joca.2012.01.011

[7] KRISHNAN R, KOPACZ M, ATESHIAN GA. Experimental verification of the role of interstitial fluid pressurization in cartilage lubrication. *Journal of Orthopaedic Research*. 2004. Available at: doi:10.1016/j.orthres.2003.07.002

[8] MURAKAMI T, YARIMITSU S, SAKAI N, NAKASHIMA N, YAMAGUCHI T, SAWAE Y. Importance of adaptive multimode lubrication mechanism in natural synovial joints. *Tribology International*. 2017. Available at: doi:10.1016/j.triboint.2016.12.052

[9] MOW VC, KUEI SC, LAI WM, ARMSTRONG CG. Biphasic creep and stress relaxation of articular cartilage in compression: Theory and experiments. *Journal of Biomechanical Engineering*. 1980. Available at: doi:10.1115/1.3138202

[10] ATESHIAN GA. The role of interstitial fluid pressurization in articular cartilage lubrication. *Journal of Biomechanics*. 2009. Available at: doi:10.1016/j.jbiomech.2009.04.040

[11] MURAKAMI T. Importance of adaptive multimode lubrication mechanism in natural and artificial joints. *Proceedings of the Institution of Mechanical Engineers, Part J: Journal of Engineering Tribology*. 2012. Available at: doi:10.1177/1350650112451377

[12] SAKAI N, HAGIHARA Y, FURUSAWA T, HOSODA N, SAWAE Y, MURAKAMI T. Analysis of biphasic lubrication of articular cartilage loaded by cylindrical indenter. *Tribology International*. 2012. Available at: doi:10.1016/j.triboint.2011.03.016

[13] MURAKAMI T, YARIMITSU T, NAKASHIMA K, YAMAGUCHI T, SAWAE Y, SAKAI N, SUZUKI A. Superior lubricity in articular cartilage and artificial hydrogel cartilage. *Proceedings of the Institution of Mechanical Engineers, Part J: Journal of Engineering Tribology*. 2014. Available at: doi:10.1177/1350650114530273

[14] FUJIE H, IMADE K. Effects of low tangential permeability in the superficial layer on the frictional property of articular cartilage. *Biosurface and Biotribology*. 2015. Available at: doi:10.1016/j.bsbt.2015.06.001

[15] MURAKAMI T, SAKAI N, YAMAGUCHI T, YARIMITSU S, NAKASHIMA K, SAWAE Y, SUZUKI A. Evaluation of a superior lubrication mechanism with biphasic hydrogels for artificial cartilage. *Tribology International*. 2015. Available at: doi:10.1016/j.triboint.2014.12.013

[16] MOORE AC, BURRIS DL. Tribological rehydration of cartilage and its potential role in preserving joint health. *Osteoarthritis and Cartilage*. 2017. Available at: doi:10.1016/j.joca.2016.09.018

[17] KLEIN J. Hydration lubrication. *Friction*. 2013. Available at: doi:10.1007/s40544-013-0001-7

[18] IKEUCHI K. Origin and future of hydration lubrication. 2007. Available at: doi:10.1243/13506501JET214

[19] NAKASHIMA K, SAWAE Y, MURAKAMI T. Study on Wear Reduction Mechanisms of Artificial Cartilage by Synergistic Protein Boundary Film Formation. *JSME International Journal Series C*. 2005. Available at: doi:10.1299/jsmec.48.555

[20] NAKASHIMA K, SAWAE Y a MURAKAMI Y. Effect of conformational changes and differences of proteins on frictional properties of poly(vinyl alcohol) hydrogel. *Tribology International*. 2007. Available at: doi:10.1016/j.triboint.2007.02.010

[21] YARIMITSU S, NAKASHIMA K, SAWAE Y, MURAKAMI T. Influences of lubricant composition on forming boundary film composed of synovia constituents. *Tribology International*. 2009. Available at: doi:10.1016/j.triboint.2008.11.005

[22] MURAKAMI T, YARIMITSU S, NAKASHIMA K, SAWAE Y, SAKAI N. Influence of synovia constituents on tribological behaviors of articular cartilage. *Friction*. 2013. Available at: doi:10.1007/s40544-013-0010-6

[23] GONG JP. Friction and lubrication of hydrogels - Its richness and complexity. *Soft Matter*. 2006. Available at: doi:10.1039/b603209p

[24] GONG JP, OSADA Y. Gel friction: A model based on surface repulsion and adsorption. *Journal of Chemical Physics*. 1998. Dostupné z: doi:10.1063/1.477453

[25] OLIVEIRA AS, SEIDI O, RIBEIRO N, COLAÇO R, SERRO AP. Tribomechanical comparison between PVA hydrogels obtained using different processing conditions and human cartilage. *Materials*. 2019. Available at: doi:10.3390/ma12203413

[26] OKA M, USHIO K, KUMAR P, IKEUCHI K, HYON SH, NAKAMURA T, FUJITA H. Development of artificial articular cartilage. *Proceedings of the Institution of Mechanical Engineers, Part H: Journal of Engineering in Medicine*. 2000. Available at: doi:10.1243/0954411001535246

[27] NOGUCHI T, YAMAMURO T, OKA M, KUMAR P, KOTOURA Y, HYON S, IKADA Y. Poly(vinyl alcohol) hydrogel as an artificial articular cartilage: evaluation of biocompatibility. *Journal of applied biomaterials : an official journal of the Society for Biomaterials*. 1991. Available at: doi:10.1002/jab.770020205

[28] MURAKAMI T, SAWAE Y, NAKASHIMA K, FISHER J. Tribological Behaviour of Artificial Cartilage in Thin Film Lubrication. 2000. Available at: doi:10.1016/S0167-8922(00)80136-4

[29] OTSUKA E, SUZUKI A. A Simple Method to Obtain a Swollen PVA Gel Crosslinked by Hydrogen Bonds. *Wiley InterScience*. 2009. Available at: doi:10.1002/app.30546

[30] YARIMITSU S, SASAKI S, MURAKAMI T, SUZUKI A. Evaluation of lubrication properties of hydrogel artificial cartilage materials for joint prosthesis. *Biosurface and Biotribology*. 2016. Available at: doi:10.1016/j.bsbt.2016.02.005

[31] SUZUKI A, SASAKI S, SASAKI S, NON T, NAKASHIMA K, YARIMITSU S, MURAKAMI T. Elution and wear of PVA hydrogels by reciprocating friction. *5th World Tribology Congress 2013 Torino*. 2013.

[32] YARIMITSU S, YOSHIDA A, SASAKI S, MURAKAMI T, SUZUKI A. Evaluation of Lubrication Property of Poly(vinyl alcohol) Hybrid Gel for Artificial Articular Cartilage. *Tribology Online*. 2016. Available at: doi:10.2474/trol.11.360

[33] YARIMITSU S, SAWAE Y. Development of PVA hydrogels for artificial cartilage with superior lubricity. *Proceedings of JSME International Conference on Materials and Processing 2022 November 6–10 2022, Okinawa, Japan*. 2022.

[34] MURAKAMI T, SAKAI N, YARIMITSU S, NAKASHIMA K, Tetsuo YAMAGUCHI, Yoshinori SAWAE a Atsushi SUZUKI. Evaluation of influence of changes in permeability with aging on friction and biphasic behaviors of artificial hydrogel cartilage. *Biotribology*. 2021. Available at: doi:10.1016/j.biotri.2021.100178

[35] SAKAI N, YARIMITSU S, SAWAE Y, KOMORI M, MURAKAMI T. Biomimetic artificial cartilage: Fibre-reinforcement of PVA hydrogel to promote biphasic lubrication mechanism. *Biosurface and Biotribology*. 2019. Available at: doi:10.1049/bsbt.2018.0031

[36] SHIRAZI R, SHIRAZI-ADL A. Deep vertical collagen fibrils play a significant role in mechanics of articular cartilage. *Journal of Orthopaedic Research*. 2008. Available at: doi:10.1002/jor.20537

[37] SAKAI N. Vertical fiber-reinforcement promoters biphasic lubrication of PVA hydrogel. *Biotribology conference, Fukuoka 2024 (USB storage)*. nedatováno.

[38] FUJIE H, MORISHITA S, YARIMITSU S. Effect of collagen-induced residual stress on the frictional property of articular cartilage. *Biosurface and Biotribology*. 2018. Available at: doi:10.1049/bsbt.2018.0008

[39] MA R, XIONG D, MIAO F, ZHANG J, PENG Y. Novel PVP/PVA hydrogels for articular cartilage replacement. *Materials Science and Engineering C*. 2009. Available at: doi:10.1016/j.msec.2009.03.010

[40] ARAKAK K, KITAMURA N, FUJIKI H, KUROKAWA T, IWAMOTO M, UENO M, KANAYA F, OSADA Y, GONG JP, YASUDA K. Artificial cartilage made from a novel double-network hydrogel: In vivo effects on the normal cartilage and ex vivo evaluation of the friction property. *Journal of Biomedical Materials Research - Part A*. 2010. Available at: doi:10.1002/jbm.a.32613

[41] YANG F, ZHAO J, KOSHUT WJ, WATT J, RIBOH JC, GALL K, WILEY BJ. A Synthetic Hydrogel Composite with the Mechanical Behavior and Durability of Cartilage. *Advanced Functional Materials*. 2020. Available at: doi:10.1002/adfm.202003451

[42] ZHAO J, TONG H, KIRILLOVA A, KOSHUT WJ, MALEK A, BRIGHAM NC, BECKER ML, GALL K, WILEY BJ. A Synthetic Hydrogel Composite with a Strength and Wear Resistance Greater than Cartilage. *Advanced Functional Materials*. 2022. Available at: doi:10.1002/adfm.202205662

[43] JOHNSON CL, DUNN AC. Tribological Characterization of Gradient-density Polyacrylamide Hydrogel Surfaces. *Experimental Mechanics*. 2021. Available at: doi:10.1007/s11340-021-00704-x

[44] RONG M, LIU H, SCARAGGI M, BAI B, BAO L, MA S, MA Z, CAI M, DINI D, ZHOU F. High Lubricity Meets Load Capacity: Cartilage Mimicking Bilayer Structure by Brushing Up Stiff Hydrogels from Subsurface. *Advanced Functional Materials*. 2020. Available at: doi:10.1002/adfm.202004062

[45] YU Y, YUK H, PARADA GA, WU Y, LIU X, NABZDYK CS,YOUCEF-TOUMI K, ZANG J, ZHAO X. Multifunctional “Hydrogel Skins” on Diverse Polymers with Arbitrary Shapes. *Advanced Materials*. 2019. Available at: doi:10.1002/adma.201807101

[46] WEI Q, LIU H, ZHAO X, ZHAO W, XU R, MA S, ZHOU F. Bio-inspired hydrogel-polymer brush bi-layered coating dramatically boosting the lubrication and wear-resistance. *Tribology International*. 2023, Available at: doi:10.1016/j.triboint.2022.108000

[47] LIU G, LIU Z, Li N, WANG X, ZHOU F, LIU W, Hairy Polyelectrolyte Brushes-Grafted Thermosensitive Microgels as Artificial Synovial Fluid for Simultaneous Biomimetic Lubrication and Arthritis Treatment *ACS Applied Materials & Interfaces*. 2024. Available at: doi:10.1021/am506026e

[48] LIN W, KLEIN J. Hydration Lubrication in Biomedical Applications: From Cartilage to Hydrogels. *Accounts of Materials Research*. 2022. Available at: doi:10.1021/accountsmr.1c00219

[49] MURAKAMI T, YARIMITSU S, SAKAI N, NAKASHIMA K, YAMAGUCHI T, SAWAE Y. Importance of adaptive multimode lubrication mechanism in natural synovial joints. *Tribology International*. 2017. Available at: doi:10.1016/j.triboint.2016.12.052

[50] JAHN S, SEROR J, KLEIN J. Lubrication of Articular Cartilage. *Annual Review of Biomedical Engineering*. 2016. Available at: doi:10.1146/annurev-bioeng-081514-123305

[51] KRISHNAN R, KOPACZ M, ATESHIAN GA. Experimental verification of the role of interstitial fluid pressurization in cartilage lubrication. *Journal of Orthopaedic Research*. 2004. Available at: doi:10.1016/j.orthres.2003.07.002

[52] IKEUCHI K. Origin and future of hydration lubrication. In: *Proceedings of the Institution of Mechanical Engineers, Part J: Journal of Engineering Tribology*. 2007. Available at: doi:10.1243/13506501JET214

[53] GONG JP. *Friction and lubrication of hydrogels - Its richness and complexity*. 2006. Available at: doi:10.1039/b603209p

[54] JOHNSON KL. *Contact Mechanics*. B.m.: Cambridge University Press, 1985.

[55] MIAO L, GUO H, ZUCKERMANN MJ. Conformation of polymer brushes under shear: Chain tilting and stretching. *Macromolecules*. 1996. Available at: doi:10.1021/ma951071z

[56] HE X, XUE F, CHEN Q, HUANG G, ZHANG R. Macromolecular motions and hydrodynamic radius variation in dilute solutions under shear action. *Polymer International*. 2015. Available at: doi:10.1002/pi.4850

[57] SHINMORI H, MAYO K, TAKEHIRO M, YAMAGUCHI T, SAWAE Y. Effects of Synovial Fluid Constituents on Friction between UHMWPE and CoCrMo. *Tribology Online*. 2020. Available at: doi:https://doi.org/10.2474/trol.15.283

[58] YARIMITSU S, NAKASHIMA K, SAWAE Y, MURAKAMI T. Influence of Phospholipid and Protein Constituents on Tribological Properties of Artificial Hydrogel Cartilage Material. *Journal of Biomechanical Science and Engineering*. 2013. Available at: doi:10.1299/jbse.8.257

[59] FEI W, GAO J, YANG X, JIANMING Y. Enhanced Mechanical Properties of PVA Hydrogel by Low-Temperature Segment Self-Assembly vs. Freeze–Thaw Cycles. *Polymers*. 2023. Available at: https://doi.org/10.3390/polym15183782

[60] BAVARESCO VP, ZAVAGLIA CAC, REIS MC, GOMES JR. Study on the tribological properties of pHEMA hydrogels for use in artificial articular cartilage. *Wear*. 2008. Available at: doi:10.1016/j.wear.2007.10.009

[61] FREEMAN, ME, FUREY MJ, LOVE BJ, HAMPTON JM. Friction, wear, and lubrication of hydrogels as synthetic articular cartilage. *Wear*. 2000. Available at: doi:10.1016/S0043-1648(00)00387-2

[62] SAKAI N, HASHIMOTO C, YARIMITSU S, SAWAE Y, KOMORI M, MURAKAMI T. A functional effect of the superficial mechanical properties of articular cartilage as a load bearing system in a sliding condition. *Biosurface and Biotribology*. 2016. Available at: doi:10.1016/j.bsbt.2016.02.004

[63] KANCA Y, MILNER P, DINI D, AMIS AA. Tribological properties of PVA/PVP blend hydrogels against articular cartilage. *Journal of the Mechanical Behavior of Biomedical Materials*. 2018. Available at: doi:10.1016/j.jmbbm.2017.10.027

[64] GREGORA J. Tribology of hydrogel for articular cartilage replacement. Online, mater's Thesis. Martin VRBKA (supervisor). Brno: Brno University of Technology, Faculty of Mechanical Engineering, 2025. Available at: https://www.vut.cz/en/students/final-thesis/detail/165364.

9 LIST OF ABBREVIATIONS, SYMBOLS AND QUANTITIES USED

Symbol	Meaning	Unit
a	Contact Radius	mm
b	Sample Thickness	mm
h	Thickness of Hydrogel (Figure 4-6)	m
p_{max}	Maximum pressure	Pa
pHEMA	Poly(2-hydroxyethyl methacrylate)	—
s	Lateral Shift (Figure 4-6)	mm
A	Contact Area	m^2
AFM	Atomic Force Microscopy	—
BC	Bacterial Cellulose	—
BUT	Brno University of Technology	—
CD	Cast drying method or a shortcut of PVA CD hydrogel	—
COF	Coefficient of Friction	1
COFeff	Effective Coefficient of Friction	1
COFeq	Equilibrium Coefficient of Friction	1
CP	Composite PVA Hydrogel (CP06, CP24, …)	—
DPPC	Dipalmitoylphosphatidylcholine (a phospholipid)	—
E	Elastic modulus / Young's modulus	MPa
FE	Finite Element (method or model)	—
FFM	Friction Force Microscope	—
F_N	Normal Force	N
FT	Freeze-thaw method or a shortcut of PVA FT hydrogel	—
F_T	Friction Force	N
FT-IR	Fourier-Transform Infrared Spectroscopy	—
GAG	Glycosaminoglycan	—
HA	Hyaluronic Acid	—
HD	Hydrodynamic Lubrication	—
LSM	Laser Scanning Microscope	—
LM	Laminar PVA Hydrogel	—
OA	Osteoarthritis	—
PAMPS	Poly(2-acrylamido-2-methyl-1-propanesulfonic acid)	—
PBS	Phosphate Buffered Saline	—
PCs	Phosphatidylcholines	—
PEEK	Polyether ether ketone	—
PLs	Phospholipids	—
PRG4	Proteoglycan 4 (lubricin)	—

PNaAMPS	PAMPS with sodium salt	—
PVA	Polyvinyl Alcohol	—
DN	Double Network	
PVP DN	Polyvinylpyrrolidone	—
R	Ball Radius	mm
Ra	Arithmetic average roughness	μm
RH	Relative Humidity	%
Rz	Average maximum profile height (roughness)	μm
S	Contac Area	mm^2
SD	Standard Deviation	—
SF	Synovial Fluid	—
SFB	Surface Force Balance	—
UHMWPE	Ultra-high-molecular-weight polyethylene	—
VHX	Optical Microscope Keyence VHX 7000	—
W	Total load pressure	N
W^P	Load supported by interstitial fluid	N
δ	Contact Deformation	m
ε	Mechanical Strain	—
φ	Fraction of Solid Contact Area; tilt angle	—, °
σ	Mechanical Stress	Pa
τ	Shear stress	Pa
G*	Complex shear modulus	Pa
G’	Storage modulus (elastic response)	Pa
G”	Loss modulus (viscous response)	Pa

10 LIST OF FIGURES AND GRAPHS

11 LIST OF TABLES

12 DATA AVAILABILITY

All the data used in the present thesis are available in the Zenodo repository. (Note: The links will be available once the related manuscripts are published in journals.)

Data of the 1st experimental part: https://doi.org/10.5281/zenodo.11196287

Data of the 2nd experimental part: https://doi.org/10.5281/zenodo.15053243